

**CHARACTERIZATION OF A REGULATORY MECHANISM FOR
POSTTRANSCRIPTIONAL LIN28A INDUCTION THROUGH
microRNA PROCESSING MACHINERY IN NEURONAL GROWTH**

by

Alexandra M. Amen

A dissertation submitted to the Johns Hopkins University in conformity with the
requirements for the degree of Doctor of Philosophy

Baltimore, MD

July, 2016

Abstract

Environmental cues produce rapid transitions in gene expression to support growth and cellular plasticity through incompletely understood mechanisms. Brain-derived neurotrophic factor (BDNF) is a signaling molecule involved in development and plasticity that is dysregulated in numerous neurologic diseases. Prior work from our laboratory demonstrated that BDNF signaling confers translational specificity by regulating microRNA biogenesis, in part through induction of Lin28a protein. Lin28 RNA-binding proteins have evolutionarily-conserved roles in posttranscriptional coordination of pro-growth gene expression, but Lin28 is traditionally considered to be absent from terminally-differentiated cells, and signaling pathways allowing stimulus-dependent induction of Lin28 remain uncharacterized. The first portion of my dissertation focuses on elucidating a novel mechanism allowing rapid Lin28a induction in mature neurons. We find that Lin28a protein undergoes rapid basal turnover in hippocampal neurons, and is stabilized by BDNF-dependent activation of mitogen-activated protein kinase (MAPK). MAPK-mediated phosphorylation of the miRNA-processing factor, HIV TAR-RNA-binding protein (TRBP), promotes binding and stabilization of Lin28a, but not Lin28b, with accompanying reduction in Lin28-targeted miRNAs (Let-7 miRNAs). Further, phospho-TRBP recapitulates BDNF-induced neuronal dendritic spine growth, in a Lin28a-dependent manner. Finally, we demonstrate MAPK-dependent induction of TRBP and Lin28a downstream of diverse growth factors in multiple primary

cell types, supporting a broad role for this newly described pathway in cellular trophic responses.

Our finding of Lin28a regulation by phospho-TRBP in neuronal cells leads to the second portion of my dissertation, investigating the possibility that TRBP and Lin28a are dysregulated in a human tumor disorder, Neurofibromatosis Type 2 (NF2). We demonstrate that loss of Merlin protein in NF2 results in elevated TRBP, phospho-TRBP, and Lin28a proteins, and reduced Let-7 miRNAs. Additionally, ongoing studies suggest that abnormal tumor cell growth in NF2 is related to Lin28a overexpression, paving the way for potential research regarding novel therapeutics for NF2. Collectively, the work presented in my dissertation uncovers a previously unrecognized mechanism for induction of Lin28a that is conserved in both acute (trophic) and chronic (tumor) settings. This molecular mechanism underlying Lin28a stabilization has implications for understanding regulation and misregulation of translational specificity in synaptic responses, and in tumor and stem cell biology, where Lin28a is constitutively elevated.

Advisor: Mollie K. Meffert, M.D., Ph.D

Acknowledgements

The amount of work necessary for the successful completion of a dissertation is never the result of a single person's effort. I want to sincerely thank Dr. Mollie Meffert, my thesis advisor, for all of her support and encouragement throughout my time as a graduate student in her lab. Mollie had a clear and successful vision for the direction of my thesis project from the outset, and did an amazing job of guiding experiments while still allowing me to explore alternate methods and hypotheses. She was always available for troubleshooting and discussion of ideas, and I can't image a better scientific training experience. I also want to thank Drs. Shanthini Sockanathan, Alex Kolodkin, and Rachel Green who have served as part of my thesis committee for the past several years and provided excellent feedback and guidance, directly contributing to the successful completion of the project.

All of the members of the Meffert lab were an integral part in keeping me happy and excited to come to work on a daily basis. In particular I want to thank one of my best friends, Claudia Ruiz, who mentored me as a rotation student and then generously allowed me to join the project she initiated, working to understand Lin28a stabilization. I also want to thank Jay Shi, a previous master's student with out lab, who is extremely talented and worked with Claudia and me to establish initial characterization of Lin28a induction. I will sincerely miss all of the current members of the lab, and want to thank them for all of our scientific discussions, late nights in lab together, all of the fun that we've had outside of lab as well. The lab is an amazingly upbeat, positive environment that helps to keep

us all invested in our projects, even when we hit a rough patch scientifically. In particular, I want to acknowledge Daniel Pham, Josh Schwatz, and Leo Hagmann. The four of us all joined Mollie's lab as graduate students within the same month, and have progressed through all major milestones together. I can't imagine my graduate experience without them.

I want to thank my incredible boyfriend, Karl Petre, for being patient with the hours I spend in lab, listening to me practice all of my scientific presentations, and always encouraging me when I was frustrated or unsure. Finally, I want to thank my parents, Barbara Amen and Tom Wieting, for introducing me early to the world of academia, and always supporting me both in my time as a graduate student, and in life generally. It would have been impossible to accomplish this without their help.

Table of Contents

Abstract.....	ii
Acknowledgements.....	v
Table of Contents	vi
List of Figures	viii
Chapter 1: Introduction	1
Gene expression regulation in synaptic plasticity	1
BDNF signaling regulates synaptic plasticity	2
Physiological effects of post-transcriptional regulation by BDNF	4
BDNF regulates the specificity of translation	7
Post-transcriptional regulation by microRNA-mediated repression.....	9
BDNF regulates miRNA biogenesis through the Lin28/Let-7 axis	11
Characterization of the Lin28/Let-7 axis in growth and development	14
Lin28 regulation in mammalian systems	16
Figures and legends	19
Chapter 2: A rapid induction mechanism for Lin28a in trophic responses.....	21
Background	21
Results	23
Rapid posttranscriptional induction of Lin28a, but not Lin28b	23
MAPK-mediated TRBP phosphorylation promotes induction of Lin28a, but not Lin28b.....	25
TRBP phosphorylation reduces its polyubiquitination	28

TRBP is a binding partner of Lin28a.....	31
TRBP phosphorylation downstream of BDNF promotes Lin28a co- association.....	33
Phospho-TRBP requires Lin28a to regulate dendritic spine growth.....	35
MAPK-dependent Lin28a induction is a shared feature in trophic responses	37
Discussion.....	38
Figures and Legends	40
Methods	67
Chapter 3: Regulation of the Lin28/Let-7 axis in Neurofibromatosis Type 2.....	81
Background.....	81
Results	84
Loss of Merlin in Neurofibromatosis tumors is associated with elevated phospho-TRBP and Lin28a	84
Loss of Merlin protein directly regulates Lin28a through TRBP	86
Lin28 expression controls growth of Neurofibromatosis Type 2 tumor cells	87
Discussion.....	88
Figures and Legends	92
Chapter 4: Conclusions and Perspectives	104
Appendix A.....	113
Appendix B: Extended Experimental Methods.....	115
References.....	165
Curriculum Vitae.....	185

List of Figures

Figure 1.1.....	19
Figure 1.2.....	20
Figure 2.1.....	43
Figure 2.2.....	45
Figure 2.3.....	48
Figure 2.4	50
Figure 2.5	52
Figure 2.6.....	53
Figure 2.7.....	55
Figure 2.8.....	58
Figure 2.9.....	60
Figure 2.10	61
Figure 2.11	63
Figure 2.12	65
Figure 2.13	67
Figure 3.1.....	92
Figure 3.2.....	94
Figure 3.3.....	96
Figure 3.4.....	98
Appendix A.....	113

Chapter 1: Introduction

Gene expression regulation in synaptic plasticity

The precise complement of neuronal proteins is fundamentally important in shaping neural function and activity, and ultimately determines synaptic response. It has long been appreciated that novel and specific gene expression is required for the endurance of synaptic changes and memory consolidation (Gal-Ben-Ari et al., 2012; Pfeiffer and Huber, 2006). Environmental stimuli lead to neuronal activity that can cause enduring changes in the strength of synapses by inducing changes in gene expression. This phenomenon is termed long-term synaptic plasticity, and is considered the cellular correlate of learning and memory. In order to better understand mechanisms underlying synaptic plasticity, molecules contributing to transcriptional specificity, including transcription factors and chromatin modifications, have been widely investigated in past years. However, high-throughput approaches in recent years have shown that the cellular transcriptome correlates only moderately with the proteome (Foss et al., 2011; Ideker et al., 2001; Schwanhausser et al., 2011; Tian et al., 2004). Additionally, genetic variants regulating transcription are suggested to be distinct from those regulating protein synthesis (Foss et al., 2011). These studies reveal that the expression of most proteins is predominantly controlled post-transcriptionally, and underscore the differential genetic control of regulation by transcription versus translation, highlighting the importance of understanding mechanisms for regulation at the level of translation.

Dysregulated translation is associated with a range of cognitive and neurologic conditions including autism spectrum disorders and neurodegenerative diseases (Bassell and Warren, 2008; Gehrke et al., 2010; Krauss et al., 2013; Liu-Yesucevitz et al., 2011; Ramaswami et al., 2013; Wang et al., 2007). Changes in RNA granule accumulation linked to disrupted local translation in neurons is observed in Fragile X Syndrome (FXS), Amyotrophic Lateral Sclerosis (ALS), and Frontotemporal Dementia (FTD), among others (Liu-Yesucevitz et al., 2011; Ramaswami et al., 2013; Wang et al., 2007). Additionally, polyglutamine repeat expansions in conditions such as Huntington's Disease (HD) are thought to bind to regulatory complexes and increase neuronal translation (Krauss et al., 2013). However, the current lack of knowledge regarding control points in protein synthesis significantly impairs our ability to decipher dysregulation in disease. Thus, elucidating how neurons control translational specificity may reveal novel targets for therapeutic approaches.

BDNF signaling regulates synaptic plasticity

Growth factors refer to a naturally occurring class of secreted proteins that generally exert their effects by supporting cellular survival, proliferation, and healing. Brain-derived neurotrophic factor (BDNF) belongs to the neurotrophin family of growth factors, and influences specifically the growth and survival of neurons in the central and peripheral nervous systems. BDNF expression is detectable in all brain regions, with the highest BDNF mRNA levels generally observed in the cerebral cortex and hippocampus, where it is characterized as a

critical regulator of learning and memory (Conner et al., 1997; Wetmore et al., 1990). BDNF signaling is crucial in early development where it plays significant roles in neuronal progenitor proliferation and differentiation, cell survival, the outgrowth of neuronal processes, and both the formation and pruning of synaptic connections. Mice homozygous for loss of BDNF (BDNF knockout) often die postnatally, and surviving mice show significant nervous system dysfunction (Ernfors et al., 1995; Jones et al., 1994; Patterson et al., 1996). Additionally, throughout adulthood, secretion of BDNF in response to neuronal activity functions to promote synaptic strengthening and enhance learning and memory, as well as to provide general trophic support for neuronal health and survival. These critical roles mean that abnormal BDNF signaling is closely associated with a range of mental health disorders, including autism spectrum disorder, depression, schizophrenia, bipolar disorder, and anxiety disorders, as well as neurodegenerative diseases, including Alzheimer's Disease and Parkinson's Disease (Andero and Ressler, 2012; McAllister et al., 1999; Muglia et al., 2003; Nagahara and Tuszynski, 2011; Santos et al., 2010; Tyler et al., 2002; Zuccato and Cattaneo, 2009).

BDNF protein is observed in the synaptic compartment, and is thought to be stored and released both pre-synaptically from dendritic sites, as well as post-synaptically in an autocrine manner (Andreska et al., 2014; Hartmann et al., 2001; Matsuda et al., 2009). Upon secretion, BDNF interacts with the high affinity tropomyosin-related kinase B (TrkB) tyrosine kinase receptor to activate multiple intracellular signaling cascades, including the MAPK, mTOR, and PLC γ

pathways. Signaling downstream of TrkB receptors mediates the trophic effects of BDNF on neurons and synaptic connections, and blocking the BDNF/TrkB interaction leads to significant impairments in synaptic plasticity and learning (Lai et al., 2012; Takei et al., 2001; Tanaka et al., 2008).

Enduring effects of BDNF on growth and plasticity require changes in gene expression, and BDNF has been shown to regulate both transcription and translation. Through the activation of select transcription factors such as serum response factor (SRF), nuclear factor kappa B (NF- κ B), and cAMP response element binding protein (CREB), BDNF is known to upregulate trophic targets at the level of transcription (Finkbeiner et al., 1997; Kajiya et al., 2009; Kalita et al., 2006; Riccio et al., 2006). However, as discussed, the level of a transcribed mRNA does not necessarily correlate with its translation, and in fact expression levels of many proteins are predominantly controlled post-transcriptionally (Foss et al., 2011; Ideker et al., 2001; Schwanhausser et al., 2011; Tian et al., 2004). Given the dramatic role that BDNF plays in neuronal health, survival, and plasticity, understanding how BDNF signaling can generate trophic programs of gene expression at a post-transcriptional level has the potential to reveal critical regulatory points in both normal and abnormal brain function.

Physiological effects of post-transcriptional regulation by BDNF

Alterations in neuronal structure, such as dendritic outgrowth and spine maturation, are major physiological components of enduring plasticity that have been shown to require BDNF-dependent changes in protein synthesis (Jaworski

et al., 2005; Tanaka et al., 2008). In a translation-dependent manner, BDNF signals through TrkB receptors to enhance dendritic complexity and branching in both hippocampal and cortical neurons (Cheung et al., 2007; Horch and Katz, 2002; Jaworski et al., 2005; Je et al., 2009a; Lazo et al., 2013; Takemoto-Kimura et al., 2007; Tanaka et al., 2008). BDNF release can act to enhance dendritic arborization of both itself (in an autocrine fashion), or a closely neighboring neuron, through signaling pathways downstream of TrkB receptor binding. Accordingly, pyramidal neurons lacking TrkB receptors have significantly reduced pyramidal dendritic arbors (Horch and Katz, 2002; Xu et al., 2000). This ability of BDNF to increase dendritic arborization has been clearly linked to its regulation of translation. For example, Jaworski et al. (2005) demonstrated that enhanced dendritic complexity in response to BDNF expression was dependent on the mTOR signaling pathway, and could be blocked by inhibiting translation initiation. Additionally, Huang et al. (2012) showed that inhibition of specific microRNAs, and thus increased translation of their target mRNAs, is required for BDNF-mediated induction of dendritic arborization.

BDNF is also a well-characterized regulator of spine dynamics, and can induce changes in dendritic spine size and number. In cultured hippocampal neurons, BDNF has been shown to robustly increase spine density on the apical dendrite of pyramidal neurons in a MAPK/ERK-dependent manner (Alonso et al., 2004; Tyler and Pozzo-Miller, 2003; Tyler and Pozzo-Miller, 2001). Again, the effect of BDNF on spine plasticity is dependent on its regulation of protein-synthesis. In general, activity-induced upregulation of dendritic spines can be

blocked by treating cultured neurons with the drug anisomycin, an inhibitor of protein synthesis (Fifkova et al., 1982; Srivastava et al., 2012). More directly, long-term increases in hippocampal spine density mediated by BDNF have been shown to require new translation utilizing a system that allows inducible cell-autonomous inactivation of protein synthesis (Je et al., 2009a). Collectively, this research indicates that posttranscriptional regulation of gene expression by BDNF can induce structural changes in both synaptic and dendritic morphology that participate in plastic responses.

Consistent with the idea of synaptic plasticity as a cellular readout of learning and memory, the requirement for BDNF in tests of hippocampal-dependent learning and memory is well established (Heldt et al., 2007; Pardon, 2010; Tyler et al., 2002). The hippocampus is thought to be a major locus of memory consolidation, and requires novel protein synthesis for this function, because *in-vivo* hippocampal injection of protein synthesis inhibitors prevents hippocampal-dependent memory formation (Power et al., 2006; Tronel et al., 2005). While few studies have directly attempted to link BDNF function with the required novel translation in hippocampal-based learning, recent research has shown that LTM in the hippocampus requires multiple cycles of translation that occur following learning paradigms, and that BDNF is elevated concurrent with the initiation of these cycles (Bekinschtein et al., 2007). Additionally, inhibition of BDNF prevented LTM formation in the same timecourse as intrahippocampal anisomycin injection (Bekinschtein et al., 2007). These findings are consistent overall with a role for BDNF in translation-dependent changes of neuronal and

synaptic function that are associated with learning and memory consolidation, and underscore the importance of understanding mechanisms of translation regulation by BDNF.

BDNF regulates the specificity of translation

Long-lasting synaptic changes underlying learning and memory result from initial, rapid changes in gene expression following neuronal activity. Effective activity-dependent regulation of neuronal gene expression requires that the appropriate proteins be simultaneously regulated to accurately enhance or reduce synaptic response. Thus, it seems likely that rapid changes in the proteome following activity necessitate altered translation of discrete groups of specific genes, rather than increased translation of all mRNAs globally, many of which may be involved in conflicting cellular responses. While past research has defined multiple mechanisms underlying specificity of gene expression at the level of transcription (Jenuwein and Allis, 2001; Smith and Matthews, 2016), mechanisms allowing for translational specificity are less well delineated. However, BDNF has been shown to effectively promote synapse growth and plasticity by coordinating a synaptic response that involves a specific increase in translation of plasticity-related proteins. Despite the ability of BDNF to affect general translational machinery and total cellular translation (Gingras et al., 1999, 2004; Huang et al., 2012; Inamura et al., 2005; Kanhema et al., 2006; Takei et al., 2001; Takei et al., 2009), the modest increase in global translation that is observed in response to BDNF has actually been attributed to a robust effect on

the translation a relatively small number of specific transcripts (Huang et al., 2012; Schratt et al., 2004). Using a candidate-based approach, several initial studies demonstrated that BDNF increases the translation of plasticity-related proteins, such as CamKII α , Arc, and glutamate receptor subunits (Aakalu et al., 2001; Jourdi et al., 2009; Kanhema et al., 2006; Kelleher et al., 2004; Takei et al., 2004; Yin et al., 2002). In contrast, BDNF has been observed to decrease translation of certain mRNAs, such as potassium channels and co-transporters (Raab-Graham et al., 2006; Rivera et al., 2002). Radiolabelled synapses stimulated with BDNF and subjected to 2D electrophoresis also revealed a robust increase in a very specific set of proteins, while some proteins were decreased, and the majority were unchanged (Yin et al., 2002).

The development of high-throughput techniques enabled an appreciation of the truly impressive extent to which BDNF mediates target specificity. In an exciting study from the Greenberg lab (Schratt et al., 2004), the authors used polysome profiling to show that only roughly 4% of transcripts present in neurons underwent increased translation in response to BDNF, and that these increases were sensitive to mTOR signaling. Additionally, multidimensional protein identification technology (MudPIT) demonstrated that a brief, 30-minute BDNF stimulation of isolated synapses was sufficient to selectively increase proteins involved in synaptic vesicle formation and trafficking, translation, and synaptic components, while translation of other pools of mRNAs was decreased or, predominantly, unaltered (Liao et al., 2007). Similarly, gel based proteome profiling revealed that a long-term (12 hour) BDNF stimulation could increase

levels of a number of proteins involved in cellular metabolism and proliferation, while again most protein levels were decreased or unchanged (Manadas et al., 2009). The authors reported that BDNF was capable of affecting both the mRNA and protein levels of its targets, but that these changes were not always correlated, supporting post-transcriptional roles for BDNF in regulating *de novo* protein synthesis or protein stability (Manadas et al., 2009).

If BDNF in fact leads to increased translation of only 4% of transcribed mRNAs, how does it act to achieve such a remarkable degree of translational specificity? One well-established method of achieving selective translation is through RNA-binding proteins, which play important roles in post-transcriptional regulation of mRNAs by enhancing or repressing the translation of certain mRNAs. MicroRNAs (miRNAs), which inhibit translation of specific mRNA targets, represent another cellular method of post-transcriptional regulation of specificity in protein synthesis. Several different RNA-binding proteins have been observed both to be present at synapses, and to regulate the translation of major targets of BDNF (Bhakar et al., 2012; Huang et al., 2002; Huang et al., 2012; Napoli et al., 2008; Wu et al., 1998). However, a more direct link is documented between BDNF signaling and regulation of miRNA expression.

Post-transcriptional regulation by miRNA-mediated repression

Although miRNA-mediated regulation of protein synthesis was only relatively recently discovered (Lee et al., 1993), in the past 20 years many ground-breaking studies have demonstrated the importance of miRNA function in

all cell types. MiRNAs are short (20-24 nucleotide), non-coding RNA molecules that are endogenously expressed. They are able to recognize and bind partially complementary sites in their target mRNAs, causing translational suppression and/or degradation of these targets. Precursor miRNAs undergo several well-established processing steps to produce functional mature miRNAs. The canonical miRNA biogenesis pathway starts with transcription of a larger precursor miRNA (pri-miRNA) in the nucleus, where it is processed into a pre-miRNA stem-loop structure (of ~70 nucleotides) by the enzyme Drosha. This pre-miRNA hairpin is then exported into the cytoplasm, where it undergoes a second processing step by the RNaseIII enzyme Dicer and its binding partner Tar-RNA Binding Protein (TRBP) into a mature miRNA duplex. Regulation of either of these processing steps can dramatically affect the levels of functional mature miRNAs, and thus the expression of their mRNA targets.

MiRNA function in the brain has been shown to be crucial for normal neuronal development and plasticity in both mammalian and non-mammalian species (Giraldez et al., 2005; Krichevsky et al., 2003; Sempere et al., 2004; Smalheiser and Lugli, 2009). Given that a single miRNA can potentially regulate expression of an entire suite of proteins, miRNAs are attractive candidates for coordinating complex responses such as neuronal development, plasticity and synaptic remodeling at a post-transcriptional level. Interestingly, in comparison to other cell types, neuronal miRNAs have been shown to undergo dramatically accelerated activity-dependent turnover (Krol et al., 2010), which could enhance

their contribution to rapid, dynamic changes in neuronal gene expression following activity.

There is strong evidence for the presence of both miRNAs and miRNA processing machinery at the synapse (Ashraf et al., 2006; Huang et al., 2012; Lugli et al., 2012; Schratt et al., 2006; Wayman et al., 2008), further supporting a potential role for miRNAs in synaptic plasticity. The miRNA processing enzyme Dicer has been found to be present and active in synaptosomes, and there is additional evidence for enrichment of both precursor (pre-miRNAs) and mature miRNAs at synapses (Lugli et al., 2005; Lugli et al., 2008). Enrichment of mature miRNAs has been correlated with the presence of the corresponding pre-miRNA, again suggesting that miRNA processing might happen locally at the synapse (Lugli et al., 2008).

BDNF regulates miRNA biogenesis through the Lin28/Let-7 axis

Given that microRNA-mediated regulation has the ability to affect a wide range of downstream targets, recent emphasis has been placed on elucidating regulators of miRNAs themselves. Initial studies addressing the potential for individual miRNA regulation by BDNF demonstrated that BDNF signaling leads to changes in function or levels of single miRNAs involved in structural components of plasticity, including spine size and dendritic outgrowth (Dajas-Bailador et al., 2012; Fiore et al., 2009; Kawashima et al., 2010; Schratt et al., 2004; Schratt et al., 2006; Vessey et al., 2010; Vo et al., 2005; Wayman et al., 2008). However, recent work from our laboratory (Huang et al., 2012) has shown that BDNF can

also act upstream of miRNA processing to coordinately regulate the biogenesis of miRNAs globally. Briefly, BDNF stimulation of cultured hippocampal neurons elevates both Dicer and TRBP proteins in a rapid, transcription-independent manner, which enhances pre-miRNA processing and is associated with a concurrent increase in many mature miRNAs (Fig. 1.1). This finding initially appears somewhat counterintuitive, given that a global increase in miRNA biogenesis would suggest a global decrease rather than increase in translation. However, we also observed that BDNF selectively decreases the processing of a specific class of miRNAs – abundantly comprised of the Let-7 miRNA family - that are inhibited by an RNA-binding protein called Lin28 (Fig. 1.1). Let-7 miRNAs repress a range of pro-growth mRNAs, including various examples that are known to be crucial for synaptic function, such as CamKII α and GluA1 (Huang et al., 2012).

Vertebrates express two functionally redundant homologous forms of Lin28, Lin28a and Lin28b, which possess highly similar coding regions that share ~80% sequence identity (Heo et al., 2009; Piskounova et al., 2011) (Fig. 1.2). However, Lin28a exists primarily in the cytoplasm where it inhibits pre- to mature Let-7 miRNA processing, while Lin28b exists primarily in the nucleus where it inhibits pri- to pre-Let-7 processing (Piskounova et al., 2011). Though both forms of Lin28 were previously considered to be transcriptionally silenced in differentiated cell types such as neurons, we found that Lin28a protein, but not Lin28b, was substantially elevated by BDNF in a rapid, transcription-independent manner, and that this accounted for the specific decrease in mature Let-7 miRNA

expression following BDNF stimulation (Huang et al., 2012). Let-7 miRNAs are particularly abundant in the brain (Lagos-Quintana et al., 2002; Wienholds et al., 2005; Wulczyn et al., 2007), and make up at least 50% of miRNAs present in mature neurons (Juhila et al., 2011; Shinohara et al., 2011). Thus, Lin28a elevation resulting in reduced Let-7 miRNA-mediated repression could account for the mRNA targets that are selectively affected by the global increase in translation caused by BDNF. Accordingly, our laboratory demonstrated that expression of a mutant Let-7 miRNA construct that was unable to be inhibited by Lin28 protein resulted in loss of specificity for targets upregulated by BDNF (Huang et al., 2012).

Taken together, this research suggests that BDNF positively regulates global miRNA biogenesis by upregulating Dicer and TRBP proteins, and negatively regulates Let-7 miRNA biogenesis specifically by increasing Lin28a protein. In this way, BDNF increases miRNA-mediated repression globally while selectively relieving translational repression of Let-7 miRNA targets. Increased miRNA biogenesis via the Dicer/TRBP arm of this hypothesis may account for the transcripts that have been shown to undergo decreased translation in response to BDNF (Raab-Graham et al., 2006; Rivera et al., 2002), and indeed knockdown of Dicer protein in cell culture prevented a BDNF-mediated decrease in such targets (Huang et al., 2012). In contrast, BDNF leads to increased translation of specific pro-growth mRNAs that harbor Let-7 miRNA binding sites by increasing Lin28a protein levels and thus inhibiting Let-7 miRNA processing. Knockdown of Lin28a prevented a BDNF-mediated increase in many important

Let-7 containing targets, such as CamKII α , that are known to contribute to the synaptic and cognitive effects of BDNF (Huang et al., 2012). Similarly, expression of a mutant Lin28-resistant Let-7 miRNA in hippocampal neurons prevented BDNF from enhancing dendritic arborization (Huang et al., 2012), suggesting that the ability of BDNF to inhibit Let-7 miRNAs through Lin28 induction is required for physiological readouts of BDNF signaling.

Characterization of the Lin28/Let-7 axis in growth and development

Lin28 is a pro-growth pluripotency factor that is highly expressed in stem cells and many cancer cells, and is downregulated during development (Moss et al., 1997; Olde Loohuis et al., 2012). It was discovered in *C. elegans* as a heterochronic gene important in developmental timing (Moss et al., 1997), and was subsequently shown to be both conserved and similarly temporally regulated in other model organisms (Moss and Tang, 2003a). In recent years, Lin28 protein has been suggested to bind to conserved sequences in certain mRNAs, subsequently regulating their translation. Specifically, Lin28 is demonstrated to directly increase synthesis of RNA binding proteins, and to inhibit translation of mRNAs targeted to the endoplasmic reticulum (Cho et al., 2012; Wilbert et al., 2012). Additionally, Lin28 may bind to specific DNA promoter regions, and thus regulate gene expression through transcription as well as translation (Zeng et al., 2016). However, Lin28 is thought to exert its proliferative effects primarily through well-documented negative regulation of Let-7 microRNA biogenesis (Heo et al.,

2008; Heo et al., 2009; Moss et al., 1997; Nam et al., 2011; Viswanathan et al., 2008).

Because they inhibit translation of a range of important pro-growth proteins, the Let-7 miRNAs exhibit an expression pattern directly opposite to that of Lin28 – they are virtually absent from stem cells, and are substantially upregulated across development (Moss et al., 1997; Olde Loohuis et al., 2012). This opposing expression of Lin28 and the Let-7 miRNAs occurs through a negative feedback mechanism. Lin28 binds and remodels the terminal loop of the pre-Let-7 miRNA via its cold shock domain, which then allows the Lin28 zinc knuckle domain to bind to a conserved ‘GGAG’ motif in the terminal loop of the pre-Let-7 (Mayr et al., 2012; Nam et al., 2011). Lin28 binding to the ‘GGAG’ motif recruits a terminal uridylyase such as TUT4 or TUT7 (Heo et al., 2009; Thornton et al., 2012), resulting in poly-uridylation and subsequent degradation or inhibition of the pre-Let-7 (Heo et al., 2008; Heo et al., 2009; Nam et al., 2011). Thus, Lin28 protein is able to prevent Let-7 miRNA maturation prior to Dicer/TRBP processing. Conversely, mature Let-7 miRNAs can inhibit translation of Lin28 mRNA through Let-7 miRNA binding-sites in the Lin28 3’ UTR (Huang et al., 2012; Rybak et al., 2008).

Just as Lin28 enhances cellular division and pluripotency through its inhibition of Let-7 miRNAs, Let-7 miRNAs function to control differentiation and cell cycle termination by inhibiting translation of growth-related genes. For example, hypodermal blast cells of *C.elegans* Let-7 mutants fail to appropriately exit the cell cycle during development (Reinhart et al., 2000). Let-7 miRNAs are

grouped as a family not only because they share the Lin28-targeted 'GGAG' motif, but also because they exhibit identical 'seed' sequence regions (nucleotides 2-8 of the mature miRNA 5' end). The seed sequence is important in generating target recognition, suggesting that each Let-7 miRNA family member inhibits an overlapping (though not identical) group of targets (Lim et al., 2003b), generally functioning to provide a regulatory stop on growth and pluripotency.

Lin28 regulation in mammalian systems

Though the Lin28/Let-7 axis was initially and predominately characterized in *C. elegans*, it is known to be highly evolutionarily conserved, from zebrafish to rodent to human (Moss and Tang, 2003a; Pasquinelli et al., 2000; Viswanathan et al., 2008). As the importance of this axis as a regulator of growth and plasticity has begun to be appreciated, a range of research has been directed towards understand the role of Lin28 in mammalian tissues. In particular, Lin28a is one of a cocktail of four factors used to re-program differentiated mammalian cells into stem cells (Yu et al., 2007), and expression of Lin28a is one of the best predictors of successful iPSC reprogramming (Buganim et al., 2012). Additionally, Lin28 has been shown to promote insulin sensitivity and glucose uptake through Let-7 miRNA reduction, leading to resistance towards high fat diet-induced diabetes in mice (Zhu et al., 2011). Also in mice, Lin28 overexpression in adults enhances tissue recovery and regeneration (Shyh-Chang et al., 2013). GWAS studies in humans have linked genetic variations in the Lin28 locus to differences in height and sexual maturation (Ong et al., 2009;

Tommiska et al., 2011). In addition, due to the pro-growth nature of Lin28 function, at least 15% of human cancers are associated with elevations in Lin28 upstream of Let-7 miRNA reductions (Wang et al., 2012). Because the Let-7 miRNAs function as a group to inhibit expression of pro-growth genes, it is unsurprising that they are downregulated in a range of cancers, and are referred to a 'tumor-suppressor' miRNAs. For example, Let-7 miRNAs are globally decreased in human lung cancer tissues, and their reduction is associated with poor clinical outcome (Calin et al., 2004; Takamizawa et al., 2004; Yanaihara et al., 2006; Yu et al., 2008). Because of this, cancer treatment therapies involving the use of Let-7 microRNA mimics are currently in development (Dai et al., 2015; Kasinski et al., 2015; Liu et al., 2014; Wang et al., 2012).

Though Lin28 protein has been demonstrated to play a critical role in cellular growth and survival, and to be potentially pathogenic when dysregulated, mechanisms allowing for control of Lin28 expression have not been well characterized. In mammalian embryonic stem cells, transcription of Lin28a is regulated by Oct4, Sox2, Nanog, and TCF3 (Marson et al., 2008). Additionally, the transcription factors c-Myc and NF- κ B are capable of transactivating Lin28b in cancer cells (Chang et al., 2009; Iliopoulos et al., 2009). However, the only signaling mechanism previously known to regulate the Lin28/Let-7 axis involves nuclear receptors in *C. elegans* and *Drosophila Melanogaster* that transmit steroid hormone signals to increase Let-7 transcription (Chawla and Sokol, 2012; Hammell et al., 2009). Work from our laboratory showing rapid, transcription-independent induction of Lin28a protein by BDNF (Huang et al., 2012) was not

only the first demonstration of a signal-dependent mechanism for Lin28 induction in mammalian cells, it was also the first demonstration of Lin28a expression and function in differentiated neurons. These findings gave us the opportunity both to further elucidate molecular regulation of gene target specificity downstream of BDNF signaling, and to achieve an understanding of mechanisms underlying Lin28 induction.

The majority of my dissertation aims to uncover mechanisms of Lin28a induction downstream of trophic signaling, as will be described in Chapter 2. The work in Chapter 2 lead us to the hypothesis that a pathway controlling Lin28a might be dysregulated in a human tumor disorder, Neurofibromatosis Type 2, which is the focus of Chapter 3. Together, we hope that this work will lead to a better appreciation of mechanisms underlying Lin28 regulation, which could be important in increasing understanding of and therapeutic approaches for both diseases and disorders associated with dysregulated BDNF signaling, as well as those resulting from abnormal expression of Lin28a.

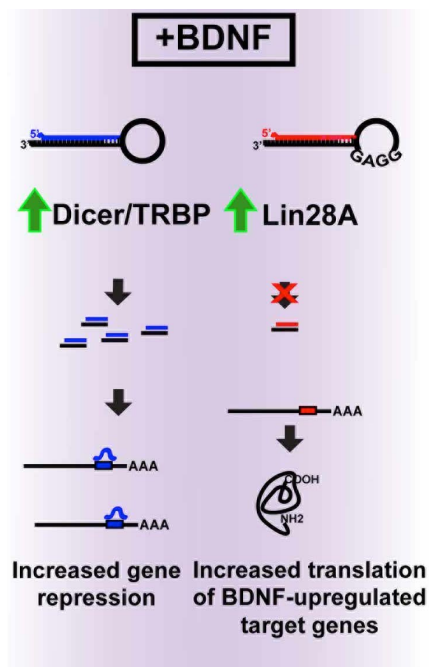
Note: As part of my dissertation, I have worked in collaboration with several other lab members whose research contributed importantly to our understanding of Lin28 regulation. Experiments performed by these collaborators are referenced in each figure legend, where appropriate. I contributed intellectually to all aspects of the research presented in this document.

Figures and legends

Figure 1.1: BDNF generates target specificity by regulating miRNA biogenesis

BDNF leads to positive regulation of miRNA biogenesis, and enhanced abundance of non-Let-7 family miRNAs, as a result of BDNF-induced increases in the miRNA processing proteins Dicer and TRBP (left side of panel). This explains why some mRNAs are excluded from translation in response to BDNF. Negative regulation of miRNA biogenesis occurs through BDNF-induced upregulation of the RNA-binding protein Lin28a, which blocks the processing of the Let-7 family of miRNAs specifically (right side of panel). This allows increased selective translation of Let-7 miRNA targets, which mediate a cellular pro-growth response to BDNF.

Figure 1.1

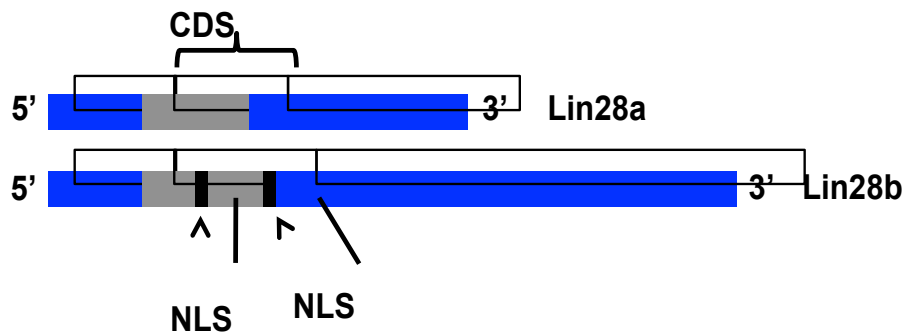


Huang et al., 2012

Figure 1.2: Lin28a and Lin28b share significant sequence homology

The vertebrate paralogs Lin28a and Lin28b both repress production of Let-7 miRNAs and were traditionally thought to be functionally redundant. The protein coding regions (coding DNA sequence, CDS) of Lin28a and Lin28b are highly homologous, sharing ~80% sequence identity. The Lin28b CDS, however, contains two nuclear localization signals not found in Lin28a, and thus Lin28b is localized to the nucleus while Lin28a is predominantly cytoplasmic (Piskounova et al., 2011). Additionally, the 3' untranslated region (UTR) of Lin28b is roughly twice the size of the Lin28a 3' UTR, suggestive of increased translational control.

Figure 1.2



Chapter 2: A rapid induction mechanism for Lin28a in trophic responses

Background

The cellular complement of proteins instructs cell identity, structure, and function. Mechanisms to rapidly tailor cellular protein composition in reaction to external trophic cues facilitate effective physiological responses supporting survival, growth, and plasticity. The heterochronic Lin28 RNA-binding proteins, first discovered in *C.elegans*, have evolutionarily-conserved roles as determinants of transitions in biological growth (Buganim et al., 2012; Shyh-Chang et al., 2013; Viswanathan et al., 2009; Zhu et al., 2010), but understanding their regulation by environmental stimuli has remained a challenge. Lin28 proteins coordinate selective protein synthesis from suites of genes that control cellular and organismal growth, in part through a mutually antagonistic relationship with the Let-7 family of microRNAs (miRNAs). Lin28 has recently been found to exert widespread effects on mammalian growth and development, including governing body size, reproductive maturation, metabolism, tissue regeneration, and cellular reprogramming (Buganim et al., 2012; Shyh-Chang et al., 2013; Zhu et al., 2010). Elevated Lin28 expression is a common oncogenic feature associated with advanced malignancy in humans (Chang et al., 2013; Mao et al., 2013; Urbach et al., 2014; Viswanathan et al., 2009), and implicated in highly prevalent and age-related diseases such as

insulin-insensitivity and type II diabetes (Frost and Olson, 2011; Perez et al., 2013; Zhu et al., 2010; Zhu et al., 2011).

Despite understanding of the Lin28/Let-7 pathway as a key regulator of growth-related genes, mechanisms by which stimuli might target Lin28 for biological responses are lacking. Lin28 levels are high in progenitor cells and gradually decline during development to negligible levels in differentiated cells, leading to assumptions of protracted Lin28 regulatory mechanisms. However, a prior observation from our laboratory (Huang et al., 2012) of rapid Lin28a upregulation in fully-differentiated neurons by a growth factor, BDNF, presented an opportunity to uncover cellular signaling pathways controlling Lin28. In this study, we demonstrate that Lin28a undergoes rapid transcription-independent induction by protein stabilization in complex with a previously unknown binding-partner, TRBP. BDNF induces MAPK-dependent TRBP phosphorylation, which both protects TRBP from proteasomal degradation and enhances TRBP binding to Lin28a. Lin28b, a paralog of Lin28a, does not associate with TRBP and is not induced by TRBP phosphorylation, exposing a mechanism for distinct stimulus-responsive regulation of Lin28a and Lin28b. Further, our data show that this rapid Lin28a induction pathway is broadly employed downstream of multiple trophic factors in diverse primary cells. These studies identify TRBP phosphorylation downstream of activated MAPK, and concomitant Lin28a stabilization, as a central mediator in neuronal pro-growth responses to BDNF, highlighting an unappreciated post-transcriptional induction mechanism for the pluripotency-associated Lin28/Let-7 pathway in rapid trophic responses.

Results

Rapid posttranscriptional induction of Lin28a, but not Lin28b

To address the regulatory mechanisms supporting stimulus-dependent Lin28a induction, we first evaluated the possibilities of altered Lin28a transcription, translation and protein stability. Primary murine hippocampal neurons stimulated with BDNF in the presence or absence of the transcription inhibitor, Actinomycin-D, showed no significant difference in the rate or amplitude of rapid Lin28a protein induction (Fig. 2.1a). Lin28a protein is posttranscriptionally induced 2-2.5 fold by BDNF over this timecourse, a magnitude shown to be sufficient to mediate physiological effects of BDNF on neuronal growth and protein synthesis (Huang et al., 2012; Kanhema et al., 2006; Kelleher et al., 2004). A band near the predicted molecular weight of Lin28a protein (25 kD) typically predominates in undifferentiated cells (e.g. embryonic stem cells and cell lines), while in differentiated primary cells we detect endogenous Lin28a protein as a predominant band or bands near 37 kD, as previously reported (Huang et al., 2012; Moss and Tang, 2003; Nowak et al., 2014; Seggerson et al., 2002) and validated by knockdown (Supplementary Fig. 1a). This banding pattern is observed using multiple antibodies raised against distinct Lin28a epitopes (Supplementary Fig. 1a), and has been attributed to posttranslational modification and alternative splicing of Lin28a (Seggerson et al., 2002).

Concordant with the Actinomycin-D results, quantitative real-time PCR (qRT-PCR) demonstrated that Lin28a mRNA levels were also not significantly

altered in a two-hour timecourse following BDNF stimulation without transcription inhibition (Fig. 2.1b). These results indicated that post-transcriptional mechanisms likely mediate rapid upregulation of Lin28a protein. The untranslated regions (UTRs) of mRNAs can regulate mRNA stability, localization, and translation efficiency. To examine a potential role for the Lin28a mRNA UTRs in conferring rapid Lin28a induction by BDNF, we next compared the induction of endogenous Lin28a to that of a FLAG-tagged Lin28a (FL-Lin28a) construct lacking the Lin28a UTRs. Rapid induction kinetics of endogenous Lin28a and FL-Lin28a were indistinguishable in a timecourse from 5 to 60 minutes following neuronal BDNF stimulation (Fig. 2.1c).

Most vertebrates possess two Lin28 paralogs, Lin28a and Lin28b, both of which can reduce mature Let-7 miRNA levels by inhibiting distinct steps in Let-7 miRNA biogenesis (Piskounova et al., 2011) to influence mRNA translation. In contrast to Lin28a, protein levels of endogenous Lin28b or a FLAG-tagged Lin28b (FL-Lin28b) lacking the Lin28b UTRs did not undergo BDNF-dependent induction over a similar time course (Fig. 2.1d and Fig. 2.2b). Though both Lin28a and Lin28b can shuttle between nucleus and cytoplasm, Lin28a is localized predominantly to the cytoplasm, whereas Lin28b is believed to be primarily nuclear. We tested the possibility that nuclear localization of Lin28b prevents its induction by BDNF, using a Lin28b construct in which mutation of both nuclear localization sequences (FL-Lin28b Δ NLS; gift of R.Gregory) results in a predominantly cytoplasmic localization (Piskounova et al., 2011). No BDNF-

responsive induction was observed in protein levels of FL-Lin28b Δ NLS in hippocampal neurons (Fig. 2.1d and Fig. 2.2b).

The lack of a requirement for the Lin28a UTRs in BDNF-dependent induction suggested direct regulation at the level of the Lin28a protein. To test this, we examined the effects of BDNF on Lin28a protein stability by radiolabel (^{35}S]Cys/Met) pulse chase analysis. Hippocampal neurons were incubated with BDNF only during the chase period in order to exclude effects on radiolabel incorporation due to altered translation. The median half-life of mammalian proteins has been estimated to be forty-six hours (Schwanhausser et al., 2011). We observed that Lin28a protein undergoes fast turnover under basal conditions, with levels of Lin28a signal reduced to $48.2\% \pm 7.6\%$ in 30 minutes. In contrast, no significant loss of Lin28a was observed over 3 hours in the presence of BDNF (Fig. 2.1e). BDNF, and excitatory neuronal activity, is generally reported to increase ubiquitin/proteasome-mediated turnover of cellular proteins ((Bingol and Schuman, 2006; Ehlers, 2003; Jia et al., 2008; Lin et al., 2011), but see (Santos et al., 2015)). However, taken together, these results indicate that rapid induction of Lin28a protein levels by BDNF is due to enhanced Lin28a protein stability.

MAPK-mediated TRBP phosphorylation promotes induction of Lin28a, but not Lin28b

We noted that the timecourse of Lin28a protein induction paralleled our previous observations of rapid BDNF-induced activation of extracellular signal-

regulated protein kinase (Erk) and phosphorylation of TRBP (Huang et al., 2012), which is a cofactor and binding partner of the miRNA-processing enzyme, Dicer. TRBP is reported to stabilize Dicer protein through co-association, and Erk-dependent phosphorylation of TRBP can induce both TRBP and Dicer protein levels ((Chendrimada et al., 2005; Haase et al., 2005; Melo et al., 2009; Paroo et al., 2009), but see (Kim et al., 2014)). To examine whether Erk activity also participates in rapid induction of Lin28a protein, we tested the effects of the MEK/Erk inhibitor, U0126, on BDNF-dependent induction of Lin28a in neurons. Interestingly, Erk inhibition eliminated Lin28a induction by BDNF and also caused a modest reduction in basal Lin28a protein levels (Fig. 2.3a), consistent with known low-level basal BDNF signaling in neurons (Jia et al., 2008; McAllister et al., 1997). As anticipated, U0126 also prevented BDNF-dependent elevation of TRBP and Dicer protein levels (Fig. 2.3a). These results suggested that TRBP phosphorylation might underlie a requirement for Erk activity in post-translational Lin28a induction by BDNF. To directly test a requirement for TRBP in Lin28a induction, we used lentiviral-mediated knockdown (KD) of TRBP in hippocampal neurons, which prevented BDNF-mediated induction of both Lin28a and Dicer proteins (Fig. 2.3b). TRBP-deficiency also produced a modest but significant reduction in the low basal levels of Lin28a (Fig. 2.3b). In contrast, Dicer KD did not alter basal Lin28a protein levels in hippocampal neurons (Fig. 2.4a). We conclude that both MEK/Erk activity and TRBP are required for BDNF-mediated Lin28a induction.

We next investigated the mechanism by which TRBP might upregulate Lin28a protein, and the role of TRBP phosphorylation in this process. Mass spectrometry analysis has shown TRBP phosphorylation at four serine residues (142,152,283,286)(Paroo et al., 2009), two of which are potential consensus Erk phosphorylation sites. Expression of either wildtype (TRBPWT) or phospho-mimic (TRBPS Δ D), but not phospho-mutant TRBP (TRBPS Δ A) (gift of Z.Paroo (Paroo et al., 2009)), in HEK293T cells was capable of significantly elevating levels of Lin28a protein expressed from a construct lacking the Lin28a UTRs (FL-Lin28a), showing that these effects require only the Lin28a protein coding region (Fig. 2.3c). In contrast, levels of Lin28b protein were not altered by expression of TRBP constructs, even when Lin28b was localized to the cytoplasm through mutation of its nuclear-localization sequences (FL-Lin28b Δ NLS)(Fig. 2.3c). A dose-titration of the TRBP constructs revealed that, at equivalent protein levels, phospho-mimic TRBP consistently produced significantly greater elevation of Lin28a protein than either wildtype or phospho-mutant TRBP (Fig. 2.3d).

If BDNF signaled through phosphorylation of TRBP to rapidly induce Lin28a, we anticipated that phospho-mimic TRBP expression might similarly induce Lin28a, while phospho-mutant TRBP might inhibit induction. To test this prediction, we compared elevation of Lin28a by BDNF in neurons subjected to lentiviral-mediated expression of equivalent levels of wild-type, phospho-mimic and phospho-mutant TRBP, under control of a neuron-specific synapsin promoter. In neurons expressing wildtype TRBP, BDNF was still able to upregulate Lin28a protein levels; however, phospho-mimic TRBP expression

elevated basal Lin28a levels and occluded further induction by BDNF (Fig. 2.3e and Fig. 2.4b). BDNF-dependent induction of Lin28a could still be observed in neurons expressing phospho-mutant TRBP in the presence of endogenous TRBP (non-target shRNA), but this was eliminated by concomitant KD of endogenous TRBP (TRBPshRNA)(Fig. 2.3e and Fig. 2.4c,d). We conclude that TRBP deficient in serine sites for Erk phosphorylation does not support BDNF-induced of Lin28a. Neuronal expression of phospho-mimic TRBP also mimicked a downstream effect of elevated Lin28a, by lowering levels of Lin28-targeted miRNAs (e.g. Let-7 family members)(Fig. 2.3f) and occluding further reduction by BDNF. These results indicate that TRBP phosphorylation is necessary and sufficient to functionally upregulate Lin28a, and they link BDNF-induced TRBP phosphorylation to rapid post-transcriptional changes in the Let-7 family miRNAs that govern synthesis of many pro-growth proteins. BDNF also enhances Dicer levels through phosphorylation and stabilization of TRBP (Huang et al., 2012), leading to increased biogenesis of many miRNAs not targeted by Lin28. As expected, a Dicer-dependent but non-Lin28 targeted control miRNA (miR-132) underwent BDNF-mediated induction that was mimicked and occluded by neuronal expression of phospho-mimic TRBP (Fig. 2.3f).

TRBP phosphorylation reduces its polyubiquitination

Our results implicated Erk-mediated TRBP phosphorylation and the concomitant increase in total TRBP protein as a critical signaling event producing rapid Lin28a induction (Fig. 2.3a-e). Previous reports using cell lines indicated that

phosphorylation might enhance TRBP stability (Paroo et al., 2009), and that TRBP was subject to cell-density dependent turnover by the 26S proteasome during a prolonged 15 hour timecourse (Lee et al., 2006). To examine the possibility that BDNF-induced TRBP phosphorylation might alter its proteasomal regulation, we first evaluated whether TRBP was subject to rapid proteasome-dependent turnover in primary cells. Brief inhibition of 26S proteasomal activity (MG132, 60 min) in hippocampal neurons resulted in the accumulation of high molecular weight forms of TRBP, which suggested basal ubiquitin-mediated turnover (Fig. 2.5a). To investigate regulation of TRBP stability by phosphorylation, we next evaluated wildtype, phospho-mimic, and phospho-mutant forms of TRBP for K48-linked ubiquitination, which is associated with proteasomal degradation. Stringent IP of FL-TRBP, FL-TRBPS Δ D, or FL-TRBPS Δ A from HEK293T cells co-expressing an HA-tagged ubiquitin mutant exclusive for K48-linkages (HA-K48-Ubiquitin, other lysines mutated to arginines)(Lim et al., 2005) showed a ladder of anti-HA immunoreactivity associated with wildtype and phospho-mutant TRBP, consistent with polyubiquitination. Quantification normalized to the amount of IPd TRBP construct showed that K48-linked ubiquitin association with phospho-mutant TRBP was significantly elevated relative to wildtype TRBP. In contrast, K48-linked ubiquitin laddering associated with phospho-mimic TRBP was reduced by nearly 5 fold relative to phospho-mutant TRBP and was also significantly reduced relative to wildtype TRBP (Fig. 2.5b). Stringency of the IP was validated by demonstrating loss of TRBP association with a Dicer-containing complex under

these high salt and detergent IP conditions (Fig. 2.5b). These results are consistent with phosphorylation of TRBP regulating the process of TRBP ubiquitination and proteasomal degradation. To understand how this regulation might occur, we considered the known binding interactions of TRBP.

The third double-stranded RNA binding domain of TRBP does not bind RNA but is instead thought to mediate protein-protein interactions with binding partners such as Dicer (Haase et al., 2005) and a tumor-suppressor protein, Merlin (Lee et al., 2004). Merlin binding to TRBP facilitates ubiquitination and proteasomal degradation of TRBP (Lee et al., 2006). We hypothesized that Merlin might exert its anti-proliferative effect by controlling protein levels of TRBP and, consequently, levels of Lin28a. Accordingly, we asked whether Merlin played a role in BDNF-mediated regulation of TRBP phosphorylation and abundance. While treatment of neurons with BDNF did not alter the total levels of Merlin protein (Fig. 2.6a), pull-down assays showed that HA-tagged Merlin (Zhao et al., 2007) expressed in HEK293T cells exhibited a co-association with wildtype TRBP (FL-TRBP) that was robustly enhanced with phospho-mutant TRBP and greatly reduced with phospho-mimic TRBP (Fig. 2.5c). This result suggests that phosphorylation of TRBP might inhibit TRBP binding to Merlin, a mechanism that could underlie the reduced ubiquitination and enhanced stability of phosphorylated TRBP and, in turn, mediate enhanced stability of Lin28a.

TRBP is a binding partner of Lin28a

While precise roles of TRBP in RNA processing are incompletely delineated, TRBP has been shown to regulate the biogenesis of miRNAs and to assist in generating the small RNA-induced silencing complex (RISC) by stabilizing associations with Dicer-containing complexes (Chendrimada et al., 2005; Daniels et al., 2009; Fukunaga et al., 2012; Paroo et al., 2009; Wilson et al., 2015). To further elucidate the role of TRBP, and in particular phospho-TRBP, in Lin28a induction, we asked whether TRBP might also stabilize Lin28a through direct co-association using recombinant TRBP and Lin28a proteins expressed and purified from bacteria. Purified Lin28a protein bound to a pull-down of purified GST-TRBP protein, but not to GST alone (Fig. 2.7a and Fig. 2.8a), demonstrating direct protein-protein interaction between Lin28a and TRBP. Lin28a protein showed significantly increased binding to phospho-mimic TRBP protein (GST-TRBP Δ D) compared to wildtype TRBP protein (Fig. 2.7a). This result is consistent with our intracellular expression titration (Fig. 2.3d), and indicates that TRBP phosphorylation may stabilize Lin28a both through increased stability of TRBP itself, and also by increasing binding affinity for Lin28a. We next tested whether endogenous Lin28 associates with TRBP-containing protein complexes in HEK293T cells, which we found express Lin28a at a molecular weight of ~25kD (Fig. S4b), although a previous study suggested that HEK293T cells may lack Lin28a expression (Heo et al., 2012). Endogenous Lin28a and Dicer both co-immunoprecipitated (co-IPd) with FLAG-tagged TRBP (FL-TRBP) and not with control IgG in HEK293T cells, and the reverse

association of endogenous TRBP and Dicer with IPd FLAG-tagged Lin28 (FL-Lin28a) was also observed (Fig. 2.7b,c). The lysate input control, GAPDH, was not co-IPd. Since TRBP expression did not induce the Lin28a paralog, Lin28b, (Fig. 2.3c), we tested whether this might be due to an inability of Lin28b to associate with complexes containing TRBP and Dicer. IP of FLAG-tagged Lin28b (FL-Lin28b) or cytoplasmic Lin28b (FL-Lin28b Δ NLS) did not demonstrate association with endogenous Dicer or TRBP (Fig. 2.7d,e), and provided additional corroboration of the specificity of the FL-Lin28a IP. Specific co-association of FL-TRBP with myc-tagged Lin28a (myc-Lin28a) and endogenous Dicer, but not with myc-Lin28b Δ NLS, was also observed (Fig. 2.8c). These results highlight a critical node of differential regulation by TRBP between the mammalian Lin28 paralogs.

We next used a sequential co-IP strategy to distinguish whether Lin28a can exist in a single complex with both TRBP and Dicer, or whether the observed co-IP might reflect separate complexes of Lin28a with either TRBP or Dicer. Lysates from HEK293T cells co-expressing myc-TRBP and FL-Lin28a were subjected to initial IP for the myc epitope, followed by elution and secondary IP of eluents for the FLAG epitope (Fig. 2.7f and Fig. 2.8d). Immunoblot of eluents from secondary FLAG IP showed that Lin28a and Dicer were both associated with the TRBP-containing complex, indicating that these components can reside in a single complex (Fig. 2.7f). While previous RISC characterizations show that RNase treatment reduces but does not eliminate TRBP association with Dicer (Daniels et al., 2009; Haase et al., 2005), we observed a striking reduction in the

co-association of cellular Lin28a with TRBP and Dicer by RNaseA (Fig. 2.8e). Intracellular associations between RNA-binding proteins are often enhanced by cooperative complexes with RNA and other proteins, which can facilitate interaction at low intracellular concentrations. The high conservation of RNA-binding domains between Lin28a and Lin28b (Mayr et al., 2012), and the failure of Lin28b to co-associate with TRBP (Fig. 4d,e and Supplementary Fig. 4c), suggests that RNA-binding is not the sole mechanism of intracellular Lin28a and TRBP interaction. Taken together, our results are consistent with direct interactions of TRBP and Lin28a (observed with recombinant, purified proteins in vitro) that are facilitated at intracellular protein concentrations by the presence of RNA.

TRBP phosphorylation downstream of BDNF promotes Lin28a co-association

Our results indicated that expression of phospho-mimic, but not phospho-mutant TRBP, significantly elevated total Lin28a levels (Fig. 2.3c,d), and that Lin28a has increased apparent binding affinity for phospho-TRBP (Fig. 2.7a). Based on these observations, we suspected that phosphorylation of TRBP might convey signal-induced Lin28a regulation, and that intracellular Lin28a might also preferentially co-associate with phospho-mimic TRBP. IP of lysates from HEK293T cells co-expressing myc-Lin28a with FL-tagged wildtype, phospho-mimic, or phospho-mutant TRBP, revealed robust association of Lin28a with phospho-mimic TRBP, which was enhanced relative to wildtype TRBP, and

reduced association of Lin28a with phospho-mutant TRBP (Fig. 2.7g). Overexpression of Lin28a was employed in these experiments to minimize possible artifacts resulting from differential induction of total Lin28a levels amongst the TRBP constructs. FL-TRBP constructs were transfected at levels designed to achieve approximately equal expression, and quantitation of co-associated Lin28a was normalized to IPd FL-TRBP level for each construct.

We next tested whether Lin28a might undergo enhanced association with phosphorylated TRBP as the physiological mechanism for Lin28a induction in neurons responding to BDNF. Depletion IP in neurons with lentiviral-mediated expression of FL-Lin28a under control of the neuron-specific synapsin promoter, revealed that BDNF significantly enhanced the association of FL-Lin28a with endogenous total TRBP, phospho-TRBP, and Dicer, as well as producing the expected elevation in total levels of all three proteins (Fig. 2.7h, depleted lysates Fig. 2.8f). Phospho-TRBP was detected using a phospho-specific TRBP polyclonal antibody we developed against an amino-terminal perfect Erk phosphorylation consensus site located adjacent to a putative Erk docking site in TRBP (Fig. 2.8g); we observe loss of antibody signal in lysates from Erk-inhibited cells (by U0126, Fig. 2.8h) and increased antibody signal in lysates from BDNF-stimulated neurons (Fig. 2.8i). While our data indicate that phospho-TRBP can function as a hub for parallel regulation of both Lin28a and Dicer, Dicer might also be regulated distinctly from Lin28a potentially through additional known Dicer partner proteins (Lee et al., 2013; Pepin et al., 2012; Rybak-Wolf et al., 2014; Wilson et al., 2015). Collectively, these data establish a context in which a

stimulus, BDNF, employs TRBP phosphorylation as a central molecular mechanism coordinating induction of both Lin28a and Dicer, which together produce gene-target specification in protein synthesis (Huang et al., 2012; Ruiz et al., 2014).

Phospho-TRBP requires Lin28a to regulate dendritic spine growth

BDNF-regulated protein synthesis plays a prominent role in enduring neuronal plasticity in part by regulating structural changes involved in synaptic response. Our laboratory has previously demonstrated that BDNF-mediated dendritic outgrowth in immature hippocampal neurons requires inhibition of Let-7 miRNAs through Lin28a induction (Huang et al., 2012). We now also observe that Lin28a overexpression in young (DIV 7) hippocampal neurons mimics increased dendritic arborization following BDNF, and occludes further response to BDNF (Appendix A.1-A.3). Similarly, BDNF regulates synaptic plasticity of terminally-differentiated excitatory neurons in part by promoting the growth of dendritic spines, which are the primary sites of excitatory synaptic contacts (Alonso et al., 2004; Je et al., 2009a, b; Tanaka et al., 2008). We used this informative biological readout to test whether a pro-growth response to BDNF requires phospho-TRBP mediated induction of Lin28a. We initially assessed the effect of phospho-TRBP on dendritic spine growth by comparing the density and volumes of dendritic spines in vehicle- or BDNF-stimulated hippocampal pyramidal neurons (DIV 17 - 19) expressing either phospho-mimic TRBP, or an empty vector control. Hippocampal pyramidal neurons expressing empty vector

exhibited robust BDNF-induced elevations in both dendritic spine density (increased by 140.6%, Fig. 2.9a,b) and dendritic spine head volume (increased by 78.2%, Fig. 2.9c,d), results consistent with previously observed effects of BDNF on the enhancement of excitatory synaptic function (Lauterborn et al., 2007; Tanaka et al., 2008). In contrast, in the absence of BDNF (vehicle condition), neurons expressing phospho-mimic TRBP showed increases in dendritic spine density and spine head volume that mimicked BDNF-mediated elevations and occluded further induction by BDNF (Fig. 2.9a-d).

We hypothesized that phospho-TRBP might support dendritic spine growth by producing a pro-growth program of protein synthesis through elevated Lin28a, which could relieve Let-7 miRNA-mediated repression of pro-growth mRNAs (Huang et al., 2012). Accordingly, we next directly tested the role of Lin28a in the promotion of dendritic spine growth by phospho-mimic TRBP. Knockdown of Lin28a through RNAi, but not expression of a control hairpin (non-target shRNA), prevented the induction of elevated dendritic spine density and spine head volume by phospho-TRBP (Fig. 2.9e-h). The effects of phospho-TRBP on spine density and volume were rescued by expression of an shRNA-resistant Lin28a construct (FL-Lin28a*) in the presence of Lin28a shRNA (Fig. 2.9e-h and Fig. 2.10a), supporting specificity of the requirement for Lin28a. Neurons expressing control non-target shRNA displayed increased dendritic spine growth in response to phospho-TRBP, similarly to wildtype neurons that were not expressing shRNA (Fig. 2.9f and 2.9h, compared to 2.9b and 2.9d). These experiments place Lin28a as an essential downstream mediator of

phospho-TRBP in a physiological growth response, which is consistent with our data showing BDNF-induction of a Lin28a-stabilizing complex through TRBP phosphorylation. We conclude that TRBP phosphorylation, and subsequent Lin28a protein stabilization, displays an essential function in neurotrophin-induced structural plasticity of terminally differentiated neurons.

MAPK-dependent Lin28a induction is a shared feature in trophic responses

Our data collectively implicated Erk-mediated TRBP phosphorylation and the concomitant increase in total TRBP protein as a critical signaling event capable of producing rapid Lin28a induction to generate a pro-growth program. The observation that phospho-TRBP could induce Lin28a protein not only in neurons but also in a HEK293T cell line (Figs. 2c, 2d, and 2e), suggested the possibility for broader use of this regulatory pathway in trophic responses. Since MAPK activation is a common feature of growth factor signaling cascades, we initially investigated whether MAPK pathway activation was sufficient to induce Lin28a. Expression of a constitutively active MEK construct (HA-CAMAPKK) (Mansour et al., 1994) in HEK293T cells induced both TRBP and Lin28a proteins (Fig. 2.11a), consistent with potential for MAPK pathway activation to control TRBP and Lin28a protein regulation more widely. We next tested whether MAPK-mediated TRBP phosphorylation might serve as a gateway to dynamic receptor-mediated regulation of Lin28a in a variety of cell types. Stimulation of primary murine cultures of dorsal root ganglion (DRG) neurons with nerve growth factor (NGF), cortical glia with glial-derived neurotrophic factor (GDNF), and

peritoneal macrophages with mouse macrophage colony stimulating factor (mM-CSF) all resulted in TRBP and Lin28a protein induction (Figs. 2.11b-d and Figs. 2.12a-c). As in hippocampal neurons, Lin28a protein in these primary cells migrates as a predominant band near 37 kD (Fig. 2.12d), as has been previously reported particularly in differentiated cells (Moss and Tang, 2003; Nowak et al., 2014; Seggerson et al., 2002). In each cell type, TRBP and Lin28 induction by growth factor were blocked by treatment with the MEK/Erk inhibitor U0126 (Figs. 2.11b-d and Fig. 2.12a-c). These results are consistent with TRBP phosphorylation, downstream of MAPK activation, serving as a general regulatory hub for Lin28a stabilization and subsequent pro-growth effects. Our findings lead us to propose a model in which BDNF-mediated phosphorylation of TRBP reduces its association with Merlin, leading to decreased proteasomal degradation of TRBP and allowing enhanced levels of a phospho-TRBP and Lin28a protein complex (Fig. 2.13), which can also include Dicer. We conclude that TRBP phosphorylation is a previously unrecognized mechanism for rapid post-translational induction of Lin28a protein and downstream control of miRNA biogenesis, which has biological relevance in acute growth factor-mediated responses.

Discussion

The conserved importance of Lin28 proteins in processes of growth and development has led to their widespread study in diverse organisms. A post-translational control mechanism enabling elevation of Lin28a may not have been

previously recognized because the understanding that Lin28a can undergo rapid stimulus-dependent induction is relatively recent (Huang et al., 2012; Ruiz et al., 2014; Shyh-Chang and Daley, 2013). Genetic studies in *C.elegans*, where Lin28 was first discovered, have reported that Lin28 levels decline during development as a result of miRNA-mediated repression (Morita and Han, 2006; Shyh-Chang and Daley, 2013), and changes in transcription have been associated with altered mammalian Lin28 levels during differentiation and in tumors (Chang et al., 2009; Iliopoulos et al., 2009; Marson et al., 2008; Shyh-Chang and Daley, 2013). In addition to development, Lin28 protein levels are also altered in a variety of biological contexts including oncogenesis, injury, and in cellular reprogramming to generate pluripotent stem cells (Buganim et al., 2012; Ramachandran et al., 2010; Rehfeld et al., 2015; Viswanathan et al., 2009). The potential broader significance of phospho-TRBP as a Lin28a regulatory linchpin in contexts apart from BDNF-dependent signaling is underscored by our finding that upregulation of phospho-ERK and TRBP downstream of diverse growth factor receptors in multiple cell types is also accompanied by Lin28a protein induction.

The vertebrate paralogs Lin28a and Lin28b arose through gene duplication, and their distinct and overlapping roles remain incompletely understood. Lin28a and Lin28b proteins share similar, although not identical, expression patterns and a high degree of sequence identity (66% in mice, 73% in humans)(Balzer et al., 2010). Both Lin28 paralogs can lower mature Let-7 miRNA levels to de-repress growth-related transcripts, but the extent of

redundancy in their net effects on gene expression and biological responses is not yet clear. Our finding of differential stabilization of Lin28a, but not Lin28b, through protein association with phospho-TRBP reveals a mechanistic difference in regulation that may have physiological relevance in growth and cellular self-renewal, and is also intriguing in light of literature reporting discrete oncogenic roles of Lin28a and Lin28b in different tumor settings (Thornton and Gregory, 2012).

Post-transcriptional regulation of gene expression is currently understood to substantially, if not predominantly, control the cellular abundance of proteins, but knowledge of regulatory mechanisms operating at this level to drive growth responses is relatively limited. Here, we define a post-translational MAPK/Erk and TRBP-dependent Lin28a induction mechanism downstream of growth factor signaling that provides dynamic receptor-mediated regulation of Lin28a capable of producing rapid transitions in growth, development and pluripotency. Previous work indicating that mitogenic signaling in tumor cell lines also depends upon TRBP phosphorylation is consistent with this pathway as a determinant of Lin28a function in broader biological contexts (Paroo et al., 2009). Our data also highlight the unexpected co-regulation of core factors in small RNA biogenesis as a molecular event underlying pro-growth protein synthesis. Improved understanding of Lin28 regulatory mechanisms may provide insight to dysregulated growth control by the Lin28/Let-7 pathway and opportunities for therapeutic manipulation in human disease and stem cell biology.

Figures and Legends

Figure 2.1: BDNF post-translationally induces Lin28a protein, but not paralog Lin28b, through protein stabilization

(a) (Top) Quantification and (bottom) representative immunoblot of Lin28a protein levels in lysates from hippocampal neurons subjected to BDNF stimulation with or without transcription blockade (Actinomycin-D) for the indicated times, normalized to GAPDH. (b) Quantification of Lin28a mRNA level by individual TaqMan qRT-PCR reaction normalized to β -tubulin III mRNA in hippocampal neurons subjected to BDNF for the indicated times. (c) (Top) Quantification and (bottom) representative immunoblots of levels of endogenous Lin28a and expressed FL-Lin28a in lysates from hippocampal neurons subjected to BDNF stimulation in the presence of Actinomycin-D for the indicated times, normalized to HSC70. We note that FL-Lin28a migrates as a single band near 25 kD, consistent with the possibility that the higher apparent molecular weight of endogenous Lin28a in neurons results from alternative splicing, posttranscriptional modification, or a combination of the two (Seggerson et al., 2002). (d) Protein levels of endogenous Lin28b and expressed FL-Lin28b or FL-Lin28b Δ NLS, normalized to GAPDH, quantified from immunoblot of lysates from hippocampal neurons subjected to BDNF stimulation in the presence of transcription blockade (Actinomycin-D). (a-d) Data plotted relative to 0 min BDNF (set as 1.0). (e) IPd [³⁵S]Cys/Met-labeled myc-Lin28a protein was assessed following a chase timecourse in the presence of vehicle (growth media) or BDNF (added following removal of [³⁵S]Cys/Met label). (Left) Representative

radiograph. (Right) Quantification of percent remaining ^{35}S -labeled myc-Lin28a protein at specified chase timepoints. N=3-8 independent experiments for all panels. * $p < 0.05$ by t test for all experiments. All error bars represent SEM.

Experiments in 2.1a-c were performed by Claudia Ruiz and were also presented in her thesis.

Figure 2.1

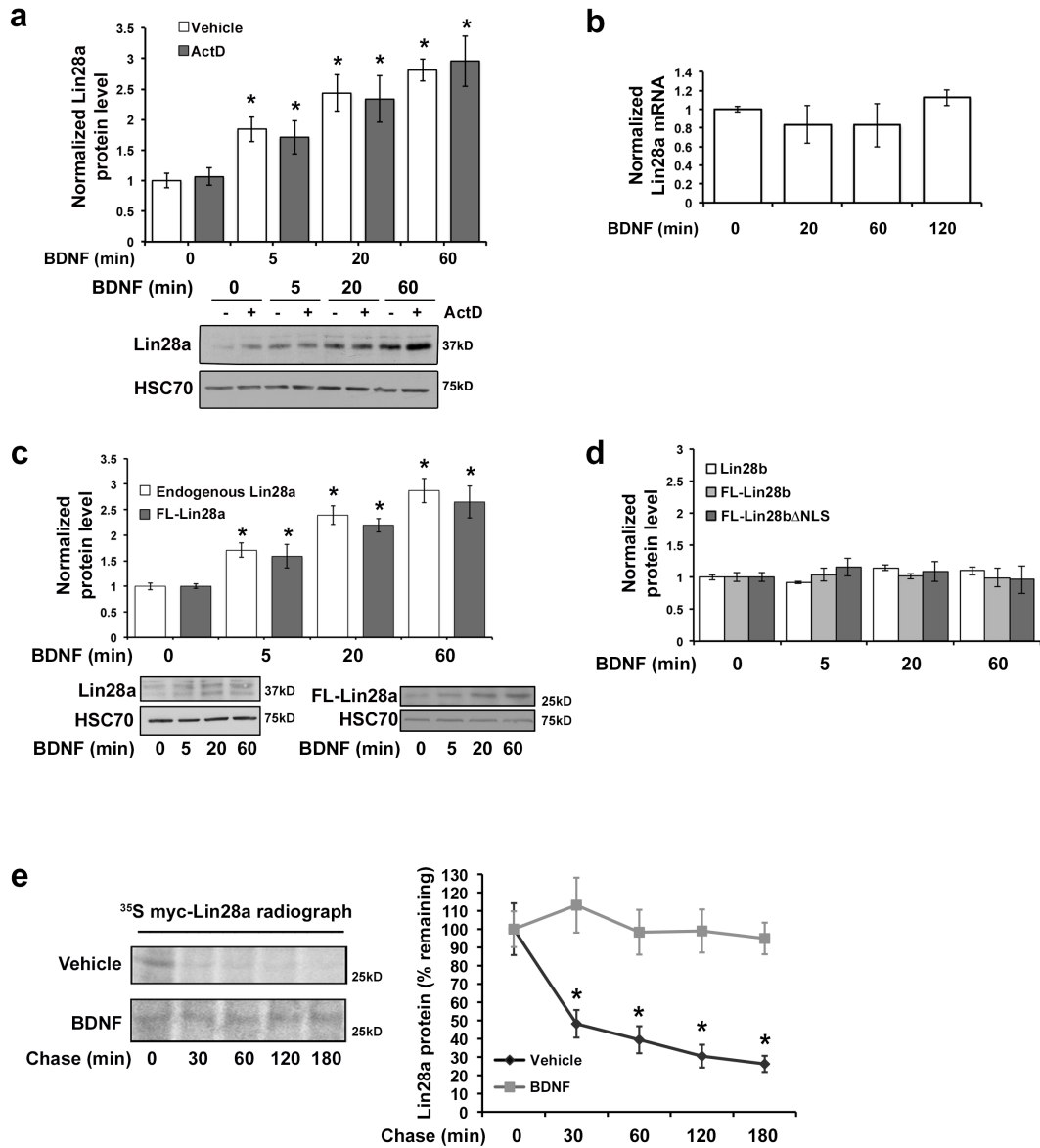


Figure 2.2: Immunoblots for Lin28a and Lin28b proteins

(a) Immunoblots using two antibodies directed towards two different Lin28a epitopes (Cell Signaling A177 and Lifespan LS-C165782 now LS-B11566), and one towards Lin28b, in lysates from hippocampal neurons infected with two different shRNAs targeting Lin28a compared to a non-target shRNA (NTshRNA, control). At the titers tested, Lin28a shRNA #1 reduces Lin28a protein detection by 84% (Cell Signaling) and 62% (Lifespan), but does not alter Lin28b detection. Lin28a shRNA #2 reduces Lin28a protein detection by 88% (Cell Signaling) and 85% (Lifespan), but does not alter Lin28b detection. Endogenous Lin28a protein is detected by immunoblot in differentiated neurons as a predominant singlet or doublet band near 37 kD (Cell Signaling A177 and Lifespan LC-C165782); a band near the predicted molecular weight of Lin28a (25 kD) is also detected by LC-C165782. These Lin28a-immunoreactive bands are each sensitive to Lin28a knockdown, and have been previously observed in differentiated cells (Huang et al., 2012; Moss and Tang, 2003; Nowak et al., 2014; Seggerson et al., 2002). Lin28a protein bands near 37 kD have been previously reported to be reflective of post-translational modification and alternative splicing (Seggerson et al., 2002). (b) Representative immunoblot from Fig. 2.1b of (top left) endogenous Lin28b protein, (top right) FL-Lin28b protein, or (bottom) FL-Lin28b Δ NLS protein in hippocampal neurons undergoing a BDNF timecourse. N=3-4 independent experiments per panel.

Figure 2.2

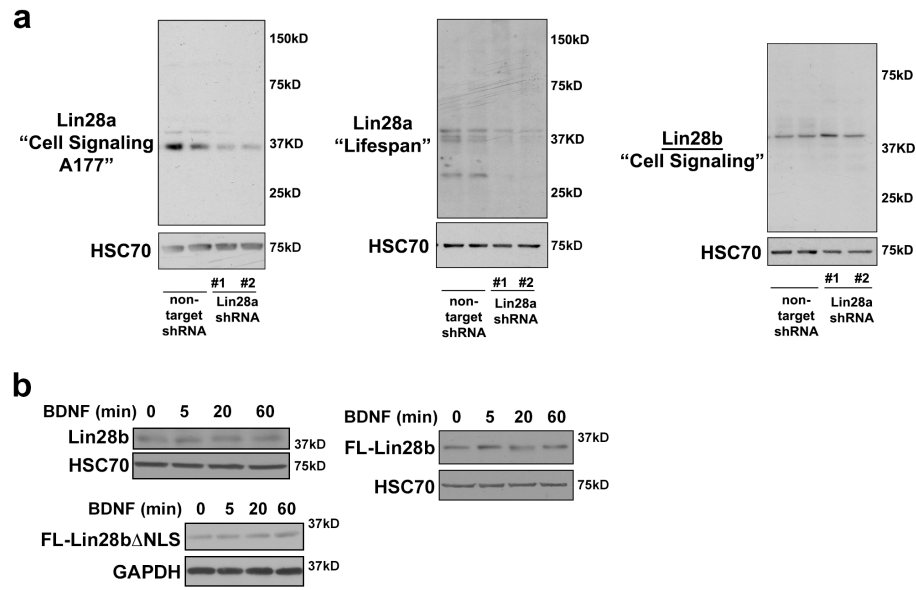


Figure 2.3: TRBP phosphorylation by BDNF regulates Lin28a induction

(a) (Left) Representative immunoblot and (right) Quantified Lin28a protein levels normalized to HSC70 from immunoblot of lysates from hippocampal neurons treated with vehicle (DMSO) or Erk 1/2 inhibitor U0126 for 30 min prior to addition of BDNF. Erk 1/2 inhibition prevents Lin28a induction by BDNF ($^{\#}p < 0.01$, ANOVA) and decreases basal Lin28a protein levels ($*p < 0.05$, *t* test). (b) (Left) Representative immunoblot and (right) quantified Lin28a protein levels, normalized to GAPDH, from immunoblot of lysates from hippocampal neurons treated with non-target shRNA (control) or TRBPshRNA, in the presence or absence of BDNF. Loss of TRBP precludes Lin28a induction by BDNF compared to control condition ($p < 0.01$, ANOVA). TRBP KD also caused a small but significant decrease in basal Lin28a protein levels ($*p < 0.01$, *t* test). (c) (Left) Representative immunoblots and (right) quantification of FL-Lin28 levels in lysates from HEK 293T cells expressing FL-Lin28a, FI-Lin28b, and FL-Lin28b Δ NLS in the presence of FL-TRBPWT, S Δ A, or S Δ D, or PCDNA3.1 (control). Protein levels are normalized to GAPDH; plotted relative to PCDNA3.1 condition (set as 1.0). $*p < 0.05$ by *t* test. (d) Scatter plot shows FL-Lin28a protein levels relative to titrated FL-TRBPWT, S Δ A, or S Δ D constructs, quantified from FLAG immunoblots of HEK 293T cell lysates and normalized to GAPDH. FL-Lin28a protein levels were positively correlated with increasing expression of all TRBP constructs, but phosphorylation status of TRBP had a significant effect ($F(2,17)=47.98$ $p<.0001$, ANCOVA), such that TRBPS Δ D caused the greatest increase in FL-Lin28a ($M=2.65$) compared to TRBPWT ($M=1.73$) and TRBPS Δ A

(M=1.20). **(e)** Hippocampal neurons co-expressing lentiviral FL-Lin28a and either FL-TRBPWT, S Δ D, or shRNA-resistant S Δ A (S Δ A*) were treated with vehicle (growth media) or BDNF (60 min). In the FL-TRBPS Δ A* condition, neurons were treated with either non-target control shRNA (NTshRNA) or shRNA targeting endogenous TRBP (TRBPshRNA). Graph shows quantification of FL-Lin28a protein levels normalized to HSC70, plotted relative to effect of FL-TRBPWT in vehicle condition, set as 1.0 (* $p < 0.05$, ANOVA). Immunoblots available in Figure 2b-c. **(a-e)** N=3-16 independent experiments for each panel. **(f)** Quantification of miRNA levels by individual TaqMan qRT-PCR reactions following 0 min or 60 minute BDNF treatment in neurons expressing control virus or TRBPS Δ D. miRNA levels were normalized to U6 snRNA and plotted relative to each vehicle-stimulated control virus condition, set as 1.0 (* $p < 0.05$, ANOVA). N=7-24 replicates. All error bars represent SEM.

Figure 2.3e was performed by Claudia Ruiz and was also published in her thesis.

Figure 2.3

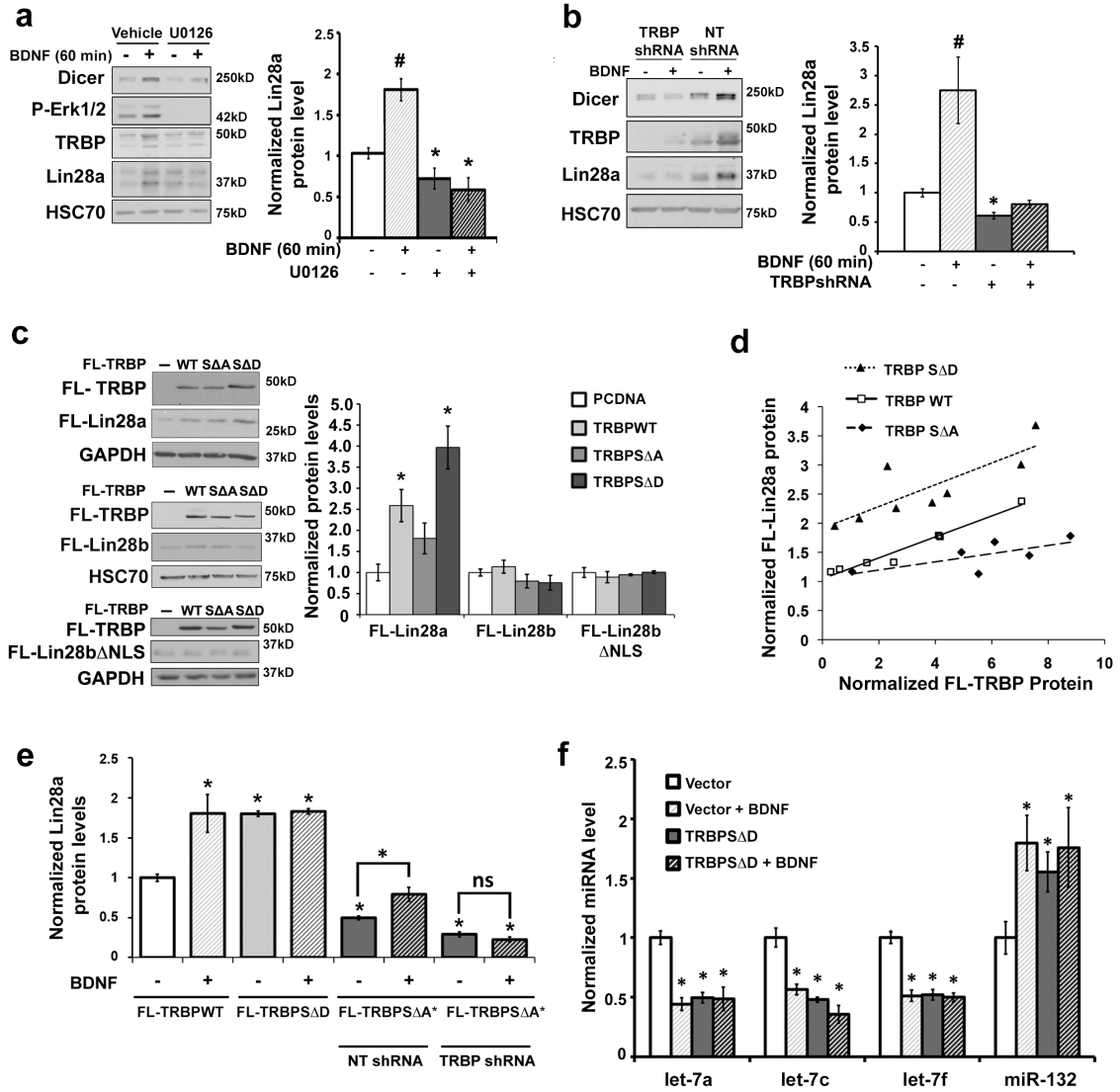


Figure 2.4: Knockdown of TRBP, but not Dicer, reduces Lin28a

(a) (Left) Representative immunoblot and (right) quantification of Dicer and Lin28a protein levels in hippocampal neurons expressing control shRNA (NTshRNA) or shRNA targeting Dicer (Dicer shRNA). (b) Representative immunoblot from Figure 2e showing FL-Lin28a protein levels in hippocampal neurons co-expressing WT or Δ D TRBP, in the presence or absence of BDNF. (c) Representative immunoblot from Figure 2e showing FL-Lin28a protein levels in hippocampal neurons co-expressing shRNA-resistant TRBPS Δ A (FL-TRBPS Δ A*), in the presence or absence of BDNF. Neurons were additionally treated with either non-target control shRNA (NTshRNA) or shRNA targeting endogenous TRBP (TRBPshRNA). Technical replicate samples were run on two separate gels to allow blotting for both FL-tagged and endogenous TRBP. (d) Quantification of Lin28a, TRBP, and FL-TRBPS Δ A* protein levels from lysates from hippocampal neurons under non-target shRNA (NTshRNA, control) or TRBP knockdown (TRBPshRNA) conditions, normalized to loading control (HSC70) and plotted relative to NTshRNA condition, set as 1.0. Error bars represent SEM. * $p < 0.05$ by unpaired Student's t test. N=3-16 independent experiments per panel.

Figure 2.4b was performed by Claudia Ruiz and was also published in her thesis.

Figure 2.4

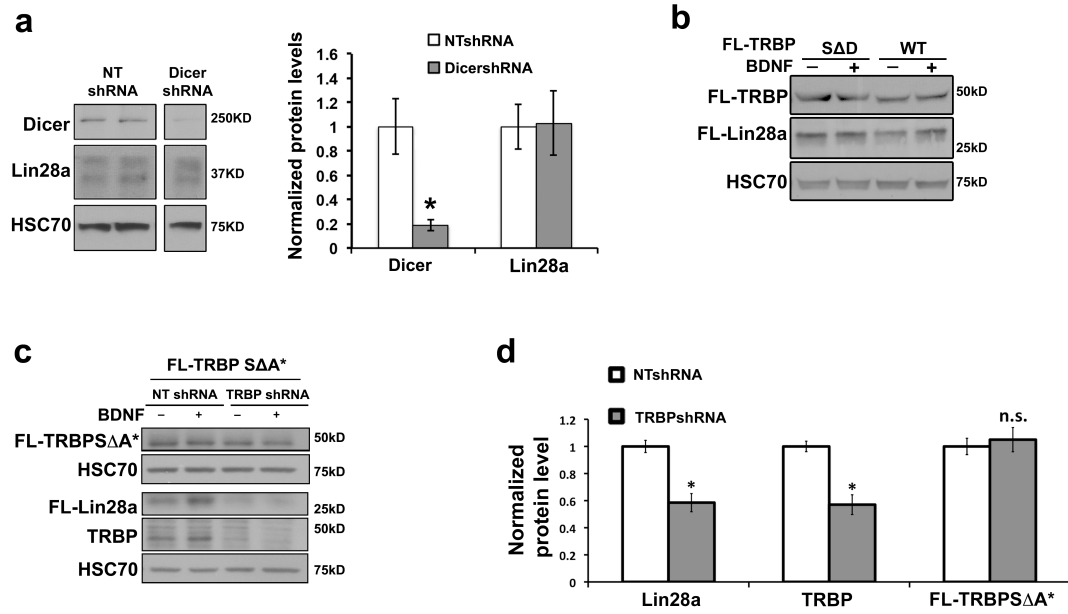


Figure 2.5: TRBP Phosphorylation reduces Merlin binding and TRBP polyubiquitination

(a) (Left) Representative immunoblot and (right) High-molecular weight (HMW) TRBP protein levels, quantified from immunoblot of lysates from hippocampal neurons treated with vehicle (DMSO) or MG132 (60 min); normalized to GAPDH and plotted relative to vehicle alone (set as 1.0). (b-c) Lysates from HEK 293T cells co-expressing FL-TRBPWT, SΔA, SΔD, or PCDNA3.1 alone (control) with either (b) HA-K48 ubiquitin or (c) HA-Merlin were IPd with anti-FLAG antibody, followed by immunoblot with anti-FLAG and anti-HA antibodies. (b and c, left) Representative immunoblots. (b and c, right) Quantification of co-associated (b) HA-K48 ubiquitin and (c) HA-Merlin protein normalized to the amount of IPd FL-TRBP for each construct, and plotted relative to FL-TRBPWT condition (set as 1.0). * $p < 0.05$ by t test for all experiments. All error bars represent SEM. N=3-8 independent experiments for each panel.

Figure 2.5

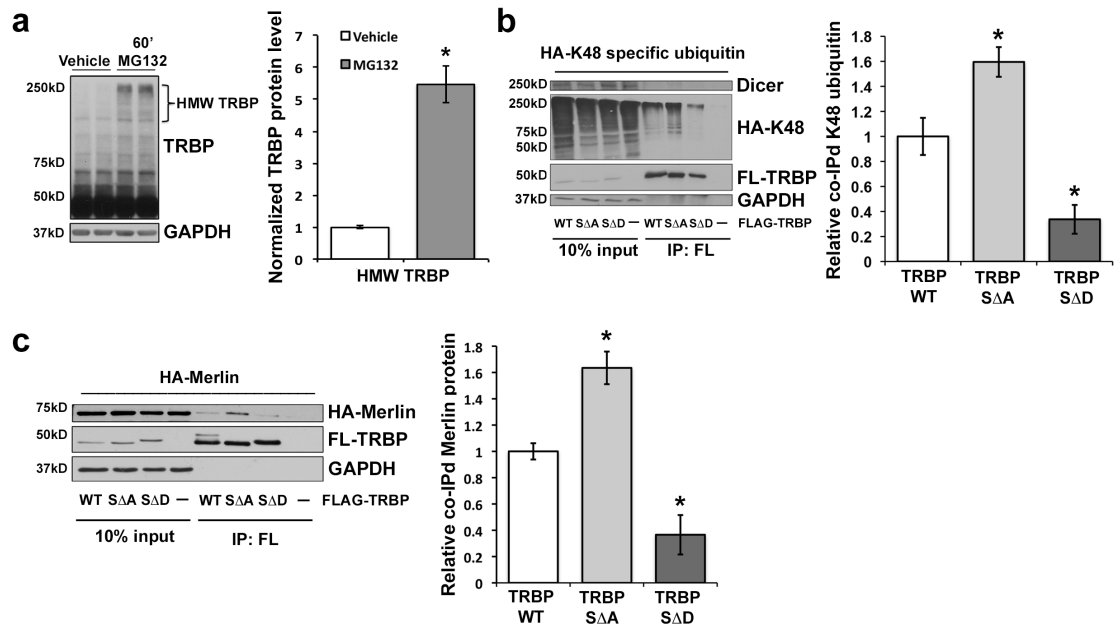


Figure 2.6: BDNF does not regulate Merlin protein levels

(a) Merlin protein levels in lysates from hippocampal neurons treated with vehicle (growth media) or BDNF (60 min). (Left) Representative immunoblot and (right) quantification of Merlin protein, normalized to GAPDH and plotted relative to vehicle (set as 1.0). Error bars represent SEM. N=8 independent experiments per panel.

Figure 2.6

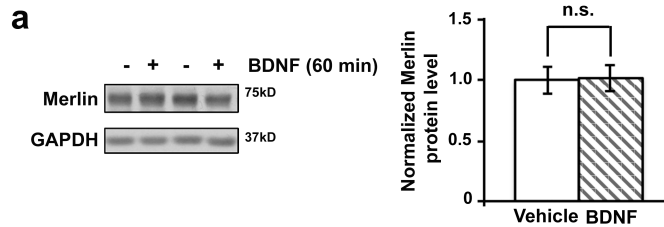


Figure 2.7: TRBP and Lin28a co-association is enhanced by TRBP phosphorylation

(a) (Left) Representative immunoblot and (right) Densitometric quantification of purified Lin28a protein co-associated with purified GST-TRBP, normalized to amount of TRBP pulled-down and plotted relative to GST-TRBPWT (set as 1.0). A lower band in the GST-TRBP conditions that migrates similarly to GST alone is thought to reflect partial cleavage of the GST tag through a protease site between GST and TRBP. Uncropped blots in Fig 2.8a. (b-e) Lysates from HEK 293T cells expressing (b) FL-TRBPWT, (c) FL-Lin28a, (d) FL-Lin28b, and (e) FL-Lin28b Δ NLS were IPd with anti-FLAG or control rabbit (rlgG) or mouse (mlgG) IgG antibodies. Representative immunoblots (b-e) show IPd proteins and co-IPd endogenous proteins. (f) Sequential IP of HEK293T cells lysates, involving initial IP for myc-TRBP followed by subsequent IP for FLAG-Lin28a. Flowchart and experimental details shown in Fig S4. (g) (Left) Representative immunoblot and (right) quantification of lysates from HEK 293T cells co-expressing FL-TRBPWT, S Δ A, S Δ D, or PCDNA3.1 alone (control) and myc-Lin28a, and IPd with anti-FLAG antibody. Myc-Lin28a was overexpressed to avoid differential effects of the FL-TRBP constructs on total Lin28a levels. Co-IPd myc-Lin28a was normalized to IPd FL-TRBP for each construct, and plotted relative to FL-TRBPWT condition (set as 1.0). (h) Lysates from hippocampal neurons expressing FL-Lin28a and treated with either vehicle (growth media) or BDNF (90 min) were IPd with anti-FLAG or control mlgG antibody. (Left) Representative immunoblot. (Right) Quantification of co-IPd TRBP and Dicer proteins plotted relative to vehicle

alone, set as 1.0. * $p < 0.05$ by t test for all experiments. All error bars represent SEM. N=3-5 independent experiments for each panel.

Figure 2.7

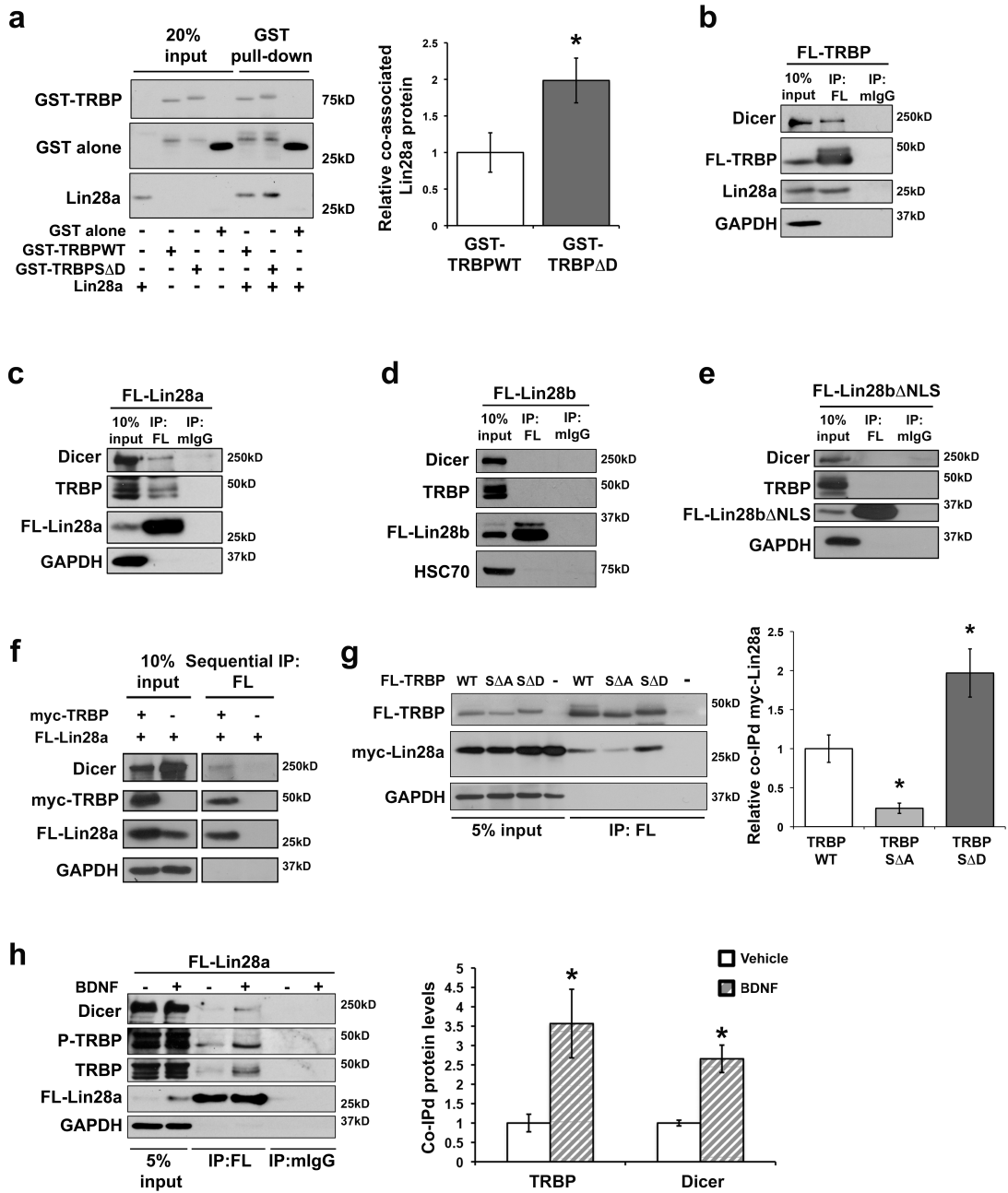


Figure 2.8: BDNF-induced TRBP phosphorylation regulates binding to Lin28a, but not Lin28b

(a) Uncropped blots of (left) purified GST-TRBP and GST alone (control) pull-downs and (right) co-associated Lin28a from Fig. 2.5a. (b) Lin28a immunoblot using antibody from Novus (NBP-149537) to detect Lin28a protein in lysates from HEK 293T cells infected with two different shRNAs targeting Lin28a compared to a non-target shRNA (NTshRNA, control). Lin28a shRNA #3 reduces Lin28a protein detection by 86%. Lin28a shRNA #2 reduces Lin28a protein detection by 76%. (c) Representative immunoblot of lysates from HEK 293T cells co-expressing FL-TRBPWT and either myc-Lin28a or myc-Lin28b Δ NLS. Lysates were IPd with anti-FLAG antibody, followed by immunoblot with anti-FLAG, anti-myc, and anti-Dicer antibodies. (d) Sequential IP flowchart. HEK293T cells were transfected with either FL-Lin28a and myc-TRBP constructs together (left side), or FL-Lin28a alone as a control (right side). Input samples from both transfection conditions were saved for immunoblot (indicated by side arrows). Each transfection condition underwent sequential IP (indicated by straight arrows). Initial myc IP was followed by elution with a myc peptide competitive inhibitor and subsequent FLAG IP. Final eluents were boiled at 95^o C and subjected to immunoblot along with input samples. (e) Lysates from HEK293T cells expressing FL-Lin28a were treated with or without RNaseA and IPd with anti-FLAG or control mouse IgG (mIgG) antibody. (Left) Representative immunoblot. (Right) Densitometric quantification of co-IPd proteins normalized to input and plotted relative to no RNase condition (set as 1.0). (f) Depletion of lentiviral FL-

Lin28a following neuronal IP was verified by running cleared lysate samples taken from the remaining neuronal cell lysate after tumbling with FLAG antibody-bound G-sepharose beads. FL-Lin28a signal is detectable in input samples prior to FLAG IP, but not in cleared lysate samples. **(g)** Mass spectrometry has demonstrated TRBP phosphorylation at serine residues 142, 152, 283, and 286. An antibody was developed in our lab towards phosphorylation at S152 (red), a perfect Erk phosphorylation consensus site. **(h)** Assay of phospho-TRBP antibody reactivity with U0126-treated lysates. HEK293T cells were incubated with either vehicle (DMSO) or MAPK inhibitor U0126 for 48 hours, followed by immunoblot with anti-phospho-TRBP antibody. **(i)** Immunoblot of TRBP and phospho-TRBP protein levels in lysates from hippocampal neurons treated with vehicle (growth media) or BDNF (60 min). Error bars represent SEM. * $p < 0.05$ by unpaired Student's *t* test. N=3-6 independent experiments per panel.

Figure 2.8

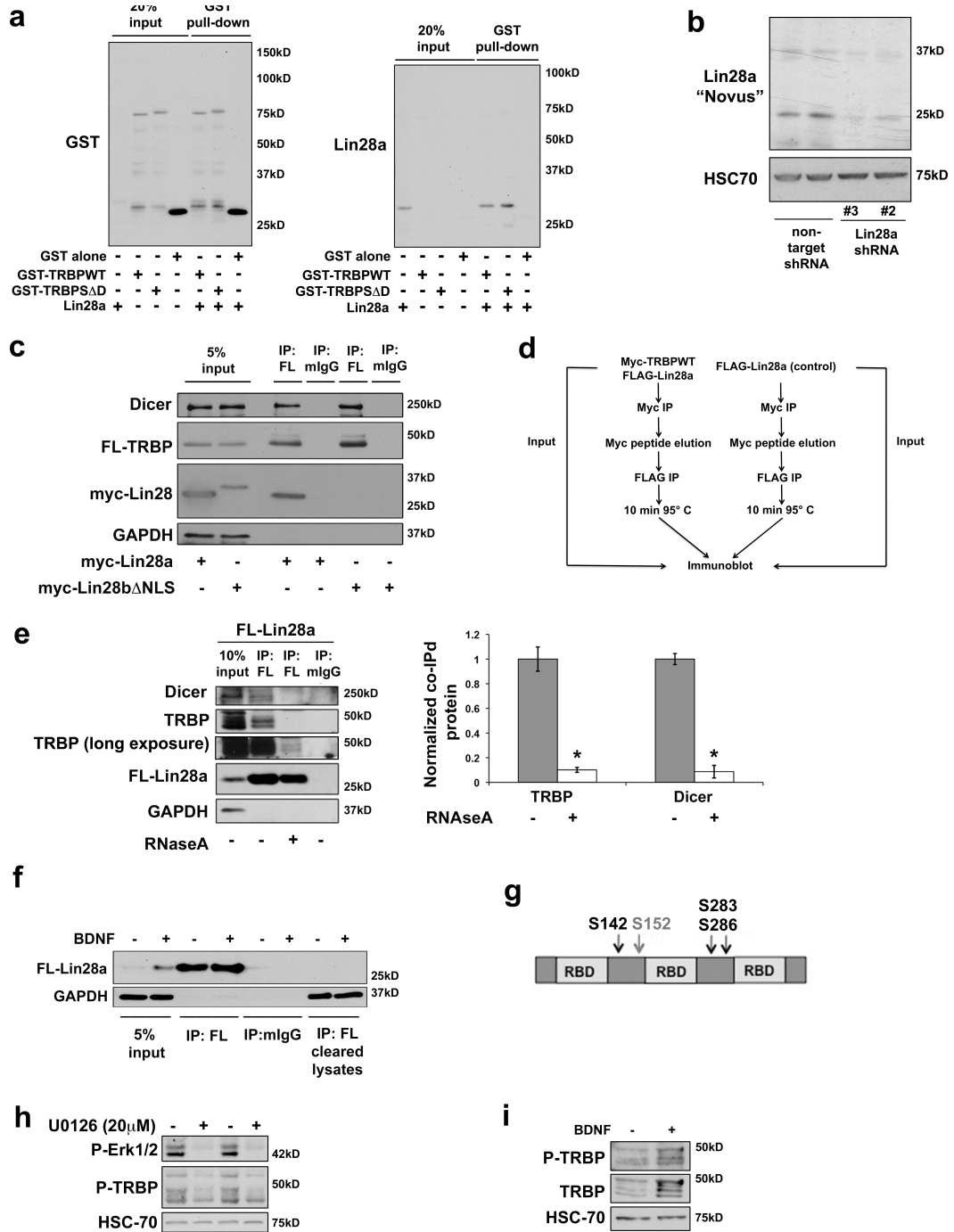
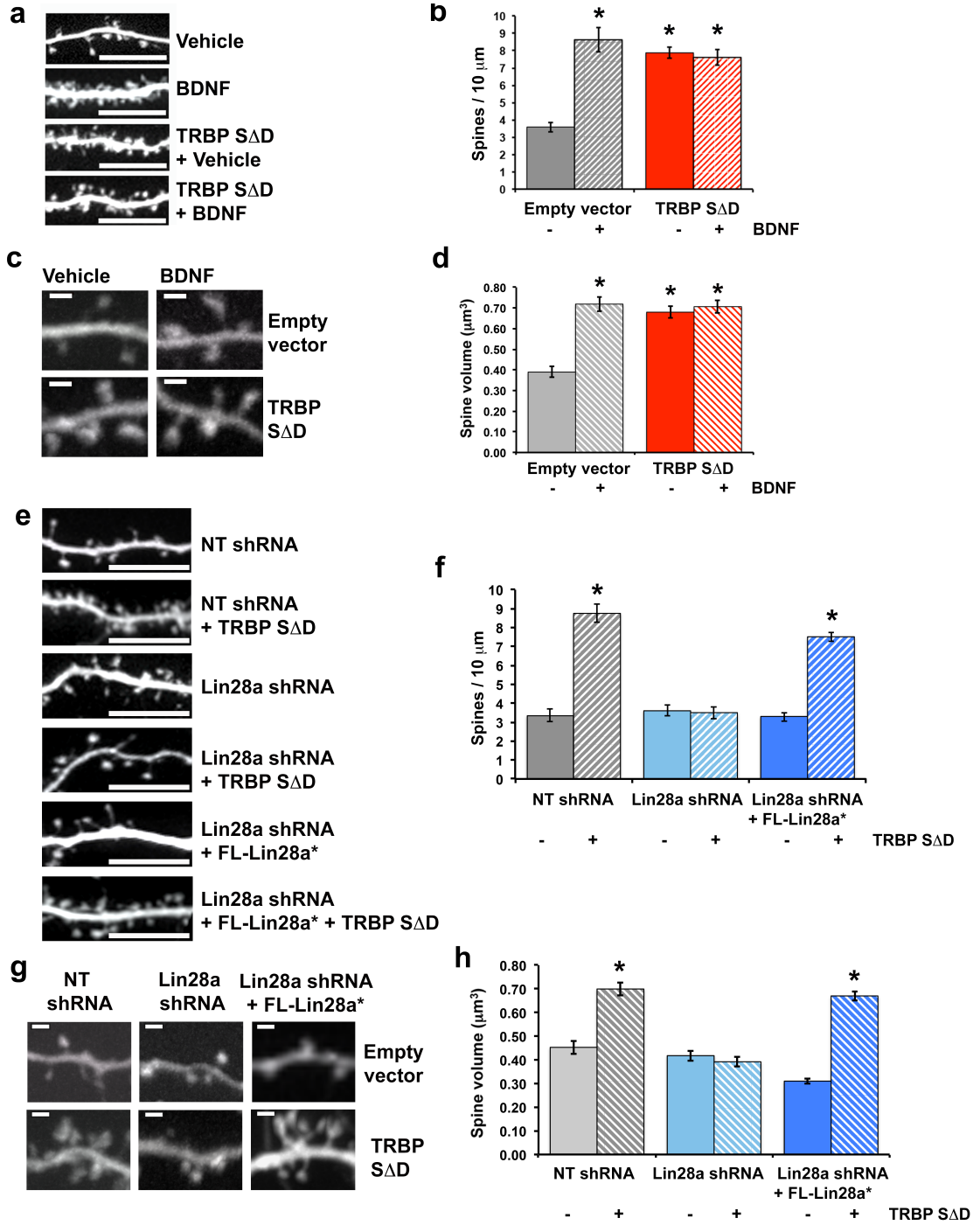


Figure 2.9: TRBP phosphorylation downstream of BDNF regulates neuronal dendritic spine growth through Lin28a

(a-d) Hippocampal neurons transfected with either empty vector or TRBPSΔD were treated with vehicle (growth media) or BDNF (12hr). (e-h) Hippocampal neurons were transfected with either empty vector (control) or TRBPSΔD in the context of expression of either non-target control shRNA (NT shRNA), Lin28a shRNA, or Lin28a shRNA plus an shRNA-resistant FL-Lin28a construct (FL-Lin28a*). (a and e) Representative confocal projections of hippocampal pyramidal dendrites. Scale bar, 10 μm. (b and f) Quantification of dendritic spine density. (c and g) Representative confocal images of hippocampal dendritic spines. Scale bar, 1.0 μm. (d and h) Quantification of average dendritic spine volume. * $p < 0.001$, t test. N=10-18 dendritic segments and 4-11 independent neurons for each panel. All error bars represent SEM.

Experiments in 2.9a-d were performed by Claudia Ruiz. Experiments in 2.9e-h were performed by Claudia Ruiz and Daniel Pham, and will also be published in Daniel Pham's thesis.

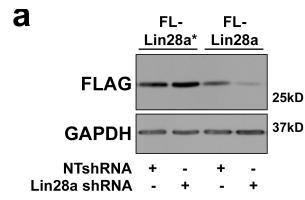
Figure 2.9



2.10: Validation of shRNA-resistant Lin28a construct

(a) Representative immunoblot of HEK293T cells co-transfected with either FL-Lin28a or shRNA-resistant Lin28a (FL-Lin28a*), alongside either non-target shRNA (NTshRNA, control) or Lin28a shRNA#1. N=4 independent experiments.

Figure 2.10



2.11: MAPK pathway activation by diverse growth factors induces TRBP and Lin28a proteins in multiple cell types

(a) (Left) Representative immunoblot and (right) quantification of immunoblots from HEK 293T cell lysates transfected with empty vector (control) or constitutively active MEK (HA-CAMAPKK), normalized to HSC70 and plotted relative to empty vector (set as 1.0). **(b)** Dorsal root ganglion neurons (DRGs), **(c)** cortical glia, and **(d)** peritoneal macrophages were stimulated with **(b)** Nerve growth factor (NGF), **(c)** Glial-derived neurotrophic factor (GDNF), or **(d)** macrophage colony stimulated factor (mM-CSF) for 90 min following a 30 min pretreatment with either DMSO (control) or pharmacological Erk inhibitor U0126. **(b-d)** (Left) Representative immunoblots. (Right) Densitometric quantification of immunoblots from cell lysates, normalized to **(b-c)** HSC70 or **(d)** β -Actin and plotted relative to no growth factor following DMSO (set as 1.0). **(b-d)** Uncropped immunoblots of Lin28a protein shown in Fig. 2.12a-c. All error bars represent SEM. * $p < 0.05$ by t test for all experiments. N=3-10 independent experiments for each panel.

Figure 2.11a was performed by Megha Subramanian and will also be published in her thesis.

Figure 2.11

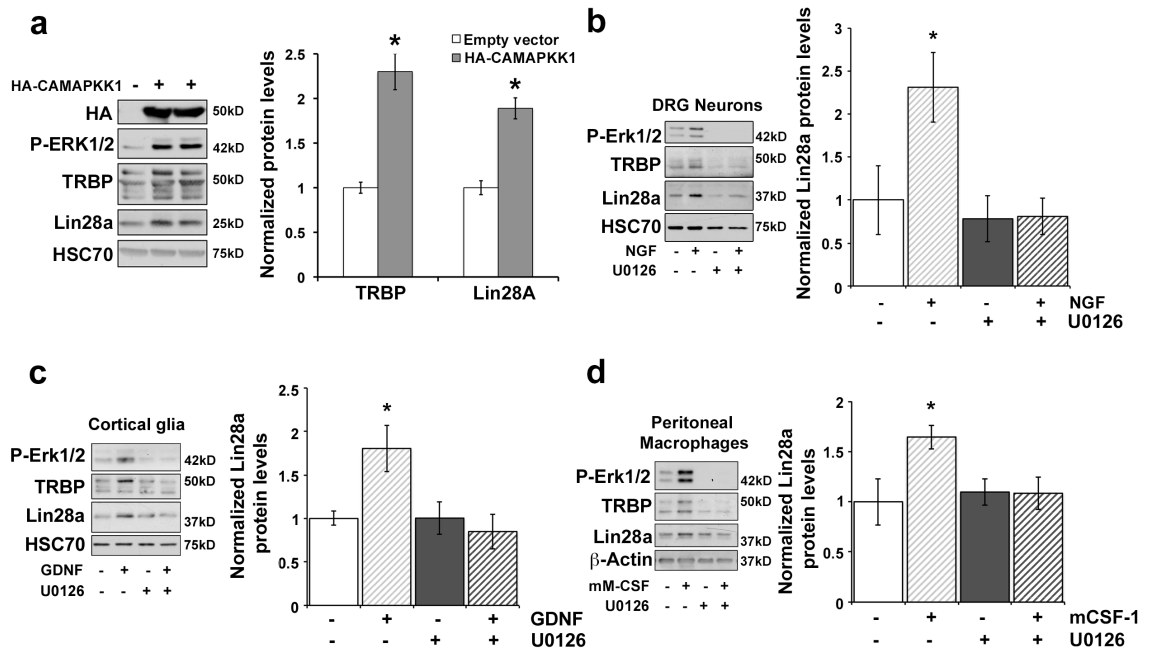


Figure 2.12: Lin28a immunoblotting in primary cell types

(a-c) Uncropped immunoblots from Fig. 2.11 of Lin28a protein using Lin28a Novus antibody in lysates from (a) DRG neurons (Fig. 2.11b), (b) glial cells (Fig. 2.11c), and (c) macrophages (Fig. 2.11d). Cells were treated with vehicle (growth media) or (a) NGF, (b) GDNF, or (c) mM-CSF following a 30 min pretreatment with either DMSO or pharmacological Erk inhibitor, U0126. (d) Lin28a immunoblot using Novus antibody (NBP-149537) to detect Lin28a protein in lysates from neurons infected with two different shRNAs targeting Lin28a compared to a non-target shRNA (NTshRNA, control). Lin28a shRNA #1 reduces Lin28a protein detection by 86%. Lin28a shRNA #2 reduces Lin28a protein detection by 75%.

Figure 2.12

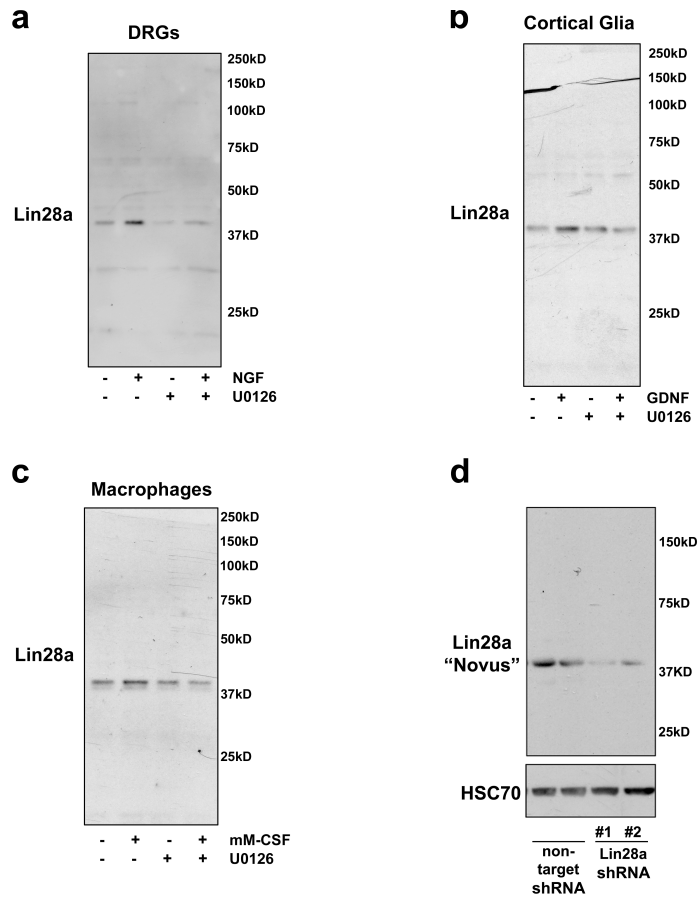
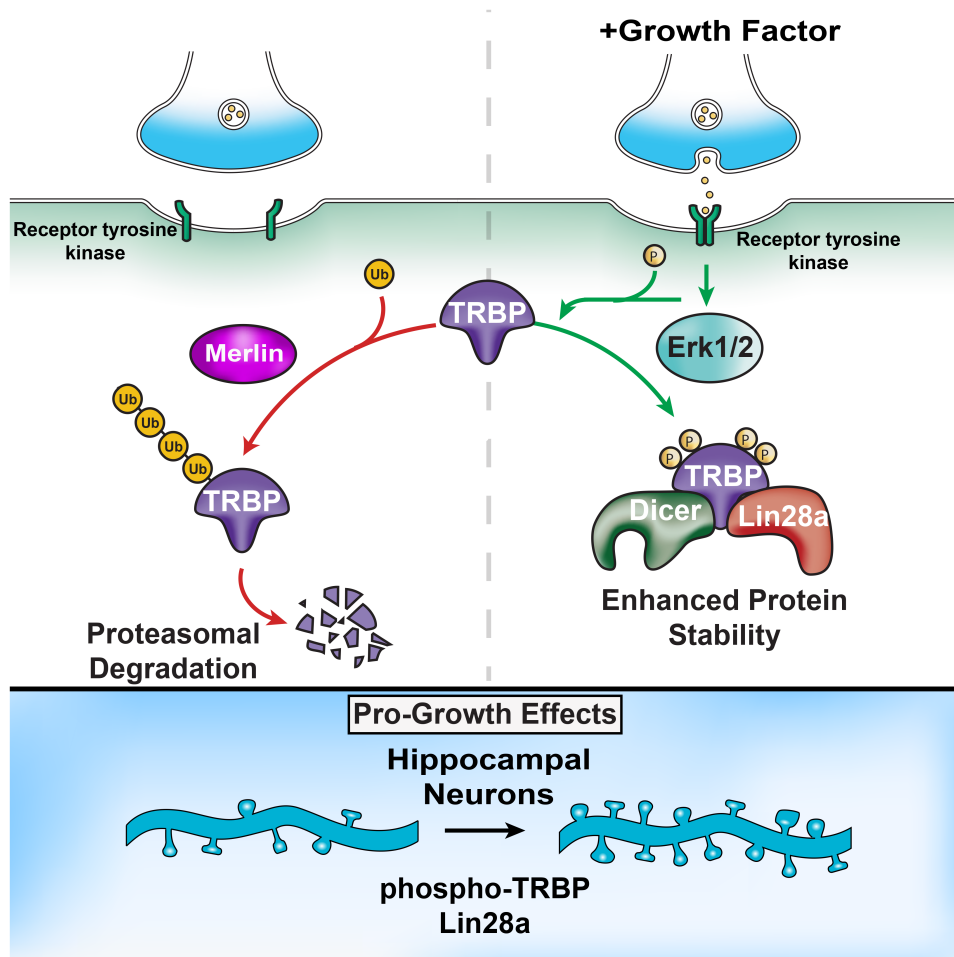


Figure 2.13: Model - Growth factor-mediated TRBP phosphorylation rapidly stabilizes Lin28a protein

Graphical model. Left panel: At baseline, TRBP undergoes polyubiquitination and degradation facilitated by Merlin protein. Lin28a protein levels are negligible as it undergoes rapid turnover. Right panel: Growth factor binding to Trk receptors leads to activation of Erk1/2 signaling and subsequent TRBP phosphorylation, which stabilizes TRBP and enhances the TRBP/Lin28a protein complex, elevating Lin28a protein levels. Downstream inhibition of Let-7 miRNAs facilitates protein synthesis of pro-growth mRNAs. Bottom panel: TRBP phosphorylation exerts Lin28a-dependent pro-growth effects on spine dynamics.

Figure 2.13



Methods

Primary cell culture and stimulation

Animal procedures conformed to care guidelines approved by the Institutional Animal Care and Use Committee.

Stimulation: BDNF (Santa Cruz, SC-4554), NGF (Millipore, #01-125), and GDNF (Sigma, SRP3200) were applied to a final concentration of 100 ng/ml; mM-CSF (Cell Signaling, #5228) to a final concentration of 50ng/ml; U0126 (Cell Signaling, 99035) to a final concentration of 30 μ M (hippocampal neurons) or 10 μ M (DRGs, glia, and macrophages); MG132 (Sigma C2211) to a final concentration of 10 mM.

Hippocampal neurons: Dissociated hippocampal cultures were prepared from postnatal day 0 (P0) mice as previously described (Meffert et al., 2003), and were maintained in Neurobasal A medium (Gibco, 10888) with B27 Supplement (Gibco 17504-44) and glutamine. On DIV 14-19, hippocampal cultures were changed into Serum Reduced Media (NBA + 0.5% B27 + glutamine) for 2 hours prior to stimulation, followed by preincubation with Actinomycin-D (Life Technologies, A7592) at a final concentration of 0.5 mg/ml for 10min if required.

Dorsal Root Ganglion: Acutely dissociated DRG neurons from 4-week old mice were cultured as previously described (Li et al., 2014). After trituration and centrifugation, cells were resuspended in DH10, plated in 24-well plates with poly-L-lysine, and cultured at 37°C for 24 hours with nerve growth factor (25 ng/ml) and glial cell-derived neurotrophic factor (50 ng/ml). After 24 hours, cells were changed into DMEM + 10% FBS + 1% glutamine. 48 hours after plating

(DIV 2), cells were changed into serum starvation media (1% FBS) for 2 hours prior to stimulation.

Cortical glia: Dissociated cortical cultures were prepared from postnatal day 0 (P0) mice as previously described (Meffert et al., 2003), plated onto 10cm tissue culture dishes, and maintained in DMEM + 10% FBS + 1% glutamine. Dishes were rinsed 24 hours after plating and passaged 48 hours after plating. Surviving cells are a mixed glial population. Cells were used within 4 passages and were changed into serum starvation media (1% FBS) for 2 hours prior to stimulation.

Peritoneal Macrophages: Mice (12-20 weeks old) were euthanized and peritoneal cells were harvested in RPMI media with 10% FBS as previously described (Link et al., 2010). Cells were plated on 24-well plates and rinsed 1 hour later with fresh media. Adherent cells are >99% macrophages. 24 hours after plating (DIV 1), cells were changed into serum starvation media (1% FBS) for 2 hours prior to stimulation.

Plasmids

The following plasmids were obtained as generous gifts: Wildtype (WT) TRBP, phospho-mutant (S Δ A) TRBP, and phospho-mimic (S Δ D) TRBP (from Dr. Zain Paroo); Flag-Lin28a (from Dr. Yinqun Huang); HA-Ubiquitin K48 (from Dr. Ted Dawson); FL-Lin28b Δ NLS mutant (from Dr. Richard Gregory); HA-CAMAPKK (pMCL-HA-MAPKK1-R4F[(Δ 31-51)S218E/S222D] from Dr. Natalie Ahn, Addgene plasmid # 40810) (Mansour et al., 1994); HA-Merlin (from Dr. Kunliang Guan, Addgene plasmid # 32836) (Zhao et al., 2007). GST-TRBPWT and GST-

TRBPS Δ D were subcloned using the pGEX-6P-1 vector. MBP-Lin28a was subcloned using the pMAL-c5X vector. Myc-Lin28a was subcloned using myc-pcDNA3.1. FL-Lin28a, FL-Lin28b, FL-Lin28b Δ NLS, FL-TRBPWT, FL-TRBPS Δ A, and FL-TRBPS Δ D were all subcloned into the synapsin promoter driven lentiviral vector FSW. Quikchange site-directed mutagenesis of a single base pair was used to generate a silent mutation for shRNA-resistant TRBPS Δ A (FL-TRBPS Δ A*). Sequence for FSW-TRBPS Δ A* following quikchange: GGCAATGAGGTGGAGCCCGATGATGACCACTTC. The shRNA-resistant Lin28a construct (FL-Lin28a*) was generated by introducing three silent mutations into the cDNA sequence that is targeted by Lin28a shRNA. Mutagenesis was performed using the Quikchange method. The sequence for FL-Lin28a* following quikchange was CTGCCACCCCAGCCCAAAAAATGICACTTCTGC CAGAGC.

Transduction

Lentiviral-mediated delivery of FL-Lin28a, Myc-Lin28a, FL-Lin28b, FL-Lin28b Δ NLS, FL-TRBPWT, FL-TRBPS Δ D, FL-TRBPS Δ A, or FL-TRBPS Δ A* was used to achieve expression of tagged proteins in hippocampal cultures for biochemical analysis at a multiplicity of infection (MOI) of 5-10, 2 - 4.5 days before harvest, depending on required expression level. Lentiviral stocks were prepared and lentiviral knockdown carried out as previously described (Huang et al., 2012; Meffert et al., 2003). Knockdown for biochemical analysis used lentiviral-mediated delivery of non-target shRNA (Sigma, SHC002), shRNA

targeting TRBP (Thermo Scientific TRCN0000102563), or shRNA targeting Lin28a (Thermo Scientific TRCN0000102576 (Lin28a shRNA#1) and TRCN0000102577 (Lin28a shRNA#2)) to infect hippocampal cultures at an MOI of 5–10, 4-5 days before harvest. 24 hours prior to imaging experiments, neurons were transiently transfected with PCDNA3.1 or TRBPS Δ D, non-target shRNA or Lin28a shRNA#1, and PCDNA3.1 or FL-Lin28a* using Lipofectamine 2000 according to the manufacturer's instructions (Invitrogen). HEK 293T cells were infected with lentivirus expressing non-target shRNA, Lin28a shRNA#2, or Lin28a shRNA#3 (TRCN0000021802) 96 hours prior to harvest for biochemical analysis of knockdown. Expression of all tagged constructs in HEK 293T cells was achieved by calcium phosphate transfection.

Immunoblotting

Primary cultures of mouse hippocampal neurons, DRG neurons, cortical glia, peritoneal macrophages, or cultured HEK293T cells were washed 2 times in cold PBS with MgCl₂ (0.9 mM) and harvested on ice with lysis buffer (50 mM Hepes, 150 mM NaCl, 10% Glycerol, 1 mM EDTA, 1% Triton-X-100, 0.2% SDS) plus freshly added protease inhibitor cocktail (Roche), phosphatase inhibitors (sodium orthovanadate 0.2 mM, sodium pyrophosphate 1 mM), and NEM (50 mM; Sigma 04260). Lysates were rotated for 10 min at 4°C, then centrifuged at 12,000 x g for 15 min. Protein concentration in supernatant was determined by Bicinchoninic acid (BCA) assay and equal protein amounts resolved on SDS-PAGE gels and electrotransferred to PVDF membrane. Membrane was blocked with 5% BSA in

Tris-buffered saline tween 20 (TBST 0.1%) for 2-4 hours and probed with primary antibodies: Lin28a (Cell Signaling A177, Lifespan LS-C165782, or Novus NBP-149537), FLAG (M2 Sigma F3165 or Sigma F7425), HA (Invitrogen 71-5500), GAPDH (Millipore 6C5), TRBP (Abcam ab72110 or Pierce LF-MA0209), Dicer (Sigma SAB4200087 or Santa Cruz sc-30226), Lin28b (Cell Signaling 5422), c-Myc (Sigma M4439 or Sigma C3956), HSC70 (Santa Cruz sc-7298), NF2/Merlin (abcam ab88957), β -Actin (Cell Signaling 4967).

Purification and pull-down of recombinant bacterial proteins

GST-TRBPWT, GST-TRBPS Δ D, and GST alone in the PGEX-6P-1 vector were expressed in BL21 bacteria (Agilent Technologies, #230132) and purified as described in Pedersen et al, 2015(Pedersen et al., 2015). Bacteria were grown in LB-amp until OD₆₀₀=0.75 after which 1mM IPTG was applied for 3 hrs at 30°C to induce protein expression. Cultures were centrifuged at 4,000 x g for 20 min at 4°C and lysed in phosphate-buffered saline (PBS) pH=7.8 with lysozyme (0.5mg/ml) for 30 min, followed by sonication 5 times with 20-s pulses at 20% amplitude. 1% Triton-X was added, and lysates were centrifuged at 4000 x g for 30 min at 4°C. RnaseA was added to lysates to a final concentration of 20 μ g/ml. Lysates were applied to 500 μ l bed volume of glutathione sepharose beads (GE Healthcare, #17-5132-01) and rotated at 4°C overnight. Beads were then added to a poly-prep column and washed, and GST-fusion proteins were eluted with glutathione elution buffer (50mM Tris HCL, pH=7.5, 10mM glutathione). MBP-Lin28a in the pMAL-c5X vector was expressed in BL21 bacteria and purified as

described, but rotated with amylose resin (NEB, #E80215). Lin28a was cleaved from the amylose-bound MBP tag with factor Xa protease (NEB, #P8010).

Purified protein concentrations were determined by Bradford Protein Assay, and equivalent amounts of GST-TRBPWT, GST-TRBPS Δ D, and GST alone were re-bound to glutathione sepharose beads by rotation at 4°C for 2 hours. Equal amounts of purified Lin28a protein were added to each sepharose-bound GST construct and rotated at 4°C for 2 hours. Beads were washed in cold PBS, pH=7.8, followed by boiling in sample buffer at 95°C for 10 minutes to elute. Eluents were subjected to SDS-PAGE electrophoresis and immunoblotting.

Immunopurification

The following antibody and peptide reagents were used for immunopurification (IP): FLAG (M2 Sigma F3165 or Sigma F7425), 3X FLAG peptide (Sigma F4799), 1X FLAG peptide (Sigma F3290), c-Myc (Sigma M4439), c-Myc peptide (Sigma M2435), Control Mouse IgG (Santa Cruz sc-2025), Control Rabbit IgG (Santa Cruz sc-2027).

Co-Immunoprecipitation:

coIP lysis buffer: 100 mM KCl, 4 mM MgCl₂, 10 mM HEPES (pH 7.3), 50 μ M ZnCl₂, 0.5% NP-40, protease inhibitor cocktail (Roche), phosphatase inhibitor (sodium orthovanadate 0.2 mM, sodium pyrophosphate 1 mM), 50 mM NEM.

coIP wash buffer: 150 mM NaCl, 1 mM MgCl₂, 50 mM HEPES (pH=7.8), 50 μ M ZnCl₂, 0.05% NP-40: protease inhibitor cocktail (Roche), phosphatase inhibitor (sodium orthovanadate 0.2 mM, sodium pyrophosphate 1 mM), 50 mM NEM.

Binding partners of TRBP and Lin28a proteins were isolated through IP of FL-TRBP or FL-Lin28a. Protein G-sepharose beads were coated with anti-FLAG antibody or control isotype-specific antibody in coIP wash buffer overnight after blocking with coIP wash buffer plus 5% BSA for 1 hour. Antibody amount was estimated as 1 μ g antibody per 100 μ g protein lysate in order to deplete the IPd protein. HEK293T cells: 1-2 days prior to transfection, cells were plated into either 24 well plates or 10cm dishes. Cells were transfected with appropriate constructs at ~70% confluency for 48 hours. Media was changed 8 hours post-transfection. Primary hippocampal cultures: Neurons (DIV 12-13) were infected with lentivirus expressing FL-Lin28a under the synapsin promoter for 86 hours. Cultures were then incubated in serum-reduced medium (0.5% B27 supplement) for 2 hours, followed by bath application of vehicle (neuronal growth media) or BDNF (100 ng/ml) for 60-90 min. All cell types: Cell lysates were harvested in coIP lysis buffer with freshly added 1mM DTT and RNAsin (Promega, 0.5 units/ml). Lysates were centrifuged (13,000xg, 15 min) and the supernatants pre-cleared by 30-min incubation with recombinant protein G-sepharose beads pre-washed in coIP wash buffer. Input samples (5-10% of IPd protein) were saved for immunoblot analysis. For IP, equal amounts of lysate protein (0.5 – 2mg, determined by Bradford protein assay) were incubated with antibody-coated beads and tumbled for 3-4 hours at 4°C, followed by 3 washes in coIP wash buffer and 1 wash in coIP wash buffer without protease and phosphatase inhibitors. Elutions from the washed beads were performed using a FLAG

peptide competitive inhibitor (Sigma, F4799 or F3290) diluted in coIP wash buffer without protease and phosphatase inhibitors, and samples were subjected to SDS-PAGE electrophoresis and immunoblotting.

Sequential IP:

HEK293T cells were transfected with either myc-TRBPWT and FL-Lin28a or FL-Lin28a alone (control) for 48 hours. Protein G-sepharose beads were bound to anti-FLAG or anti-c-Myc antibodies, and cells from both conditions were lysed and subjected to IP as previously described in “Co-Immunoprecipitation” using anti-c-Myc conjugated G-sepharose beads. Elutions from the washed beads were performed using a myc peptide competitive inhibitor (Sigma M2435). Eluents then underwent a second IP using anti-FLAG conjugated beads. Following the second IP, washed beads were incubated in sample buffer at 95°C for 10 min, eluents resolved by SDS-PAGE electrophoresis, and immunoblotted.

Co-Immunoprecipitation with RNase:

HEK293T cells were transfected with FL-Lin28a for 48 hours, then lysed and subjected to IP as described in “Co-Immunoprecipitation”. During the IP tumbling step, lysates were incubated with either RNasin (Promega, 0.5 units/ml) to maximize RNA stability, or RNaseA (200 µg/ml) to inhibit RNA.

FL-TRBP limiting immunoprecipitation:

Protein G-sepharose beads were coated with anti-FLAG antibody in intentionally limiting amounts, estimated at about 1 µg antibody per 400 µg protein lysate. Cells were then lysed and subjected to IP as previously described in “Co-Immunoprecipitation”. Limiting antibody allowed for equal pull-down of each FL-

TRBP mutant construct - which express at highly different levels - in order to allow visual appreciation and more accurate quantification of TRBP-associated proteins.

Stringent immunoprecipitation (for ubiquitination assessment):

Stringent lysis buffer: 100mM KCl, 10 mM HEPES (pH=7.3), 4 mM MgCl₂, 50 μM ZnCl₂, 1% Triton-X, 0.25% SDS, 50 μM PR-619, protease inhibitor cocktail (Roche), phosphatase inhibitor (sodium orthovanadate 0.2 mM, sodium pyrophosphate 1 mM), 50 mM NEM.

Stringent wash buffer: 1M NaCl, 1 mM MgCl₂, 50 mM HEPES (pH=7.8), 50 μM ZnCl₂, 20% Glycerol, 1% NP40, 0.1% SDS, protease inhibitor cocktail (Roche), phosphatase inhibitor (sodium orthovanadate 0.2mM, sodium pyrophosphate 1mM), 50 mM NEM.

FLAG antibody coating of protein G-sepharose beads was carried out as previously described in “Co-Immunoprecipitation”. HEK293T cells were transfected with HA-K48 specific ubiquitin and either PCDNA3.1, FL-TRBPWT, FL-TRBPΔA, or FL-TRBPΔD constructs. Cells underwent bath application of the deubiquitinase inhibitor PR-619 (10μM; LifeSensors SI9619) for 1 hour prior to harvest. Cell lysates were harvested in stringent IP lysis buffer with freshly added 1mM DTT, and underwent centrifugation, pre-clearing, and BCA. Equal amounts of protein (1.5-2mg) were incubated with antibody-coated beads and tumbled for 4 hours at 4°C, followed by washing with stringent wash buffer. The washed

beads were incubated in sample buffer at 95°C for 10 minutes and subjected to SDS-PAGE electrophoresis and immunoblotting.

³⁵S pulse chase

Cultured hippocampal neurons were infected at DIV 12-14 with lentiviral myc-Lin28a for 72 hours. Following viral-mediated expression, neurons were pre-incubated in media containing reduced serum as previously described, followed by 2 washes and 10 min incubation with methionine- and cysteine-free DMEM (Mediatech, Inc.). ³⁵S labeling was performed in the same methionine- and cysteine-free DMEM with the addition of ³⁵S-methionine/cysteine (³⁵S Met/Cys EasyTag Mix, Perkin Elmer) to a final concentration of 100 mCi/ml for 3 hours. Following the 3 hour labeling period, ³⁵S-methionine/cysteine containing media was washed out and replaced with normal serum-reduced media (NBA + 0.5% B27 + glutamine), after which neurons were subjected to either vehicle (neuronal growth media) or BDNF bath application, as previously described, for a designated period lasting 30-180 minutes. Cells were washed and lysed with stringent IP lysis buffer. As described in “Co-Immunoprecipitation” and “Stringent Immunoprecipitation”, Lysates were processed for IP and stringent IP was performed using anti-myc coated protein G-sepharose beads. The washed IP beads were incubated in sample buffer at 95°C for 10 minutes and subjected to SDS-PAGE electrophoresis. Radioactive signal of IPd myc-Lin28a was quantified using a Typhoon phosphoimager (Molecular Devices). Myc-Lin28a protein expression and IP was verified via immunoblot.

Imaging and quantification:

For live cell imaging, confocal images of hippocampal pyramidal neurons (determined by morphology) were acquired using a 40x (whole cell) or a 100x (dendrite) objective on a Yokogawa spinning disk system (Cell Observer, Carl Zeiss) at 37°C. Laser power and exposure time were adjusted to minimize photobleaching and avoid saturation. All experiments were from a minimum of 3 independent cultures, no more than 4 neurons per dish, and no more than 3 dendritic segments per neuron. Z-stacks containing the entire neuron or process of interest were analyzed using Imaris 7.6.5 (Bitplane).

Dendritic spine analysis

Neuronal cultures were randomly assigned to treatment conditions and the experimenter was blinded during data acquisition and analysis. 3D reconstructions of hippocampal neurons were analyzed with Filament Tracer (Imaris 7.6.5 Bitplane, Inc.). Dendritic segments were traced and volume rendered using automatic thresholds and dendritic protrusions 0.4-2.0 μ m in length with or without a spine head were assigned as spines. Tertiary dendritic branch segments were chosen for spine density analysis. For each dendritic segment a manual spine count was conducted in Imaris Surpass mode. Dendritic spine density was calculated by counting the number of spines per 10 microns of dendritic length. The dendrite length was measured using Filament Tracer and each spine was marked using Spots (Imaris 7.6.5 Bitplane, Inc.). Dendritic

protrusion length was measured using Measurement Points. Individual dendritic spine length was manually marked from its point of insertion in the dendritic shaft to the distal tip of the spine. Spine volume was measured by manually tracing 3D images of dendritic spines using Filament Tracer's AutoDepth feature. An accurate 3D model of dendritic spines was generated using the diameter function, which calculates the correct diameter and represents the complete morphology of the selected spine based on the 3-D image. Imaris MeasurementPro provided spine volume measurements.

RNA analysis

Total RNA from primary cultures of mouse hippocampal neurons was isolated in Tri-Reagent (Molecular Research Center, Inc.) according to the manufacturer's protocol. Cultures were homogenized in Tri-Reagent directly. RNA pellets were air-dried and resuspended in nuclease-free water. RNA concentration and quality were assayed by spectrophotometric measurements at optical density (OD) 260/280/230 nm. Reverse transcription of Lin28a mRNA was completed using 2 μ g total RNA with the TaqMan High Capacity RNA to cDNA Kit (Applied Biosystems, 4387406). The following reverse transcription program was used: 1) 37°C incubation for 60 minutes, 2) 95°C inactivation for 5 minutes. Products of RT reaction were then assayed via qPCR using TaqMan mRNA qPCR probes: Lin28a (Applied Biosystems, Mm00524077_m1), β -tubulin 3 (Applied Biosystems, Mm00727586_s1), and GAPDH (Applied Biosystems, Mm99999915_g1). The qPCR program used was the following: 1) 95°C denature

for 15 seconds, 2) 60°C reanneal and extension for 60 seconds, 3) repeat of steps 1 and 2 for 40 cycles. For individual microRNA abundance assays (Applied Biosystems), 20 ng of total isolated RNA was prepared for reverse transcription with stem-looped primers specific for individual mature miRNAs in a final volume of 15 µl according to manufacturer's protocol: 1) 4°C for 5 min, 16°C for 30 min, 2) 42°C for 30 min, 3) 85°C for 5 min, and subjected to TaqMan MicroRNA Assays (Applied Biosystems) for Let-7a (assay ID: 000377), Let-7c (000379), Let-7f (000382), miR-132 (000457). The abundance of U6 snRNA (002282) and sno234 (001234) in each sample was used as an internal control to normalize all miRNA species. RT-qPCR was performed using a Stratagene Mx3000P machine and software. Quantification was carried out using the standard-curve method and no preamplification. RQ was calculated as $2^{-\Delta Ct^{BDNF}} / 2^{-\Delta Ct^{mock}}$ where $\Delta Ct =$ (cycle threshold for miRNA of interest) – (cycle threshold for reference control).

Statistical analysis

Two-tailed unpaired student's *t* tests were used with $\alpha=0.05$. Where specified, statistical analysis included one-way ANOVA for independent samples with a Bonferroni-Holm *post hoc* test, $\alpha=0.05$. Statistical significance between scatterplot conditions was determined using one-way ANCOVA for independent samples.

Chapter 3: Regulation of the Lin28/Let-7 axis in Neurofibromatosis Type 2

Background

Neurofibromatosis is an inherited autosomal dominant disorder affecting growth of nerve tissue that leads to tumorigenesis. The course of the disease is typically characterized by recurring neurofibroma and schwannoma tumors of the nervous system, skin, and internal organs, which are often benign but may become malignant. Neurofibromatosis Type 1 (NF1) is a relatively common disorder, while Neurofibromatosis Type 2 (NF2) is less common - with a prevalence of about 1 in 40,000 - but typically more debilitating (Evans et al., 1992; Spyra et al., 2015). Neurofibromatosis Type 1 and 2 occur as a result of mutations in the *NF1* and *NF2* genes, respectively.

Neurofibromatosis Type 2 is caused by autosomal dominant mutations in the *NF2* gene, located on chromosome 22, which lead to loss of function of NF2 protein (more commonly called Merlin). Mutations are typically splice site mutations, missense mutations, large deletions, or truncating mutations, of which truncating mutations cause the most severe phenotypes (Evans et al., 1998; Rutledge et al., 1996). NF2 patients may inherit a mutated copy of the *NF2* gene, although more than 50% carry *de novo* germline mutations (Evans et al., 1992). Interestingly, it seems that cells harboring one mutated copy of the *NF2* gene acquire postzygotic mutations in the other NF2 allele through unknown mechanisms, in a cell type specific manner, leading to mosaicism (Evans et al.,

1998; Kluwe et al., 2003; Kluwe and Mautner, 1998; Moyhuddin et al., 2003). This causes loss of heterozygosity in specific tissues, and is thought to result in NF2 tumorigenesis. Accordingly, analysis of tumor tissue from patients with NF2 indicates loss of function mutations in both *NF2* genes, whereas other tissues may be heterozygous or genetically normal (Evans et al., 1998; Kluwe et al., 2003; Kluwe and Mautner, 1998; Seizinger et al., 1986; Spyra et al., 2015).

Schwann cells, the predominant glial population of the peripheral nervous system, serve to myelinate peripheral axons, and for unknown reasons are particularly sensitive to acquisition of the second-hit *NF2* mutations that result in loss of heterozygosity and tumor formation. Thus, the hallmark of Neurofibromatosis Type 2 is non-malignant bilateral vestibular schwannoma tumors occurring predominantly on the 8th cranial nerve (Evans et al., 1992; Kluwe et al., 2003; Spyra et al., 2015). However, patients may develop several other tumors types as well, such as cranial and spinal meningiomas, and skin tumors (Evans et al., 1992). Although the majority of schwannoma tumors are non-malignant, their presence and growth commonly cause such debilitating physical issues as deafness, muscle wasting, tinnitus, and imbalance, and in late stages are also associated with seizures, blindness, vertigo, paralysis, and shortened lifespan (Evans et al., 1992; Mautner et al., 1996; Parry et al., 1994; Vakharia et al., 2012). There is a push for therapeutic development, but current treatment options are limited to invasive brain surgery, which not uncommonly must be repeated due to recurrence, and carries with it a high risk of injury or morbidity due to the location of the tumors (Blakeley et al., 2012).

Though mutations in the *NF2* gene/Merlin protein have been characterized in relation to Neurofibromatosis Type 2, they are also observed in a range of other cancer types, including breast cancer, malignant mesothelioma, and glioblastoma (Arakawa et al., 1994; Cheng et al., 1999; Guerrero et al., 2015). However, despite the fact that Merlin protein is a known, potent, tumor-suppressor, its mechanistic role in preventing tumor formation has remained elusive, hindering development of potential pharmacological treatment strategies. As was previously noted in Chapter 2, Merlin protein is thought to mediate polyubiquitination and degradation of TRBP through co-association (Lee et al., 2004; Lee et al., 2006). My work in Chapter 2 indicates that Merlin protein may preferentially cause ubiquitin-mediated turnover of un-phosphorylated TRBP, potentially preventing TRBP phosphorylation and stabilization. Since the absence of Merlin might be expected to cause reduced TRBP polyubiquitination (and, therefore, enhanced levels of TRBP and phospho-TRBP), we considered the scenario that Lin28a protein could be abnormally stabilized and therefore elevated in *NF2* tumors as well. Indeed, a recent study broadly linked Merlin protein function to regulation of tumor-suppressor Let-7 miRNAs (Hikasa et al., 2016). This chapter of my thesis work focuses on elucidating whether loss of normal Merlin protein function in Neurofibromatosis Type 2 may be associated with disrupted baseline control of TRBP and, subsequently, Lin28a protein levels (Fig 3.1). Because Lin28 elevation and Let-7 miRNA inhibition have known roles in oncogenesis (Viswanathan et al., 2009; Wang et al., 2012), we hypothesized

that misregulation of Lin28a could be one explanation for tumor formation in the molecular setting of Neurofibromatosis Type 2.

Results

Loss of Merlin in Neurofibromatosis tumors is associated with elevated phospho-TRBP and Lin28a

To determine whether loss of Merlin protein in Neurofibromatosis Type 2 might result in elevated TRBP and Lin28a proteins, we first were interested in comparing protein levels in lysates harvested from primary NF2 tumors with those from samples not harboring mutations in Merlin. Dr. Alan Belzberg from the Johns Hopkins Neurosurgery Department kindly donated primary human schwannoma tumor tissue from 3 patients with Neurofibromatosis Type 1 (3 samples total) and 6 patients with Neurofibromatosis Type 2 (7 samples total), with the generous consent of the patients. Although Neurofibromatosis Type 2 is specifically associated with mutations in *NF2*/Merlin, both tumor types demonstrated absence of normal Merlin protein compared to untransformed human Schwann cells (Fig. 3.2a,b). While this finding prevented us from using NF1 tumors as a control for loss of Merlin in NF2, it is interesting to consider that tumorigenesis in NF1 may be related to alterations in Merlin protein as well. Using instead normal, untransformed human Schwann cells as a control, lysates from NF2 tumors showed robust elevations in Lin28a concomitant with elevations in TRBP, phospho-TRBP, and Dicer proteins (Fig. 3.2b), providing initial support for our hypothesis that Merlin acts as a tumor suppressor in part through control

of TRBP and Lin28a. NF1 tumors may contain elevated Lin28a, TRBP, and phospho-TRBP compared to normal Schwann cells as well (Fig. 3.2a,b), again raising the possibility that tumorigenesis in NF1 and NF2 could occur through overlapping mechanisms. Interestingly, Dicer protein was lower in NF1 than NF2 tumors (Fig. 3.2a,b), though the significance of this finding requires further investigation.

Immortalized mutant *NF2* cell lines derived from schwannomas of patients with Neurofibromatosis Type 2 are often used for molecular and biochemical studies of tumorigenesis in NF2. One such common example is the HEI193 line (Hung et al., 2002). We used HEI193 cells (obtained from Dr. Lim), which are characterized as homozygous for loss of *NF2* and Merlin protein, compared to normal cultured human Schwann cells. Immunoblots of protein lysates confirmed that Merlin protein is absent in HEI193 cells, and that Lin28a, TRBP, and phospho-TRBP are dramatically elevated (Fig. 3.2c), as we previously observed in human tumor samples. If Lin28a were elevated in HEI193 cells relative to normal Schwann cells, we hypothesized that Let-7 miRNAs might be lower, due to enhanced repression by Lin28a. Quantitative real-time RT-PCR suggests that Let-7a and Let-7g miRNAs are significantly lower in the HEI193 tumor cells compared to untransformed Schwann cells, consistent with our finding of elevated Lin28a (Fig. 3.2d). These data suggest that the HEI193 cell line is likely an acceptable representation of the molecular changes we observed in primary NF2 tumor cells, and further demonstrate misregulation of the Lin28/Let-7 axis following loss of Merlin.

Loss of Merlin protein directly regulates Lin28a through TRBP

Our findings suggested a correlation between loss of Merlin protein and elevations in TRBP and Lin28a in primary tumors, but we were next interested in determining whether loss of Merlin was causative in producing Lin28a elevations. To first examine whether Merlin is capable of directly regulating TRBP and Lin28a proteins (e.g. keeping them at a low, baseline level) in normal Schwann cells, we performed lentiviral shRNA knockdown of Merlin protein in primary cultured human Schwann cells. In response to shRNA-mediated reductions in Merlin protein, we saw significant elevations in TRBP, phospho-TRBP, and Lin28a proteins (Fig 3.3a), consistent with the possibility that Merlin protein controls levels of TRBP and Lin28a. In order to demonstrate directly that loss of Merlin protein leads to TRBP and Lin28a elevations in NF2 tumor cells, we re-introduced Merlin protein into HEI193 cells using lentivirus to generate low-level sustained expression in the majority of cells. We find that re-introduction of Merlin to these cells by exogenous expression (a lentiviral-mediated rescue for 4 days) causes significant reductions in TRBP, phospho-TRBP, and Lin28a proteins, again supporting a model in which loss of Merlin in Neurofibromatosis Type 2 results in induction of TRBP and Lin28a proteins (Fig. 3.3b). Interestingly, while Merlin re-introduction may rescue TRBP expression to lower levels similar to those observed in untransformed Schwann cells, rescue of Lin28a back to basal levels is only partial. This could be due to long-term feedback regulation, whereby elevated Lin28a leads to decreased Let-7 miRNAs, which in turn allows

for increased Lin28a translation. Assaying the effects of longer-term Merlin reintroduction on Let-7 and Lin28a levels could be used to test this possibility.

According to our model, we hypothesize that loss of Merlin protein results in elevated TRBP and Lin28a by reducing TRBP polyubiquitination and thereby increasing TRBP stability, which we observed in Chapter 2 is capable of subsequently stabilizing Lin28a. In order to determine whether TRBP regulates Lin28a in the setting of NF2 tumors, we performed shRNA-mediated knockdown of TRBP protein in HEI193 cells using a lentiviral shRNA construct targeting TRBP. We see that the reduction in TRBP protein levels following TRBP knockdown is associated with significant reductions in Lin28a (Fig. 3.3c), suggesting that TRBP still mediates Lin28a induction even in a chronic context of long-term dysregulation by loss of Merlin.

Lin28a expression controls growth of Neurofibromatosis Type 2 tumor cells

Given that elevated Lin28a in NF2 tumor cells is associated, as expected, with reduced Let-7 miRNAs, we hypothesized that Lin28a overexpression in NF2 tumor cells is causal to their accelerated growth and division. Let-7 miRNAs normally inhibit translation of genes involved in cell cycle exit, as well as invasive oncogenic factors such as Ras and c-myc (He et al., 2010; Reinhart et al., 2000). Thus, reducing Lin28a protein in NF2 tumor cells might be expected to slow their rate of division. To initially test this hypothesis, we treated HEI193 cells with either one of two different shRNAs targeting Lin28a or non-target shRNA

(control) and measured 5-bromo-2'-deoxyuridine (BrdU) incorporation. Because Neurofibromatosis tumor cells are not typically invasive or malignant, measuring tumor growth by rate of cell division is an accepted approach in the field (Agnihotri et al., 2014; Sher et al., 2012). We find that cell division is dramatically reduced in cells treated with Lin28a shRNA compared to cells treated with non-target shRNA (Fig. 3.4a-d). In the absence of Lin28a, there are fewer total cells (measured by DAPI staining)(Fig. 3.4b), compared between dishes in which cells were initially plated at equivalent densities. There are also significantly fewer BrdU-positive nuclei, such that the ratio of BrdU-positive nuclei to total nuclei is significantly reduced in the Lin28a shRNA condition (Fig. 3.4c,d). Reduced Lin28a protein expression in the Lin28a shRNA conditions was confirmed by immunoblot (Fig. 3.4e). These findings suggest that Lin28a protein plays an important role in growth rate of NF2 tumors.

Discussion

Disruption of the Lin28/Let-7 axis has been repeatedly linked to cancer formation and progression through downstream induction of pro-growth oncogenes (He et al., 2010; Viswanathan et al., 2009; Wang et al., 2012). However, neither Lin28a nor the Let-7 miRNAs have been previously studied in direct relation to Neurofibromatosis disorders. Here, following hypotheses based on mechanistic findings of the phospho-TRBP/Lin28a/Let-7 regulation delineated in Chapter 2, we propose that loss of Merlin function in NF2 leads directly to induction of Lin28a, downstream of phospho-TRBP. Given the lack of clarity in

the literature currently regarding the mechanism by which Merlin functions as a tumor suppressor, this model may provide novel insight into control of cellular growth by Merlin through the Lin28/Let-7 axis.

Although Lin28a dysregulation has not before been linked to NF2, a recent paper suggested that Merlin protein may positively regulate processing of Let-7 miRNAs by negatively regulating Lin28b function during contact inhibition in HeLa cells (Hikasa et al., 2016). The authors confirmed this mechanism in a lung cancer cell line with mutant Merlin, though they did not address NF2 (or NF1) tumors. Additionally, the authors did not examine Lin28a levels in their HeLa cell system, so that it remains unclear to what extent the observed changes in HeLa cell Let-7 miRNAs following loss of Merlin are due to regulation of Lin28a compared to Lin28b. Similarly, in our model we cannot currently rule out the possibility that Lin28b plays a role in altering Let-7 miRNAs in NF2 tumor cells as well. Causality is difficult to tease apart, because reduced Let-7 miRNAs, as a result of changes in Lin28a or Lin28b, may subsequently lead to elevated Lin28a and Lin28b translation, due to Let-7 miRNA sites in their 3' UTRs (Rybak et al., 2008). Future experiments could be aimed at examining the effects of knockdown or overexpression of Merlin on Lin28a and Lin28b constructs that express the Lin28 protein coding regions only. Regardless, these findings raise the interesting possibility that mutations in the *NF2* gene could inhibit Let-7 processing through downstream regulation of both Lin28a and Lin28b.

Growth and division of NF2 tumor cells appears to depend on Lin28a expression, suggesting the possibility that uncontrolled cell division in NF2

tumors could be due to a Lin28-mediated decrease in Let-7 miRNAs. Future experiments will test the possibility that expression of a Lin28-resistant Let-7 construct might similarly prevent NF2 tumor cell growth. Further, *in vivo* effects of manipulating the Lin28/Let-7 axis will be investigated by monitoring growth of flank-injected tumor cells in *NU/NU* mice following either shRNA-mediated Lin28a knockdown or Let-7 miRNA overexpression. These studies are of particular interest given the current development of Let-7 miRNA mimics as therapeutics in human cancer (Dai et al., 2015; Kasinski et al., 2015; Liu et al., 2014; Wang et al., 2012). If loss of Merlin leading to cancer growth could be prevented by exogenous upregulation of Let-7 miRNAs, these findings have the potential to lead to the generation of Let-7-related therapies for NF2.

Given that mutations in the *NF2* gene are associated with tumorigenesis broadly, observation of misregulated Lin28a and Let-7 miRNAs in NF2 may also have widespread implications for other tumor disorders. Merlin is mutated in breast cancer, glioblastoma, and meningioma, among others (Arakawa et al., 1994; Cheng et al., 1999; Guerrero et al., 2015), and our studies suggest that normal Merlin protein is lacking from NF1 tumor tissue as well. NF1 results from mutations in chromosome 17 and is theoretically independent from mutations to the *NF2* gene; however, given that NF2 patients exhibit loss of heterozygosity and occasionally acquire mutations in both copies of the gene postzygotically (Evans et al., 1998; Kluwe et al., 2003; Kluwe and Mautner, 1998; Moyhuddin et al., 2003), the location of the *NF2* gene must be particularly susceptible to acquired mutations, which is perhaps further catalyzed in NF1. NF1 has been

more widely studied than NF2, and is an autism spectrum disorder as well as a tumor disorder (Mbarek et al., 1999). It is exciting to consider that possible therapeutics targeting the Lin28/Let-7 axis aimed towards treatment of NF2 could also be applicable for the variety of other conditions resulting from inactivated Merlin.

Figures and Legends

Figure 3.1: Model - Possible induction of TRBP and Lin28a in Neurofibromatosis Type 2

Graphical model. Left panel: In normal cells, Merlin protein catalyzes polyubiquitination and degradation of TRBP, resulting in controlled low basal levels of TRBP, Dicer, and Lin28a. Right panel: In Neurofibromatosis Type 2, loss of Merlin protein function results in elevated TRBP and phospho-TRBP, leading to enhanced binding and stabilization of Dicer and Lin28a and subsequent tumorigenesis.

Figure 3.1

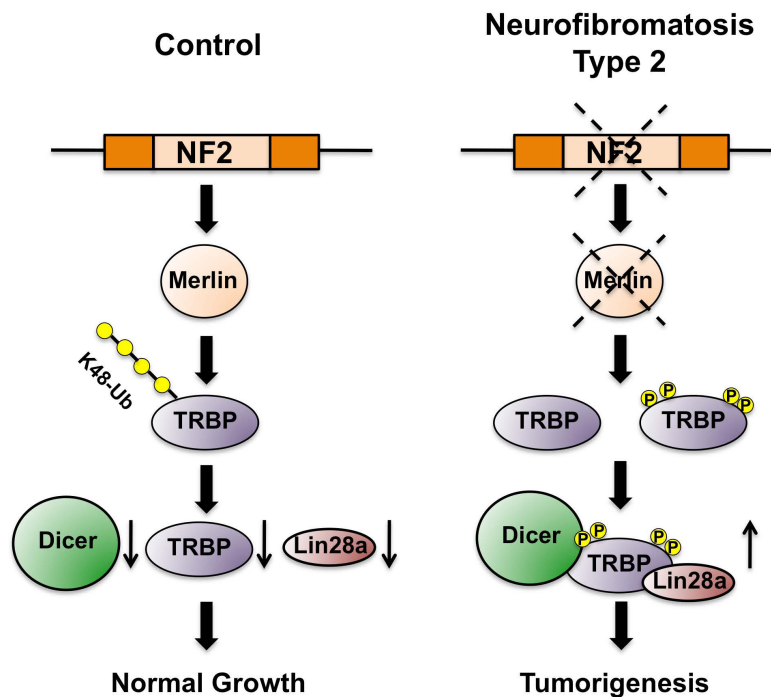


Figure 3.2: Merlin deficiency in Neurofibromatosis is associated with elevated phospho-TRBP and Lin28a, and decreased Let-7 miRNAs

(a) Immunoblot of lysates from NF2-deficient and NF1-deficient tumor cells demonstrates similar levels of TRBP and Lin28a proteins, but also similar loss of normal Merlin protein. Dicer is elevated in NF2-deficient tumors compared to those deficient in NF1. (b) Immunoblot of lysates from NF2/Merlin-deficient human Schwannoma tumors demonstrates elevated levels of TRBP, phospho-TRBP, Lin28a, and Dicer proteins compared to untransformed human Schwann cells. # denotes separate NF2-deficient Schwannomas taken from the same patient. (c) (Left) Representative immunoblot and (right) quantification of protein levels from normal Schwann cell lysates compared to NF2-deficient HEI193 cell lysates. Protein levels were normalized to GAPDH and plotted relative to Schwann cell protein levels, set as 1.0. (d) Quantification of miRNA levels by individual TaqMan qRT-PCR reactions in normal Schwann cells compared to NF2-deficient HEI193 cells. miRNA levels were normalized to U6 snRNA and plotted relative to Schwann cell miRNA levels, set as 1.0. N=3-7 independent experiments for all panels. * $p < 0.05$ by t test for all experiments. All error bars represent SEM.

Figure 3.2

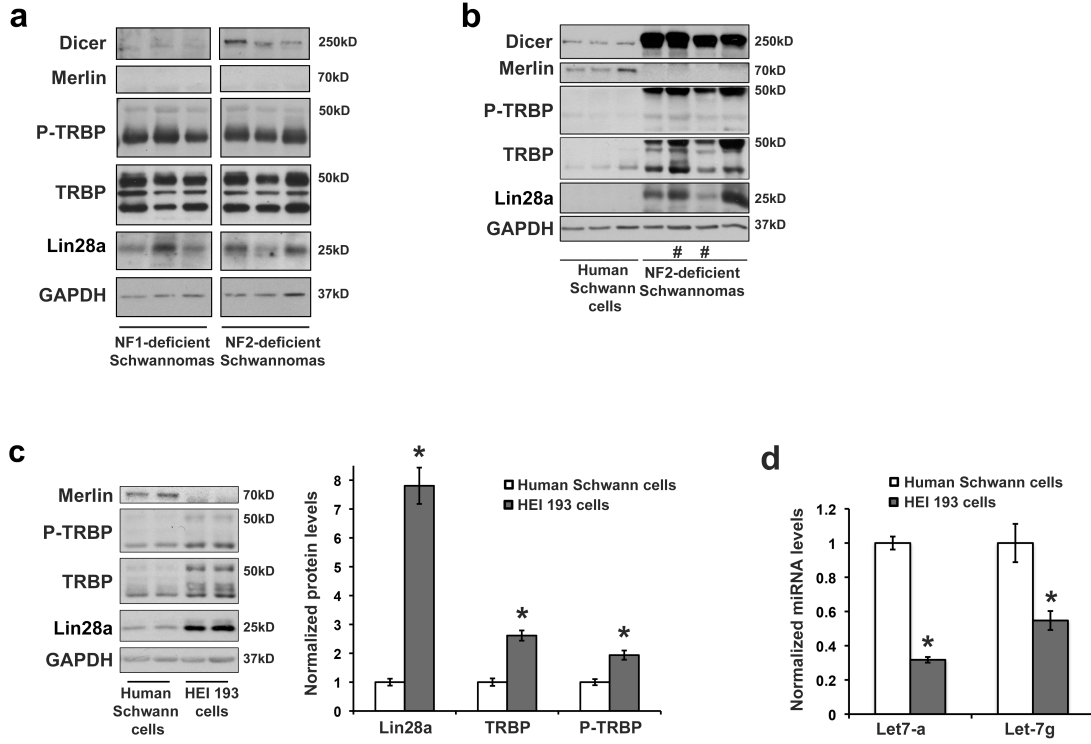


Figure 3.3: Loss of Merlin protein in Schwann cells causes abnormal Lin28a elevation through TRBP

(a) (Left) Representative immunoblot and (right) quantification of protein levels in lysates from Schwann cells treated with either non-target shRNA (NTshRNA, control) or shRNA targeting Merlin. Protein levels are normalized to GAPDH and plotted relative to NTshRNA, set as 1.0. (b) (Left) Representative immunoblot and (right) quantification of protein levels in lysates from Merlin-deficient HEI193 cells treated with either empty vector (control) lentivirus, or lentivirus expressing Merlin. Protein levels are normalized to HSC70 and plotted relative to empty vector, set as 1.0. (c) (Left) Representative immunoblot and (right) quantification of protein levels in lysates from HEI193 cells treated with non-target shRNA (NTshRNA, control) compared to 10 μ L or 15 μ L of shRNA targeting TRBP (TRBP shRNA). Protein levels are normalized to HSC70 and plotted relative to non-target shRNA, set as 1.0. N=4-7 independent experiments for all panels. * $p < 0.05$ by t test for all experiments. All error bars represent SEM.

Figure 3.3

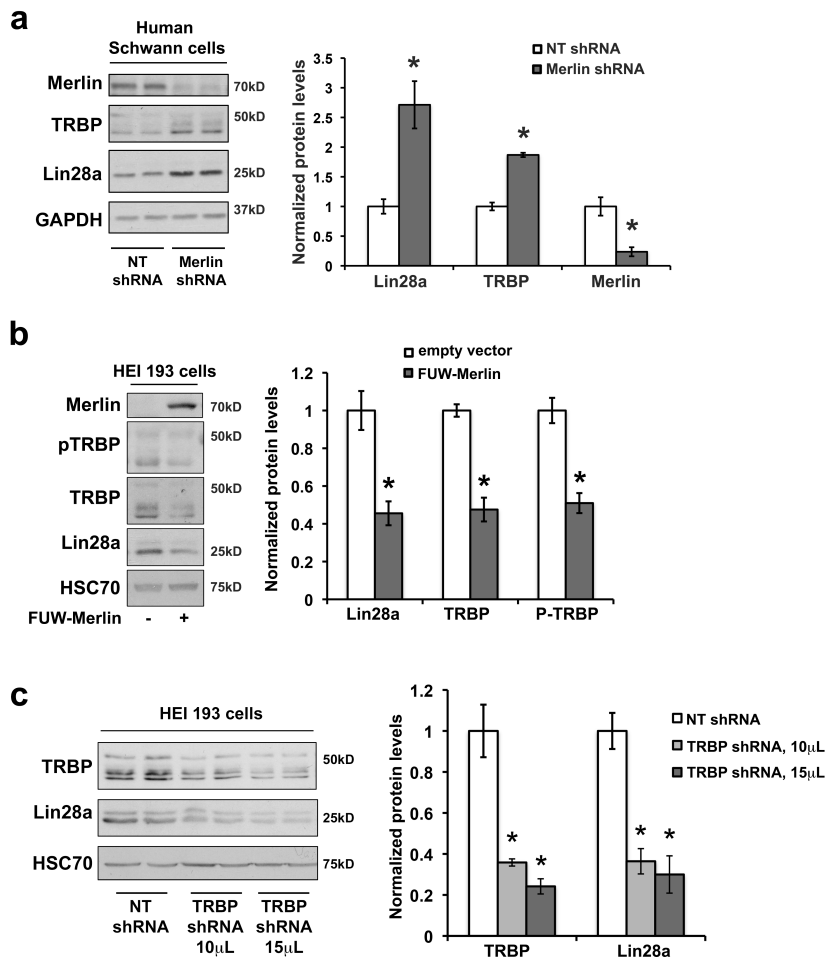
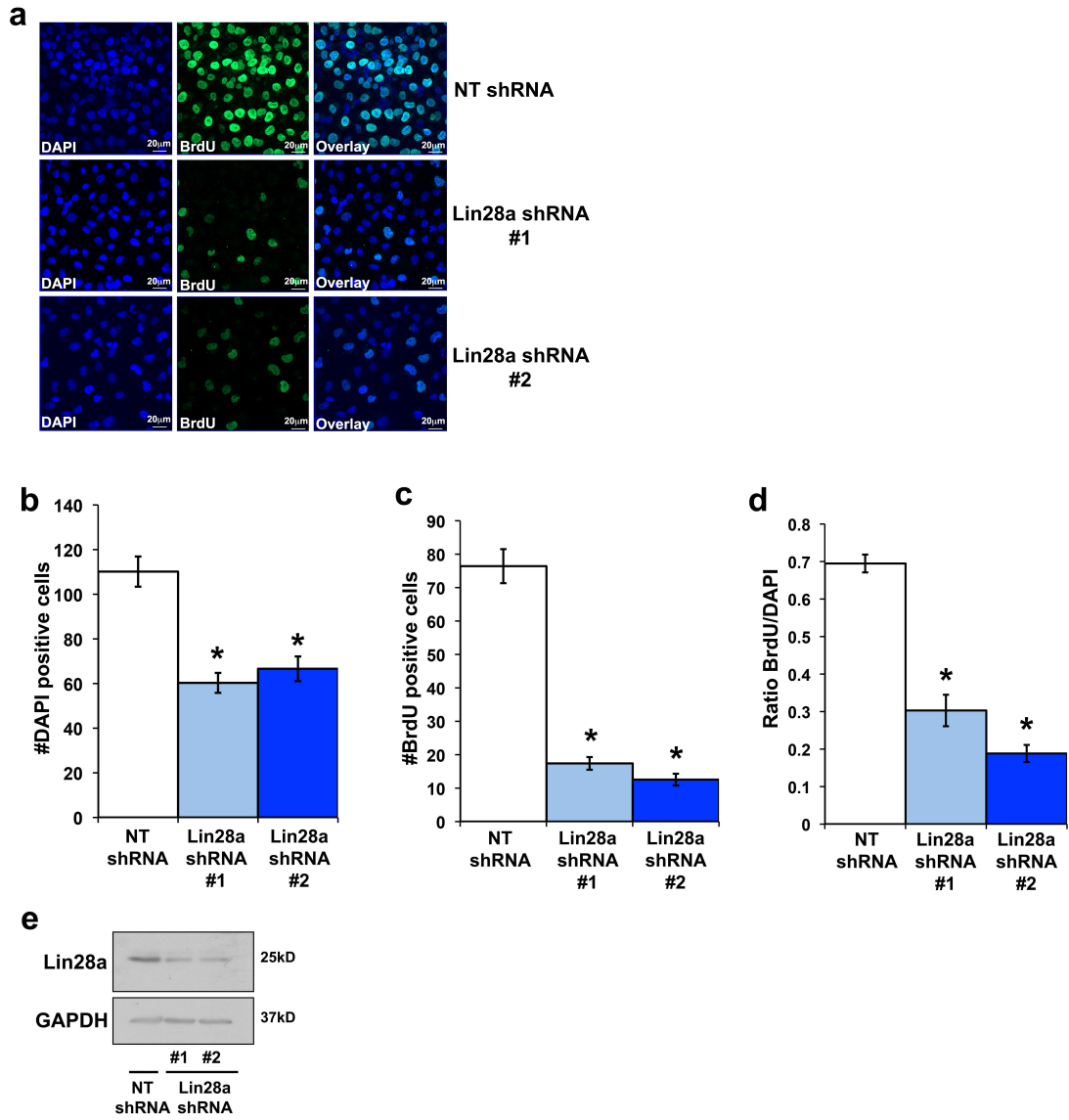


Figure 3.4: Lin28a elevation contributes to Neurofibromatosis Type 2 tumor growth

(a) HEI193 cells were treated with either non-target shRNA (NTshRNA, control), or one of two shRNAs targeting separate regions of the Lin28a mRNA (Lin28a shRNA #1 and Lin28a shRNA #2). Cells were incubated with BrdU for 8 hours, then fixed and stained for DAPI (blue) and BrdU (green). (b-d) HEI193 cells treated with Lin28a shRNA compared to those treated with NTshRNA demonstrated (b) fewer total cells, measured via DAPI signal, (c) fewer dividing cells, measured via BrdU incorporation, and (d) an overall reduced fraction of dividing cells. Results are from 9-12 independent microscopic fields per condition, no more than 3 fields per dish. $*p < 0.01$ by ANOVA for all experiments. All error bars represent SEM. (e) Immunoblot for Lin28a protein levels in HEI193 cells treated with NTshRNA, Lin28a shRNA#1, or Lin28a shRNA #2 demonstrates reduced Lin28a protein expression in the Lin28a shRNA #1 condition (68%) and the Lin28a shRNA#2 condition (67%) compared to NTshRNA.

Figure 3.4



Methods

Immunoblotting

Cells were washed 2 times in cold PBS with $MgCl_2$ (0.9 mM) and harvested on ice with lysis buffer (50 mM Hepes, 150 mM NaCl, 10% Glycerol, 1 mM EDTA, 1% Triton-X-100, 0.2% SDS) plus freshly added protease inhibitor cocktail (Roche), and phosphatase inhibitor cocktail (Sigma P004 and P5726). Lysates were rotated for 10 minutes at 4°C, followed by high-speed centrifugation for 15 minutes at 12,000 X g. Protein concentration in the supernatant was determined by Bicinchoninic acid (BCA) assay and equal protein amounts resolved on SDS-PAGE gels and electrotransferred to PVDF membrane. Membrane was blocked with 5% BSA in Tris-buffered saline tween 20 (TBST 0.1%) for 1-3 hrs and probed with primary antibodies: Lin28a (Novus NBP-149537), HA (Invitrogen 71-5500), NF2/Merlin (abcam ab88957), TRBP (Abcam ab72110 or Pierce LF-MA0209), Dicer (Sigma SAB4200087), GAPDH (Millipore 6C5), phospho-TRBP (generated by our laboratory, as described in Chapter 2 Fig. 2.8).

Schwannoma and Schwann cell sample preparation

Human schwannoma samples from patients with Neurofibromatosis Type 2 (NF2) and Neurofibromatosis Type 1 (NF1) were collected at the Johns Hopkins Peripheral Nerve Surgery Center under Institute Review Board approval (A.Belzberg and K.Ostrow) and with the generous consent of the patients. 3 separate NF1 tumor samples were taken from 3 different patients, and 7 separate NF2 tumor samples were taken from 6 different patients, all with

confirmed mutations in the *NF1* or *NF2* gene. Tumors were flash frozen on liquid nitrogen, crushed, and then rotated in lysis buffer (as previously described) with protease and phosphatase inhibitors for 3 hours, followed by high-speed centrifugation for 15 minutes (12,000 x g). Supernatant was saved for analysis.

Cell lines

Human Schwann cells were from (ScienCell #1700), and were cultured in Schwann cell medium (ScienCell #1701). The HEI193 cell line was generously supplied by Dr. Lim from UCLA, generated and immortalized as previously described (Hung et al., 2002). HEI193 cells were cultured in DMEM with 10% FBS and 1% glutamine. All cells were harvested as previously described when confluent.

Transduction

Lentiviral-mediated delivery of HA-Merlin (gift from Kunliang Guan, Addgene #32836, and cloned into the FUW lentiviral vector) was used to achieve Merlin expression in HEI193 cells for biochemical analysis at a multiplicity of infection (MOI) of 5-10, 4 days before harvest. Lentiviral stocks were prepared and lentiviral knockdown carried out as previously described (Huang et al., 2012; Meffert et al., 2003). Knockdown for biochemical and imaging analysis used lentiviral-mediated delivery of non-target shRNA (Sigma, SHC002), shRNA targeting TRBP (Thermo Scientific TRCN0000102563), shRNA targeting Lin28a (Thermo Scientific TRCN0000102576 (Lin28a shRNA#1) and TRCN0000021802

(Lin28a shRNA #2), and shRNA targeting Merlin (TRCN0000039975), 4-5 days prior to analysis.

RNA analysis

Total RNA from primary cultures of mouse hippocampal neurons was isolated in Tri-Reagent (Molecular Research Center, Inc.) according to the manufacturer's protocol. Cultures were homogenized in Tri-Reagent directly. RNA pellets were air-dried and resuspended in nuclease-free water. RNA concentration and quality were assayed by spectrophotometric measurements at optical density (OD) 260/280/230nm. For individual microRNA abundance assays (Applied Biosystems), 20ng of total isolated RNA was prepared for reverse transcription with stem-looped primers specific for individual mature miRNAs in a final volume of 15 μ l according to manufacturer's protocol: 1) 4°C for 5 min, 16°C for 30 min, 2) 42°C for 30 min, 3) 85°C for 5 min, and subjected to TaqMan MicroRNA Assays (Applied Biosystems) for Let-7a (000377), Let-7g (002282), and miR-132 (000457). The abundance of sno234 (001234) in each sample was used as an internal control to normalize all miRNA species. RT-qPCR was performed using a Stratagene Mx3000P machine and software. Quantification was carried out using the standard-curve method and no preamplification. RQ was calculated as $2^{-\Delta\text{CtBDNF}} / 2^{-\Delta\text{Ctmock}}$ where $\Delta\text{Ct} = (\text{cycle threshold for miRNA of interest}) - (\text{cycle threshold for reference control})$.

BrdU incorporation assay

HEI193 cells were plated and randomly assigned to treatment conditions. The experimenter was blinded during data acquisition and analysis. 48 hours after plating, dishes were incubated for 24 hours in serum starvation media (0% FBS), which was then replaced with full media containing 10 μ M 5-bromo-2'-deoxyuridine (BrdU; Sigma, B5002) for 8 hours. After washing with PBS, cells were fixed in 4% PFA/4% sucrose/PBS for 40 min, and permeabilized for 40 min in 0.2% triton X-100/PBS. Cells were then rinsed in PBS, and incubated in 2M HCL for 20 min at 37°C, followed by incubated in 0.1M borate buffer for 5 min, twice, to neutralize acid. Cells were blocked in 10% BSA/PBS for 1 hr at room temperature, then incubated with anti-BrdU antibody (Sigma, B8434) overnight at 4°C. The following day, dishes were washed in PBS and incubated with Alexa 488 secondary antibody for 1 hour at room temperature. During the last wash following secondary antibody incubation, DAPI stain (ThermoFisher, D1306) was added for 10 minutes. Cells were imaged using a Tokogawa spinning disk system (Cell Observer, Carl Zeiss). Confocal images of HEI193 cells were acquired using a 25x (for analysis) or 40x (tiled for representative images) objective. Laser power and exposure time were adjusted to minimize photobleaching and avoid saturation. Blue (DAPI) and green (BrdU) cells were manually counted.

Statistical analysis

Two-tailed unpaired student's *t* tests were used with $\alpha=0.05$. Where specified, statistical analysis included one-way ANOVA for independent samples with a Tukey HSD *post hoc* test, $\alpha=0.05$.

Chapter 4: Conclusions and Perspectives

The ability of neurons to swiftly and coordinately alter protein expression in response to environmental stimuli is key to their individual and collective function in synaptic networks. Given that it takes a minimum of 20 - 30 minutes for the earliest transcriptional regulation to begin to cause proteome alterations, post-transcriptional control of gene expression in the nervous system is likely crucial to producing normal neuronal function, but is currently not well understood. Previous research from our laboratory demonstrated that BDNF confers translational specificity by impacting the miRNA biogenesis pathway in part through Lin28a protein induction (Huang et al., 2012). This initial work both highlighted the importance of miRNA regulation by Lin28a in BDNF function, and suggested that BDNF could be used as a model to understand stimulus-dependent regulation of post-transcriptional gene target specificity.

A single miRNA has the potential to affect translation of entire suites of mRNAs, and therefore miRNAs and miRNA regulators are attractive candidates in coordinating elaborate biological responses. However, the finding that BDNF regulates miRNA biogenesis by inducing levels of Lin28a protein was highly unexpected, given that Lin28 was previously considered to be transcriptionally silenced in mature, terminally-differentiated cells, and only re-upregulated in pathological states such as cancer. In the first portion of my dissertation, we aimed to unravel the mechanism by which BDNF acts to elevate Lin28a protein (but not Lin28b), subsequently decreasing Let-7 miRNAs. We found that, under basal conditions, Lin28a protein is present at low but detectable levels in mature

hippocampal neurons and is subject to rapid degradation. Exposure to BDNF stabilizes Lin28a protein by inducing TRBP phosphorylation downstream of Erk kinase. Phospho-TRBP serves as a binding partner for Lin28a, leading to Lin28a stabilization, and downstream inhibition of Let-7 miRNA processing. We observed that stabilization of Lin28a by phospho-TRBP is required for physiological effects of BDNF on spine dynamics. Excitingly, we also saw that trophic induction of TRBP and Lin28a downstream of MEK/Erk exists in multiple primary cell types in response to various growth factors, both in and outside of the nervous system, suggesting that a mechanism for Lin28a regulation downstream of Erk-mediated phospho-TRBP could be broadly conserved.

Experiments performed in the first portion of my dissertation led us to uncover the potential for control of Lin28a by Merlin protein, which is mutated in the human tumor disorder Neurofibromatosis Type 2 (NF2). Based on prior reports showing ubiquitination of TRBP by Merlin (Lee et al., 2004; Lee et al., 2006), and my own work in Chapter 2 demonstrating a role for Merlin in phosphorylation-dependent TRBP regulation, we hypothesized that loss of Merlin could lead to elevated phospho-TRBP and, consequently, Lin28a. Although Lin28 is a known oncogene and Let-7 miRNAs are considered tumor-suppressors (Wang et al., 2012), dysregulation of the Lin28/Let-7 axis has not previously been characterized in NF2. In the second portion of my dissertation, we observed that loss of Merlin in NF2 tumors causes elevation of TRBP and phospho-TRBP, which results in induction of Lin28a and is associated with decreased Let-7 miRNAs. Excitingly, loss of Lin28a in these tumor cells reduces their rate of

growth. Ongoing experiments related to this project will aim to determine whether Lin28a exerts its pro-growth effects directly through Let-7 miRNA inhibition in the setting of NF2 tumors. This is being tested by expressing either wildtype Let-7 or a Lin28-resistant Let-7 miRNA mutant and observing whether rate of tumor cell division is similarly slowed. We are also in the process of developing assays to examine tumor formation and growth *in vivo* using immunocompromised mice. Flank injection of NF2 tumor cells in *NU/NU* mice has been previously shown to result in observable tumor formation within 7 days (Prabhakar et al., 2010). We hope to characterize *in vivo* growth of NF2 tumors following treatment with shRNA targeting Lin28a, or a Lin28-resistant Let-7. If growth of the tumor *in vivo* is slowed by expression of a Let-7 miRNA, this may suggest the exciting potential for Let-7 miRNA mimics as therapy in NF2 (Dai et al., 2015; Kasinski et al., 2015; Liu et al., 2014; Wang et al., 2012).

Previous studies investigating mechanisms underlying growth inhibition by Merlin have observed that Merlin negatively regulates the MAPK pathway (Jung et al., 2005; Lim et al., 2003a). Our characterization of Lin28a induction in trophic responses revealed that Lin28a is stabilized downstream of MEK/Erk-mediated TRBP phosphorylation. Considered together, these findings raise the possibility that loss of Merlin protein in NF2 tumors could elevate TRBP and Lin28a both through reduced TRBP polyubiquitination, as well as through enhanced TRBP phosphorylation downstream of Erk activity. To begin to determine whether Erk kinase may regulate TRBP and Lin28a in the context of NF2 tumors, we treated tumor cells with two different Erk inhibitors (U0126 and

AZD6244) and made initial observations of widespread cell death within 48 hours. Ongoing experiments will directly measure apoptosis following Erk inhibition *in vitro* to confirm these findings. Erk activation is associated with pro-growth phenotypes through activation of a range of signaling pathways, and therefore overexpression of phospho-mimic TRBP, for example, may help us to elucidate whether possible apoptotic phenotypes following Erk inhibition are related specifically to regulation of phospho-TRBP/Lin28a versus more general effects. Regardless, given that drugs inhibiting Erk are currently approved for human use (e.g. Lovastatin), these findings could have exciting implications for therapeutic treatment, and will be followed up with Erk inhibition using FDA approved pharmaceuticals (e.g. lovastatin) in *in vivo* models of NF2 tumor expression. Collectively, this work has the potential to demonstrate a crucial role for phospho-TRBP-mediated stabilization of Lin28a in tumor cell biology in addition to trophic signaling.

One unexpected observation arising from our characterization of a posttranslational mechanism for induction of Lin28a protein in trophic responses and tumor cells was the elucidation of differential regulation of Lin28a and Lin28b. Organisms such as *C. elegans* and *Drosophila melanogaster* contain only one Lin28 homolog (with sequence identity to Lin28a), but the vertebrate genome contains two Lin28 paralogs, a and b (Balzer et al., 2010; Piskounova et al., 2011). Traditionally, Lin28a and Lin28b are thought to be functionally redundant, both serving to inhibit Let-7 miRNA activity. However, the research presented in my dissertation demonstrates differential stimulus-specific response of the two

paralogs. We see that Lin28a exclusively is upregulated by BDNF, likely because Lin28a, but not Lin28b, is a binding partner of phospho-TRBP. This work exposes distinct biological roles for Lin28a versus Lin28b, and suggests that they may mediate separate aspects of stimulus response. Ongoing work in our laboratory is aimed at characterizing a potential role for Lin28b in long-term maintenance of plasticity, as opposed to Lin28a, which is rapidly and briefly induced by trophic stimuli. Lin28a and Lin28b are both critical players in development as well as tumorigenesis, and we anticipate that an increased understanding of distinct regulatory mechanisms will have important implications for not only trophic signaling and translational specificity, but also for stem cell and tumor cell biology as well.

Generally speaking, knowledge of mechanisms conferring translational specificity is particularly crucial in neuronal cell types, because neurons are asymmetrical cells with distinct subcellular compartments in which protein composition must be selectively regulated in order to achieve appropriate function (Holt and Schuman, 2013). Although the experiments performed in my dissertation demonstrate trophic Lin28a induction, the methods involve whole-cell lysis, and therefore allow for analysis of protein levels on a cell-wide basis only. This begs the question of subcellular location of induction of Lin28a by BDNF. Does BDNF lead to induction of Lin28a protein throughout the neuron, or in a specific region, such as the stimulated synapse? Ongoing research in our laboratory attempts to address the question of localized Lin28a protein expression both pre and post stimulation, using microfluidic chambers to

physically isolate dendrites from the neuronal cell body. These techniques allow for the application of BDNF to a single dendritic segment, after which Lin28a levels in the stimulated dendrite and dendritic spines can be compared to Lin28a in nearby unstimulated dendrites, as well as the cell body. The elucidation of the mechanistic basis for rapid Lin28a induction described in this thesis is now being brought to bear on these questions of localized regulation.

Regulation of protein synthesis is thought to underlie the enduring changes in synaptic activity that are known to require new translation, and physiological effects of BDNF that are dependent on novel protein synthesis are well-documented. Typical protein synthesis-dependent readouts of BDNF in differentiated neurons include increases in dendritic complexity and dendritic length, and regulation of dendritic spine volume, number, and density (Jaworski et al., 2005; Je et al., 2009a). Additionally, BDNF-dependent protein synthesis plays an important role in hippocampal-based learning, and rodents with impaired BDNF signaling exhibit a reduced capacity for learning and memory (Pardon, 2010; Santos et al., 2010; Tyler et al., 2002). Our work has demonstrated that BDNF relies on Lin28a induction, and subsequent Let-7 miRNA inhibition, in order to both enhance dendritic arborization in young neurons, and modulate spine density and size in mature neurons. These findings suggest the possibility that hippocampal-based learning may be impaired in animals lacking Lin28a function. To test this hypothesis, a transgenic Lin28a mouse line from the lab of G. Daley (Zhu et al., 2011), in which exon 2 of genomic Lin28a is flanked by LoxP sites (*Lin28a^{fl/fl}*), has been crossed with a

CAMKII α -CreER^{T2} transgenic line. This new line will allow us to achieve neuronal-specific conditional Lin28a knockout, prior to tasks such as Morris Water Maze and contextual fear learning, which are known to require BDNF (Minichiello et al., 1999; Tyler et al., 2002). We anticipate that removing Lin28a function will cause transgenic animals to perform poorly on tasks requiring BDNF signaling. Additionally, we will examine whether treatment with Let-7 miRNA inhibitors (antiMirs, designed with clinical intent) (De Palma and Naldini, 2010; Frost and Olson, 2011; Stenvang et al., 2012) has the ability to mimic the effects of Lin28a induction on cognitive performance, in settings where either Lin28a or BDNF expression is reduced. Since BDNF signaling is disrupted in numerous neurologic and psychiatric disorders, the use of Let-7 antiMiRs has exciting potential clinical relevance for cognitive and neurological disease.

Dysregulation of both translation and BDNF are directly associated with a variety of cognitive diseases and disorders (Bassell and Warren, 2008; Krauss et al., 2013; Nagahara and Tuszynski, 2011; Ramaswami et al., 2013; Wang et al., 2007; Zuccato and Cattaneo, 2009). Autism spectrum disorders, in particular, are linked to both disrupted translation and impaired BDNF signaling (Bassell and Warren, 2008; Correia et al., 2010; Darnell et al., 2011; Kelleher and Bear, 2008). Work from this thesis elucidating the crucial role of the MAPK pathway in regulation of Lin28a control of pro-growth translation, allowed our laboratory to form hypotheses regarding a potential role for Lin28a in autism. We hypothesize that abnormal translation in autism could result from changes in Lin28a expression, leading to altered Let-7 miRNA levels. Specifically, a current project

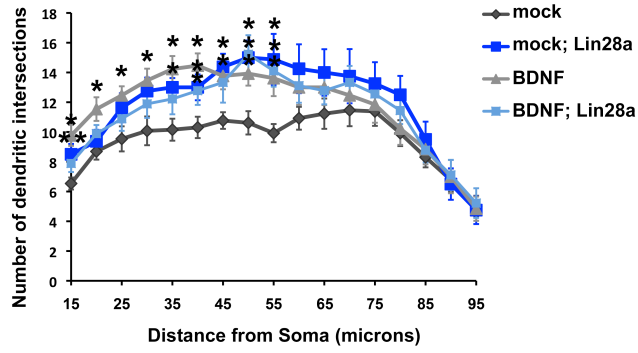
in our laboratory is focused on characterizing misregulated Lin28a expression in the autism spectrum disorder Fragile X Syndrome, which is associated with hyperactivity, anxiety, attention deficit, and cognitive impairment, and is linked to dysregulated translation and abnormal BDNF function (Bassell and Warren, 2008; Castren and Castren, 2014; Kelleher and Bear, 2008). Additionally, work in my dissertation regarding the role of Lin28a in Neurofibromatosis preliminarily indicates that Lin28a could be elevated in NF1, another autism spectrum disorder, as well. Current models suggest that autism spectrum disorders may be a result of uncontrolled neuronal growth, or loss of synaptic pruning in development (Bolton et al., 2001; Courchesne et al., 2011; Tang et al., 2014). Given the pro-growth function of Lin28a, we anticipate that abnormal Lin28a elevation in autism could contribute to these effects.

Overall, the work performed for my dissertation has characterized a previously unappreciated mechanism for regulation of Lin28a protein in the nervous system, which ultimately serves to induce selective translation of pro-growth proteins. We have shown that despite previous assumptions of Lin28a silencing during development, it is active and functional in mature hippocampal neurons following trophic stimulation. We hypothesize that mature, differentiated neurons make use of the Lin28/Let-7 pathway by keeping Lin28a levels low at baseline, but producing rapid Lin28a elevation in response to pro-growth trophic stimuli, causing transient decreases in Let-7 miRNAs and increased translation of genes involved in growth and plasticity. We have demonstrated that phospho-TRBP serves as a regulatory hub for Lin28a induction, both in the context of

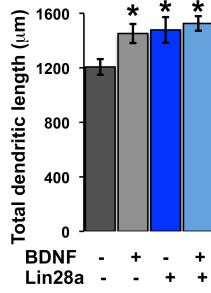
rapid trophic responses, and also in the long-term context of a tumor disorder, Neurofibromatosis Type 2. Our findings suggest that Lin28a can be regulated by various trophic stimuli through phospho-TRBP in mature cells broadly, although further research is needed to fully characterize the observed Erk-dependent Lin28a inductions in other cell types. Preliminary data suggests that while Erk activation downstream of receptor tyrosine kinase (RTK) signaling mediates TRBP/Lin28a induction, activation of other receptor types which also converge on the MAPK pathway may not have the same effect. These observations are indicative of possible parallel pathways involved in RTK activation that may contribute to Lin28a stabilization, and require further study. Additionally, a major remaining question is how mature cells maintain low basal levels of Lin28a protein – specifically, what mechanisms are in place to produce the rapid baseline turnover of Lin28a in hippocampal neurons? Ongoing work in our laboratory will attempt to provide insight into basal Lin28a control. Collectively, work in my dissertation characterizes a novel mechanism for regulation of Lin28a protein in the nervous system, and demonstrates the importance of this mechanism in both synaptic plasticity and tumor cell biology. These findings will have important implications for those seeking to better understand pro-growth outcomes of trophic signaling, as well as those interested in constitutive pathogenic elevation of Lin28a.

Appendix A

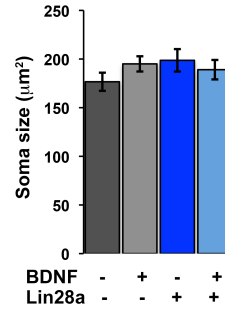
A.1



A.2



A.3



A.4: Lin28a mimics and occludes the effects of BDNF on dendritic arborization

(A.1) BDNF-mediated increases in dendritic complexity are mimicked by low-level overexpression of exogenous Lin28a. In the presence of Lin28a overexpression, BDNF has no further effect on dendritic complexity. Dendritic complexity is measured by counting the number of dendritic branches at varying distances from the cell soma. (A.2) BDNF causes a small but significant increase in total dendritic length, mimicked by Lin28a overexpression. Lin28a occluded further effects of BDNF on total dendritic length. (A.3) Soma size was unchanged between conditions, suggesting that neurons were overall of similar health and size following experimental treatments. * $p < 0.05$ by t test for all experiments. All error bars represent SEM. N=9-13 neurons per condition, from at least 3 separate cultures, no more than 3 neurons per dish.

Appendix B

Extended Experimental Methods

Hippocampal Neuron Dissociation and Culture

Prepare culture dishes: Incubate overnight with Poly-L-lysine (0.5 mg/ml) in sterile 0.1 M Sodium Borate pH 8.4.

Wash dishes 1X with sterile PBS prior to use and allow to dry briefly, store in TC incubator.

Note: If plating into MatTek dishes, wash dishes and allow them to dry during papain treatment. Drying allows plating into the coverslip well without spillage into the surrounding dish.

Make a hole in the top of a sterile 75 cm² culture flask and connect the hole by tubing to Oxygen/CO₂ (95/5 %)

Prepare the following fresh sterile solutions

Trituration Media: 20 ml DMEM
 200 µl BSA (200 mg/ml stock, 2 mg/ml final)
 0.5 ml Pen/Strep/Glucose/Pyruvate

200 μ l DNase (5 mg/ml stock, 0.05 mg/ml final)

Centrifugation 5 ml of above Trituration Media

Media: plus 400 μ l BSA (200 mg/ml stock, 16 mg/ml final)

-add three drops sterile 0.1 N NaOH, or until media is slightly pink

Papain Solution: 1.5 ml HBSS/NaHCO₃/EDTA (6.67X stock)

128 μ l cysteine (25 mg/ml stock, .32 mg/ml final)

0.25 ml Pen/Strep/Glucose/Pyruvate

8 ml H₂O

Store on Ice

Immediately prior to use, warm to RT, add 1/2 to flask and gently aerate with 95%O₂ /5 % CO₂; add Papain LATER

Dissection Solution: 2 ml HBSS (10X w/o Ca²⁺/Mg²⁺/NaHCO₃)

200 μ l HEPES (1 M stock, 1 mM final)

0.5 ml Pen/Strep/Glucose/Pyruvate (40X stock)

17.3 ml H₂O

Dissection / Digestion Procedure

- 1) Dissect Hippocampi from P0-P1 mice (use dissecting scope)

Note: Keep Hippocampi on ice in Dissection solution

- 2) When dissection is finished, transfer tissue to aerated flask containing Papain solution and add 100 U papain.
- 3) Digest for ~ 15 min at RT, depending upon papain age and temperature. Monitor by eye watching for feathering of the tissue edges.

Trituration Procedure

- 1) Label three 15 ml conicals, #1 - #3
- 2) Once digestion is over, move flask to TC hood. Allow tissue to settle, then remove tissue to #1 conical using a 5 ml plastic pipette
- 3) Allow tissue to settle and remove as much of the digestion solution as possible from above the tissue. Add 4 ml Trituration Solution with mixing, allow tissue to settle, and again remove as much solution as possible from over the tissue.
- 4) Add 3 ml Trituration Solution and triturate tissue gently up and down ~4 times with a sterile pasteur pipette, then allow tissue chunks to settle.
- 5) Remove solution from the top, which is a single cell suspension, and transfer to #2 conical.
- 6) Firepolish a sterile pasteur pipette to slightly decreased diameter and repeat trituration. Again add 3 ml Trituration Solution, allow chunks to settle, and remove top solution to #2 conical.

7) Repeat the above Trituration procedure firepolishing pipettes to progressively smaller diameters, until nearly all tissue is homogenized into single cell suspension.

Note: Typically requires 3-4 pipette diameters

8) Transfer solution from conical #2 to conical #3 using a small bore pasteur pipette. Re-triturate bits at the bottom of #2 if necessary.

9) Layer 5 ml Centrifugation Solution underneath triturated cells in conical #3. Centrifuge to pellet cells for ~10 min at 900 x g, room temperature.

10) Remove supernatant and resuspend cell pellet in Growth Media with Pen/Strep. Count cells with hemocytometer.

a. Plate at ~1.1 million cells/ml for wells. Roughly, 550,000 cells/well in 24 well plate, plated in 500 μ l.

b. Plate at ~2 million cells/ml for matteks. Roughly, ~160,000 cells/dish in MatTeks.

11) Put plated cells in incubator

12) The next morning, suck off 1/2 - 2/3 media and replace with fresh media without Pen/Strep.

Note: Cells can be plated in pen/strep/glutamine, but should be switched to media WITHOUT pen/strep within ~12 hours.

Growth Media: 50 ml - 48.5 ml Neurobasal A
 1 ml B-27 supplement (50X)
 0.5 ml Pen/Strep/L-Glutamine (100X) OR 0.25

ml L-Glutamine

Note: We have also used glial conditioned media, especially when the B27 is less than optimal.

Aliquot Stocks

B27 supplement (50X) 1 ml eppendorf aliquots, store at - 20°C (Gibco #17504-036)

BSA (200 mg/ml) BSA fraction V, 2 g / 10 ml sterile nanopure H₂O
Sterile filter, 1 ml eppendorf aliquots, store at - 20°C

Cysteine (25 mg/ml) L-cysteine in sterile nanopure H₂O
Sterile filter, 200 µl aliquots, store at - 20°C

DNAse I (5 mg/ml) 20 mg/ 4ml sterile nanopure H₂O
Sterile filter 400 µl aliquots, store at - 20°C (Worthington
#LS002004, Code D, 5mg ~ \$25)

Glucose 40 g/ 200 ml sterile nanopure H₂O
Sterile filter, store at RT

Glutamine (200X) L-Glutamine (200 mM) (Gibco #25030-032)

HBSS (10X) w/o Ca^{2+} / Mg^{2+} / NaHCO_3 - 100 ml bottle (Gibco #14180-053)

HBSS (10X) w/o Ca^{2+} / Mg^{2+} , + EDTA, NaHCO_3 - 100 ml bottle as above (#14180 053)

Add 0.5 mM EDTA final, 0.1 ml of 0.5 M stock

Add 50 mM NaHCO_3 final, 9.6 ml of 524 mM stock

Hepes (1M) pH 7.5

Papain (0.2 units/ μl) Resuspend vial in sterile nanopure H_2O at 4°C O/N, sterile filter into 15 ml conical, store at 4°C (Worthington #LS003119, code PAPL, 100mg~\$60)

Pen/Strep/Glutamine (100X)

1:1 mix of

Penicillin(10000units) - Streptomycin(10000 μg)

(Gibco#15140-031)

L-Glutamine (200 mM) (Gibco #25030-032)

Sterile filter, 1 ml eppendorf aliquots, store at -20°C

Pen/Strep/Pyruvate/Glucose (40X)

200 μl Pen/Strep

200 μl Glucose (200 mg/ml stock)

400 μ l Sodium Pyruvate (100 mM)

200 μ l sterile nanopure H₂O

Sterile filter, 1 ml eppendorf aliquots, store at - 20°C

Sodium Pyruvate (100 mM) (Gibco # 11360-070), store at - 4°C

Peritoneal Macrophage Harvest and Culture

Growth Media: RPMI with addition of 10% fetal bovine serum, 1% glutamine, and 1% pen/strep

- 1) Euthanize adult mouse (12-20 weeks old) in a CO₂ chamber, followed by cervical dislocation
- 2) Disinfect abdominal area with 70% ethanol
- 3) Cut and pull apart skin to expose abdominal cavity
- 4) Using a 21 gauge needle, inject 10ml ice cold media into abdominal cavity

Note: Inject media just under the skin into lower left quadrant of the abdomen, in order to avoid puncturing major organs. In particular, if the intestinal wall is punctured, the abdominal cell population will be contaminated.

- 5) Shake mouse to allow for distribution of media throughout abdominal cavity for 30-60 sec
- 6) Using the same 21 gauge needle and syringe, suction media back out of abdominal cavity

Note: When removing cell-containing media, avoid puncturing surrounding areas, as you will risk blood cell contamination.

- 7) Empty media into a chilled 15ml conical, on ice

Note: Pour out the cell suspension rather than ejecting through needle, in order to avoid shearing the cells.

- 8) Spin cells down at 2,000 x g for 10 min
- 9) Suction media off cell pellet, and re-suspend in fresh media
- 10) Count cells using hemocytometer and plate into 24 wells plates
 - a. Plate cells at around 600,000 cells/well in 0.5ml/well
- 11) Leave cells in 37°C incubator for 1-2 hours, then wash well 2X with warm media. Remaining, adherent cells are 99% macrophages.

Processing of Primary Tumor Tissue

Tumor tissue was harvested under Institute Review Board approval at the Johns Hopkins Peripheral Nerve Surgery Center under the expertise of Dr. Allen Belzberg

Note: Neurofibromatosis tumor tissue is highly fibrous and difficult to digest

Lysis Buffer: 50 mM Hepes, 150 mM NaCl, 10% Glycerol, 1 mM EDTA, 1% Triton-X-100, 0.2% SDS

- 1) Using a sterile blade, cut tumor tissue into $\sim 2\text{cm}^2$ chunks.
- 2) Flash-freeze tumor tissue in a liquid nitrogen bath. Ensure samples are entirely frozen.
 - a. Store unused samples at -80°C .
- 3) Chill a clean, sterile metal slab on the liquid nitrogen bath, and cover with a sheet of Saran wrap.
- 4) Place 1 frozen tissue sample on the metal slab, and crush using a hammer.

Note: Crushing allows for lysis from a mix of cells in all portions of the tissue, instead of the outermost layers only

Note: If sample is fully frozen, when crushed it should become a fine powder that can be scraped off of Saran wrap

- 5) Place powdered tissue into a 1.5ml tube containing 300-500 μ l lysis buffer with protease and phosphatase inhibitors, and rotate at 4°C for 3 hours.
- 6) Centrifuge for 15 minutes, 4°C, at 12,000 x g. Save supernatant for analysis.
- 7) Determine protein concentration of supernatant (BCA), and load equal amounts of protein on a polyacrylamide gel to analyze protein levels via immunoblot.

Purification and pull-down of recombinant bacterial proteins

Adapted from Pomerantz laboratory protocol

Day 1

- 1) Inoculate 10ml LB plus antibiotic with 1 colony from BL21 bacteria transformed with plasmid of interest

Note: Touch pipette tip to colony, then touch tip to 5ml LB/antibiotic liquid culture and eject tip in a second 5ml LB/antibiotic liquid culture

Day 2

- 1) Inoculate 250ml LB/antibiotic with 10ml starter culture from Day 1. Grow at 37°C
- 2) Monitor bacterial growth until OD 600 = 0.75 (logarithmic phase, usually about 2 hrs of growth)
- 3) Once OD 600=0.75, add IPTG to final concentration of 1mM to induce plasmid expression, and grow for **2 - 4 hrs**
- 4) Cool bacteria quick on ice water bath for 15-25 min
- 5) Spin down bacteria at 7700 x g for 10 min at 4°C
- 6) Resuspend bacterial pellet in 12.5ml cold PBS, pH=7.4

Note: At this step, bacterial resuspension can be stored overnight at -20°C to aid lysis. Alternatively, experimenter can proceed immediately to the subsequent steps

Day 3

Lysis

- 1) Quick thaw bacteria at 37°C
- 2) Add bacterial protease inhibitors to recommended concentration, and lysozyme to 0.5mg/ml
- 3) Incubate 30 min room temp
- 4) OPTIONAL: freeze bacteria and thaw at 37°C 2-3X to aid lysis
- 5) Sonicate: 20 sec pulses X 5, at 20% amplitude
- 6) Add Triton-X to 1% and incubate on ice 0-10 min
- 7) Spin 10,000 x g for 10 min at 4°C. Take supernatant for analysis.

Note: If desired, save supernatant sample for analysis of protein expression

Pull-down

- 1) Wash about 1200µl 30% bead slurry with PBS, pH=7.4 per sample (about 400µl bed volume of beads; glutathione sepharose beads for GST binding, or amylose resin for MBP binding). Re-suspend beads as 25% slurry in PBS, pH=7.4 (e.g. 1200µl PBS to 400µl beads)
- 2) Add 12.5ml lysed bacterial supernatant to 1600µl 25% slurry of appropriate beads
- 3) Rotate beads and supernatant at 4°C for 2hr-overnight

Wash and elution

Column GST tag elution:

- 1) Spin down beads at 500 x g for 5 min at 4°C and decant supernatant

Note: Save supernatant sample for analysis of protein pull-down

- 2) Re-suspend beads in small volume PBS, pH=7.4 (around 500µl) and apply to Biorad Poly-prep chromatography column

- 3) Wash with 8ml PBS, pH=7.4 (20X bead volume) and collect drainage

Note: Save wash drainage sample to confirm protein is not lost

- 4) Elute in 200µl fractions with freshly made 10mM Glutathione in 50mM Tris-Cl, pH=7.5

- a. Plug column before addition of each elution fraction, and incubate 50-10 min before collecting elution

- b. Add 1µl eluted fraction to 100µl Bradford reagent to preliminarily select for concentrated fractions

Note: Addition of Glutathione to Tris-Cl may significantly lower pH and reduce elution efficiency – check pH of elution buffer post Glutathione addition

- 5) Pool most concentrated fractions (usually 1-3) and subject to dialysis at 4°C to remove glutathione

- a. Dialysis buffer: 20mM HEPES pH=8.0, 20% glycerol, 0.2 mM EDTA, 1mM DTT

- b. Use slide-a-lyze tubes with 20K pore size

- c. Dialyze for 2 hours, change dialysis buffer, then let go overnight

- 6) Quantitate protein concentration by Bradford protein assay
- 7) Quick freeze purified proteins, store at -80°C

Xa Protease cleavage elution:

- 1) Wash beads 2X in factor Xa reaction buffer (20mM Tris-Cl, 50mM NaCl, 1mM CaCl₂, pH =6.5)
- 2) To 400µl bed volume of beads, add 600µl factor Xa reaction buffer with 0.2U/µl factor Xa. Rotate overnight at 4°C.

**Concentration of factor Xa and rotation time should be optimized

- 3) Collect eluent and add PMSF to final concentration of 0.3mM to stop protease activity. Incubate 30 min at 25°C.
- 4) Collect eluent and and quantitate protein concentration by Bradford protein assay
- 5) Quick freeze purified proteins, store at -80°C

Binding assay

- 1) Wash 60µl 30% sepharose bead slurry with cold PBS, pH=7.4 and resuspend in 20µl to make 50% slurry
- 2) Rotate about 50µg of either GST-TRBPWT, GST-TRBPSΔD, or GST alone with 40µl 50% sepharose bead slurry, 2hrs-overnight at 4°C
- 3) Add about 25µg pure Lin28a protein to bead-bound GST-TRBPWT, GST-TRBPSΔD, or GST alone (approximately 2X TRBP per 1X Lin28a)
- 4) Rotate 2-4hrs, 4°C

- 5) Wash 3X with cold PBS, pH=7.4, by adding 1.5ml to each tube, inverting, centrifuging at 200 x g for 30 sec, and suctioning off buffer
- 6) Add 60 μ l PBS with SDS loading buffer to each sample and boil for 8-10 min to elute. Analyze samples by immunoblot.

Lentiviral Production Protocol

IMPORTANT: The biosafety office at your institution must be notified prior to use of this system for permission and for further institution-specific instructions. BL2 conditions should be used at all times when handling the virus. If oncogenes or potential oncogenes are to be expressed, then BL3 conditions must be used in accord with Caltech Biosafety protocols or those of your institution. Also note that MSCV based vectors with amphotropic or pantropic envelopes also require BL3 conditions if they express oncogenes or potential oncogenes. Contaminated surfaces must be decontaminated with 1% SDS in 70% ethanol. Gloves should be worn at all times when handling lentiviral preparations, transfected cells or the combined transfection reagent and we routinely double-glove when working with lentiviral reagents. Just remember that although this virus has been significantly modified for biosafety, it used to be HIV and with a VSVG pseudotype human cells can be infected even if they are not dividing. That said, the following modifications have been made to prevent viral replication.

1. Packaging vector lacks both LTRs and has no viral packaging signal (y)
2. The following viral genes have been deleted from the packaging vector: env, tat, rev, vpr, vpu, vif and nef.
3. Rev is supplied in trans on a different vector (RSV-Rev).
4. The vector expressing the packaged viral genome has a self-inactivating LTR (TATA box deletion) and expresses no viral gene

products.

5. Envelope, in this case VSVG, is expressed on a separate vector.

For more information please refer to the following papers.

Packaging vectors (pMDLg/pRRE, CMV-VSVG and RSV-Rev):

Dull et al., A Third-Generation Lentivirus Vector with a Conditional Packaging System. *J. Virol.* 1998 72(11): 8463-8472.

Naldini L, Blomer U, Gallay P, Ory D, Mulligan R, Gage FH, Verma IM, Trono D. In vivo gene delivery and stable transduction of nondividing cells by a lentiviral vector. *Science.* 1996 Apr 12;272(5259):263-7.

Self inactivating LTR:

Miyoshi H, Blomer U, Takahashi M, Gage FH, Verma IM.
Development of a self-inactivating lentivirus vector.
J Virol. 1998 Oct;72(10):8150-7.

1. Preparation of 293 cells

Passage 293T cells regularly to prevent clumping. The day before transfection, trypsinize and triturate aggressively. Count cells and dilute them to 0.5×10^6 cells/ml. For concentration reasons, at least 3 x 10 cm plates is best, resulting in 30 ml of viral supernatant.

10 cm plates: 10 ml of cells

15 cm plates: 23 ml of cells

Transfect 12-24 hours after seeding.

2. Transfection

DNA from HR' backbone (lentivirus) sometimes doesn't grow well in DH5 cells.

Transform all constructs into Sure or Top10 cells for maxi preps.

Chapter 1: 10 cm plate: In a 15 ml polypropylene tube mix the following:
5 µg of HR' construct (your viral construct) plus 5 µg pMDLg/pRRE, 5 µg RSV-Rev and 5 µg of VSV-G packaging plasmids. Add 124 µl of 2M CaCl₂, and fill up to 1 ml with ddH₂O.

Chapter 2: 15 cm plate: 7.5 µg of HR' vector plus 7.5 µg pMDLg/pRRE, 7.5 µg RSV-Rev and 7.5 µg VSV-G packaging plasmids. Add 248 µl of 2M CaCl₂, and fill up to 2 ml with ddH₂O.

Chapter 3: To transfect cells, add 1 ml (10 cm plate) or 2 ml (15 cm plate) of 2x HBSS pH=7.05 to the tube containing DNA/CaCl₂/H₂O using a 10ml sterile pipette; quickly and vigorously bubble mixture by pressing eject button on pipette. Drip the 4ml DNA/CaCl₂/HBSS mixture onto a plate of 293T cells, swirl and put the plate back in the incubator. It is wise to dispose of the combined transfection reagent and contaminated tips in the regular biohazard waste. Tips should be first enclosed in a container to prevent "poking through" the bag (e.g. first sealed in a 50 ml conical tube and then disposed of in the biohazard waste).

Chapter 4: 8 hours after adding DNA + HBSS, aspirate medium, and change to 10 ml (10 cm plate) or 20 ml (15 cm plate) of new medium. Pasteur pipettes must be decontaminated by aspirating 100% bleach from a beaker before they are disposed of. Always decontaminate hood surface and potentially contaminated equipment with 70% EtOH at this time whether or not you spilled supernatant. If you know you spilled, please thoroughly decontaminate with 1% SDS in 70% EtOH and then clean up SDS residue with 70% EtOH. Bleach the trap and lines and dispose of liquid within trap after use.

Chapter 5: Allow cells to expand and produce virus for 40 - 48 hours after changing the media. Transfection efficiency using this protocol should approach 50%-80%.

3. Collection and Concentration

Before collecting the viral supernatant, turn on ultracentrifuge and reduce temperature to 4°C.

Recover supernatant and spin for 5 minutes at 1000-1500 rpm to pellet down cell debris. Otherwise, the supernatant may clog the filter. The clinical centrifuge next to the water bath, not the common centrifuge, must be used.

OPTIONAL- If the 293T cells do not appear to be lifting off the plate, we frequently skip this centrifugation step and go straight to filtration.

c. Filter supernatant with a 0.45µm filter (Nalgene). Filters, plates and other contaminated material from this stage must be disposed of in the infectious waste containers managed by the University. If this is unavailable, please dispose of your waste into a separate biohazard bag and autoclave immediately. Always decontaminate hood surface and potentially contaminated equipment with 70% EtOH at this time whether or

not you spilled supernatant. If you know you spilled, please decontaminate with 1% SDS in 70% EtOH.

- d. Add filtered supernatant, up to 30 ml per tube, to 25 x 89 mm Nalgene ultratubes (open-top, thick-walled, polycarbonate). Spin for 90 minutes in a SW 28 swinging bucket rotor at 25000 rpm, 4°C. This also corresponds to 25900 rpm in an SW41Ti rotor.
- e. Pour off supernatant into a beaker (put bleach in the beaker to inactivate the virus) and invert tubes over a Kimwipe that has been draped over a 15 cm plate. The plate prevents draining supernatant onto the tissue culture hood surface. After 5 minutes, aspirate the media residue collected at the opening of the tubes. Bleach Pasteur pipettes before disposal. Dispose of kimwipes and plates in infectious waste container.
- f. Add 100 µl of cold Hanks or PBS (+ Ca & Mg, no bicarbonate) to the tubes and seal tubes with parafilm. Incubate tubes at 4°C for at least 12 hours to dissolve the pellet. After incubation, pipette up and down gently and aliquot the virus into in epp. tubes. Freeze at -70C or use immediately. Dispose of tips in a 50 ml conical tube and seal the tube before disposing in the Caltech infectious waste containers.

4. Cleanup

IMPORTANT: Swinging centrifuge buckets must be rinsed in 70% EtOH after each use regardless of whether a spill is known to have occurred. Ultracentrifuge tubes for lentiviral concentration should be treated overnight in 70% ethanol/1% SDS to inactivate remaining virus and then washed liberally with water for storage. Tubes should not be stored in 70% EtOH long term since it affects strength of the tube. Just prior to reuse, wash ultracentrifuge tubes liberally with water again to assure removal of SDS and finally with sterile PBS. Any objects that come in contact with virus containing media should be decontaminated with 1% SDS in 70% ethanol or autoclaved.

The same procedure should be followed when infecting cells with the virus. When adding virus to cells, use filter tips to transfer virus from eppendorf tubes to cells. Dispose of tips in 50 ml sealed conical tube in Caltech waste container. Please do not use your fingers to remove tips from the pipetman as this is likely to contaminate your gloves with virus which could result in the spread of virus to other surfaces. Rinse Pipetman thoroughly with 70% Ethanol after use. Virus is inactivated after 5-6 hours in 10% serum media. After this time the media can be aspirated into the common container that contains Wescodyne.

5. Infection

Note: infect in as small a volume as is possible while still covering the cells. This forces the virus into contact with the cells and results in very efficient infection.

Some people use the viral supernatants without concentrating (the ultracentrifuge step), but the supernatant from 293Ts and the serum can have unpredictable and toxic effects esp. on primary cells.

- a) Reduce culture media to 300 μ l/well OR 80 μ l/MatTek
- b) Add appropriate amount of shRNA in a total volume of 50 μ l/well OR 20 μ l/MatTek
- c) Replace media after 8-12 hours

Note: Add back media so that cells do not dry out, but do not suction/replace viral-containing media for the next 24 hours
- d) Change media every 24 hours. Allow infection to proceed for the desired amount of time, optimized for experiment and construct; typically, around 48-96 hours.

Co-Immunoprecipitation Protocol

Co-IP lysis buffer: 100mM KCl, 4mM MgCl₂, 10mM HEPES (pH 7.3), 50μM ZnCl, 0.5% NP-40 (add to 10mL: protease inhibitors, phosphatase inhibitors, 20μM NEM)

Co-IP wash buffer: 50mM HEPES (pH=7.8), 150mM NaCl, 1mM MgCl₂, 50μM ZnCl, 0.05% NP-40 (add to 10mL: protease inhibitors, phosphatase inhibitors, 20μM NEM)

***For buffers in co-IPs stabilized by RNA, use DEPC water

Day 1

- 1) Block protein G sepharose beads in 1.5ml NT2 buffer + 5% BSA for 1 hour.
 - i. want 30μl 50% bead slurry per sample

- 2) Centrifuge beads at 200 x g for 25 sec at 4°C, suction off supernatant, and re-suspend in co-IP wash buffer with protease inhibitors, phosphatase inhibitors, and NEM (to 50% slurry).

- 3) Coat beads with Flag antibody or control isotype-specific serum (IgG) rotating at 4°C overnight.

- a. Use about 1 μ g antibody per 100 μ g protein sample

Day 2

- 1) Prepare beads:

- a. Wash beads

- i. Antibody coated beads from day 0 + beads for preclearing (30 μ l 50% slurry per sample). Wash with 1.5ml chilled co-IP wash buffer (invert, spin 200 x g for 25 sec at 4°C, suction off buffer with needle and repeat).

- b. Resuspend beads in 2x excess of co-IP wash buffer with protease inhibitors, phosphatase inhibitors, and NEM (45 μ l per IP final volume).

Neurons only

- 2) BDNF stimulation:

- a. Incubate primary mouse hippocampal cultures, DIV14-17, in serum-reduced media (0.5% B27) for 2 hrs
 - b. Add 40 μ l 1ng/ μ l BDNF (diluted in NBA) to a final concentration of 100ng/ml. Incubate 60-90 minutes.

- 3) Lysis:

- a. Wash cells 2x with ice-cold PBS + 0.9mM MgCl₂

- b. Harvest lysate in polysomal lysis buffer with protease inhibitor cocktail, phosphatase inhibitors, NEM, and freshly added 1mM DTT. Let cells sit in lysis buffer on ice 10 min, scrape, and rotate at 4°C 10 minutes.
 - i. For 24 wells plates, to concentrate lysate, lyse first well in 70µl, subsequent wells in 40µl transferring lysate before scraping.
 - ii. For 10cm dishes, lyse in 800µl/dish
 - c. Centrifuge lysate at 12000 x g, 4°C for 15 minutes. Remove supernatant.
- 4) Protein assay (Bradford) to determine concentration
- 5) Remove a 2.5-10% lysate protein sample, add SDS, boil, and freeze to run on gel later
- 6) Lysate pre-clearing:
- a. Pre-clear lysate with protein G sepharose beads pre-washed in co-IP wash buffer buffer. Add 45µl 3x bead dilution to lysates.
 - b. Incubate 45 min rotating at 4°C, then spin 200 x g for 1 minute at 4°C and remove cleared lysate to new tube.

- 7) Add 45 μ l antibody bound beads (now 15 μ l beads in 33% suspension) to protein lysate.
 - a. Use p200 tips with ends cut off
 - b. Incubate rotating 3-4 hours at 4°C

- 8) Washes:
 - a. Wash 3x with 1.5 μ l cold co-IP wash buffer with protease inhibitors, phosphatase inhibitors, and NEM by filling tube, resuspending, and then briefly spinning the beads in an eppendorf tube at 200 x g, 4°C for 25 sec. Use vacuum line with needle to suction off supernatant (careful not to remove the beads!)
 - b. For third wash, let rotate at 4°C for 5-10 minutes before suctioning off supernatant.
 - c. Wash 1x with 1ml cold co-IP wash buffer WITHOUT protease inhibitors/phosphatase inhibitors/NEM, spin for 1 minute at 200 x g 4°C, and remove buffer entirely with vacuum suction.

- 9) Elution with FLAG peptide
 - a. Add 30 μ l of peptide, diluted in NT2 to 100 μ g/ml (1:40 from stock)
 - b. Rotate 30 min-1 hr at ROOM TEMP
 - c. Spin 10 sec at 12000 x g at ROOM TEMP
 - d. Collect 30 μ l of eluent 1
 - e. Repeat steps 2x and collect eluents 2 and 3

- f. Combine eluents (60 μ l) and spin for 10 sec at 12000 x g
- g. Pipet off 30 μ l of eluent
- h. Boil samples with loading dye for SDS-PAGE analysis

Day 2

1) Prepare beads:

a. Wash beads

- i. Wash antibody coated beads from day 1 and beads for preclearing (see Day 2 Step 6). Wash twice with 1.5ml chilled IP wash buffer (invert, spin 200 x g for 25 sec at 4°C, suction off buffer with crushed pipette tip and repeat).

- b. Resuspend beads in 2x excess of stringent IP wash buffer + protease/phosphatase inhibitor (e.g. resuspend 15µl beads in 30µl NT2).

2) Harvest/lysis:

- a. Wash cells 2x with ice-cold PBS + 0.9mM MgCl₂

- b. Harvest lysate in IP lysis buffer with protease inhibitor cocktail, phosphatase inhibitors, and freshly added 1mM DTT. Let cells sit in lysis buffer on ice 10 min, scrape, and rotate at 4°C 10 minutes.

- i. For 24 wells plates, to concentrate lysate, lyse first well in 70µl, subsequent wells in 40µl transferring lysate before scraping.

- ii. For 10cm dishes, lyse in 800µl/dish

- c. Centrifuge lysate at 13.2 x g, 4°C for 15 minutes. Remove supernatant.

- 3) Protein assay (Bradford) to determine concentration
- 4) Remove a 10% lysate protein sample, add SDS buffer, boil, and freeze to run on gel later
- 5) Lysate pre-clearing:
 - a. Pre-clear lysate with protein G sepharose beads pre-washed in stringent IP wash buffer (step 1)
 - b. Preclear with 1 μ l beads (20 μ l 50% bead slurry, 30 μ l 33% bead slurry)
 - c. Incubate 30 min rotating at 4°C, then spin 200 x g for 1 minute at 4°C and remove cleared lysate to new tube.
 - d. Repeat, incubating for 30 min rotating at 4°C. Spin for 200 x g for 1 minute at 4°C and remove cleared lysate to new tube.
- 6) Add 30 μ l antibody bound beads (10 μ l beads in 33% suspension) to protein lysate.
 - a. Incubate rotating 3-4 hours at 4°C
- 7) Washes
 - a. Wash 3x with 1.5ml cold stringent IP wash buffer + protease and phosphatase inhibitors by filling eppendorf tube, resuspending, and then briefly spinning the beads at 200 x g, 4°C for 25 sec. Use

vacuum line with crushed pipette tip to suction off supernatant
(careful not to remove the beads!)

- i. For third wash, let rotate at 4°C for 10 minutes before suctioning off supernatant.
- b. Wash 1x with 1ml cold stringent IP wash buffer WITHOUT protease/phosphatase inhibitors, spin for 1 minute at 200 x g 4°C, and remove buffer entirely with vacuum suction.

8) Elution with FLAG peptide

- a. Add 30µl of peptide, diluted in stringent IP wash buffer to 100µg/ml
- b. Rotate 1-2 hr at ROOM TEMP
- c. Spin 10 sec at 12000 x g at ROOM TEMP
- d. Collect 30µl of eluent 1
- e. Repeat steps 2X and collect eluents 2 and 3
- f. Combine eluents (about 90µl) and spin for 10 sec at 12000 x g
- g. Pipet off 30µl of eluent, 2x, to make 2 loading samples for each condition
- h. Boil samples with loading dye for SDS-PAGE analysis

OR

9) Elution by boiling

- a. Resuspend beads in stringent IP wash buffer + 6X SDS loading buffer (72µl /sample total)
- b. Boil 90°C for 5-10 minutes

- c. Spin 10sec at 12000 x g at ROOM TEMP
- d. Pipette off supernatant and save for gel

RNA isolation, purification, and analysis

Note: At all steps, keep tubes on ice whenever possible

Lysis

- 1) Lyse cells in 1ml TRI-REAGENT per sample
- 2) Let sit for 5 minutes, vortex if necessary 10 sec to permit complete dissociation of nucleoprotein complexes. Samples can be frozen at 80°C until experimenter is ready to proceed with the protocol.

Phase separation

- 1) Add 200µl chloroform per 1ml of TRI-REAGENT. Mix well for 30 sec by inversion.
- 2) Let sit on ice for 3 min to allow layers to separate
- 3) Centrifuge at 12,000 x g for 15 min at 4°C (DNA contamination will be present in RNA if temperature is higher than 4°C)
- 4) 3 phases form: colorless upper aqueous phase (RNA); white interphase (DNA); lower red, phenol-chloroform organic phase (protein)

RNA precipitation

- 1) Transfer the aqueous phase (around 400-600µl per 1mL TRI-REAGENT) to a fresh tube (be careful to not be greedy, avoid DNA contamination)
- 2) Add 600µl isopropanol, mix well, and incubate for 20 min
- 3) Centrifuge at 12,000 xg for 20 min at 4°C

RNA wash

- 1) Decant supernatant into separate tubes to ensure no pellet is lost
- 3) Add 1ml 75% RNase-free ethanol to tubes containing pellets and invert to mix ***pellet will not go into solution
- 4) Centrifuge at 12,000 x g for 5 min at 4°C
- 5) Repeat ethanol wash

RNA solubilization

- 1) Decant ethanol into separate tubes to ensure no pellet is lost
- 2) Air dry for 3-5 min ***do not dry past when pellets start to turn transparent, or solubility will significantly decrease
- 3) Resuspend pellets in 20µl sterile DEPC water.
- 4) Read RNA concentration using a NanoDrop spectrophotometer. OD 260/280 (protein contamination) and 260/230 (organic solvent, EDTA contamination) ratios should both be >1.8.
- 5) Immediately proceed to reverse transcription for cDNA, without freeze-thaw.

Reverse transcription for mRNA

- 1) Using TaqMan High Capacity RNA to cDNA Kit, make RNA/primer mixture: 2µg RNA, 2µl random decamer (Applied Biosystems), 2µl oligo(dT) primer (Promega), plus water up to 16µl.

2) Master mix: 14 μ l/reaction, 30 μ l for total reaction

-MultiScribe Reverse Transcriptase (Applied Biosystems): 2 μ l

-RT buffer (10X): 3 μ l (100mM Tris pH 8.3, 500mM KCl)

-dNTP (10 nM, Qiagen) 8 μ l

-RNaseOut (Invitrogen): 1 μ l

3) Thermal cycler setting

-RNA/primer mixture: heat at 75°C for 3 min

-Cool to 4°C for 3 min, PAUSE

-Add master mix 20 μ l, mix well by gentle pipetting and hit GO TO
NEXT

-Incubate 37°C for 1 hour

-Inactivate 95°C for 5 min

Reverse transcription for individual microRNA

1) RNA: 10ng in 5 μ l

2) Master mix: 10 μ l/reaction, 15 μ l total reaction

-RT buffer: 1.5 μ l

-dNTP (100 nM, Qiagen): 0.15 μ l

-RNaseOut (Invitrogen): 0.2 μ l

-Individual stem-looped RT primer (20X or 60X)

-Water to 10 μ l

3) Thermal cycler setting

-4°C, 5 min

-16°C, 30 min

-42°C, 30 min

-85°C, 5 min

BrdU Incorporation Protocol

Labeling

- 1) Plate HEI193 cells at 1×10^4 /35mm glass bottom MatTek cell culture dish for 24 hours
- 2) Serum starve (0% FBS) for 24 hours
- 3) Replace media with complete media containing 10 μ M BrdU for 8hrs.

Harvest for Immunoblot

- 1) Prior to IHC, take one MatTek dish from each condition and harvest cells on ice
 - a. Let sit 10 min in 40 μ l lysis buffer per MatTek
 - b. Scrape cells on ice
 - c. Rotate lysate for 10 min at 4°C followed by high speed centrifugation for 15 min at 12,000 x g at 4°C
 - d. Save supernatant for analysis
- 2) Analyze protein lysate by immunoblot to biochemically confirm efficacy of treatment conditions

IHC

- 1) Rinse briefly in warm PBS (200 μ L/dish; warm at 37°C)
- 2) Suction off PBS and fix in 4% PFA/4% sucrose/PBS for 30-40 min at room temp

**Thaw PFA buffer at 37°C

- 3) Remove PFA with 200 μ L pipette into PFA waste
- 4) Rinse 3X with PBS
- 5) Suction and permeabilize for 30-40 min in 0.2% triton X-100/PBS
- 6) Rinse 3x with PBS
- 7) Incubate in 2M HCl at 37 degrees C for 30 min
- 8) Wash 1X PBS
- 9) Incubate in 0.1M borate buffer for 5 min, twice
- 10) Wash 2X PBS
- 11) Block in 10% BSA/PBS for at least 1 hr at room temp
- 12) Primary antibody (mouse anti-BrdU) overnight in 10% BSA/PBS at 4°C
- 13) Wash 3x PBS, let sit 10 min room temp
- 14) Secondary antibody (Alexa 488 mouse)
- 15) Wash 2x PBS, let sit 10 min room temp
- 16) Wash 1x PBS containing DAPI stain (2 drops/1mL PBS), let sit 10 min
room temp
- 17) Add 150 μ L mounting media and coverslips
- 18) Seal with agar

- 2) Centrifuge beads at 200 x g for 25 sec at 4°C. Suction off supernatant, and re-suspend in stringent IP wash buffer (to 50% slurry).
- 3) Coat beads with myc antibody rotating at 4°C overnight.
 - a. Use about 1µg antibody per expected 100µg protein sample

Day 4: Pulse Chase

- 1) Wash wells 2X with DMEM **without cysteine/methionine**, then pre-treat for 15 minutes in DMEM **without cysteine/methionine** + 0.5% B27 + glutamine (place cells in incubator).
- 2) Add ³⁵S methionine to wells for labeling phase
 - a. Dilute ³⁵S (stock: 11mci/ml) to 600µci/ml in DMEM-cys,met. Suction wells down to 250µl volume and add ³⁵S in 50µL volume to a final concentration of 100µci/ml.
 - b. Label for 3 hours in incubator
- 3) Chase
 - a. Wash wells 3X with NBA + 2% B27 + glutamine. Deposit wash waste in liquid radioactivity beaker.
 - b. Add back NBA + 2% B27 + glutamine

- c. BDNF/mock stimulation: Suction volume down to about 360 μ l in well. Add 40 μ l 1ng/ μ l BDNF (or empty media, mock) to final concentration of 100ng/ml.
 - d. Incubate cells with BDNF/empty media for desired chase period.
- ***I stagger my labeling/chase phase between samples so that I harvest all samples at the same time, regardless of the length of the chase***

4) Harvest

- a. At the end of desired chase period, place cells on ice and wash 2X with PBS + .9mM MgCl₂ (deposit waste in liquid radioactivity beaker)
- b. Harvest lysate in stringent IP lysis buffer (pH=7.3) + protease inhibitor cocktail + phosphatase inhibitors and freshly added 1mM DTT. Let cells sit in lysis buffer on ice 10 min prior to scraping.
 - i. If necessary, to concentrate lysate, add 70 μ l to first well and 40 μ l to subsequent wells. Transfer lysate from previous to next well prior to scraping.
- c. Rotate harvested lysate for 10min at 4°C
- d. Centrifuge lysate at 13.2 X g at 4°C for 15 minutes. Remove supernatant.

5) Protein assay (BCA) to determine concentration of samples

6) Remove 5-10% lysate (depending on amount to IP) for input sample. Add SDS, boil, and freeze to run on gel later.

7) IP

- a. Prepare beads: Wash myc antibody coated beads from day 3 with 1.5ml chilled stringent IP wash buffer (invert, spin 200 x g for 25 sec at 4°C, suction off buffer) twice. Resuspend in 2X excess of stringent IP wash buffer with protease and phosphatase inhibitors (e.g. 30µl of stringent IP wash buffer to 15µl beads per IP)
- b. Add 45l 33% myc-bead slurry to protein lysate for IP. IP around 1mg protein per sample.
 - i. Use p200 tips with ends cut off
 - ii. **Incubate rotating 3-4 hours at 4°C**

8) Washes

- a. Wash 3X with 1.5 µl cold stringent IP wash buffer with protease and phosphatase inhibitors by filling tube, resuspending, and then briefly centrifuging at 200 x g, 4°C for 25 sec. Use vacuum line to suction off supernatant; crush pipette tip with tweezers to decrease tip diameter.
- b. Wash 1X with 1.5ml cold stringent IP wash buffer WITHOUT inhibitors and spin for 1 minute at 200 x g 4°C. Remove buffer entirely.

9) Elution

- a. Add 36 μ l stringent IP wash buffer + 6X SDS buffer to each bead sample. Boil 10 minutes.
- b. Spin down 10 sec 12000 x g at room temp. Pipette off liquid sample and save for SDS-PAGE analysis.

Day 5: Phosphoimage and SDS-PAGE analysis

- 1) Run acrylamide gel with both input and IP elution samples; transfer during day or O/N
- 2) Let membrane dry and place in phosphoimager cassette O/N
- 3) Use typhoon imager (Green lab) to obtain phosphoimage of myc-Lin28a IP
- 4) Myc immunoblot
 - a. Use rabbit anti-myc antibody (sigma) at 1:5000 for 2 hours RT

Remember to clear phosphoimager cassette right before and after use

Quickchange Mutation Protocol to Generate shRNA-resistant Constructs

Primer Design

- 1) Design two complementary primers containing desired mutation
 - a. Flank mutation by ~15 unmodified nucleotides (25-45 total nt)
 - b. Minimum %GC > 40%
 - c. Terminate in one or more G/C
 - d. $T_m > -78^\circ\text{C}$
- 2) Sequences:
 - a. FSW-TRBPS Δ A*:
GGCAATGAGGTGGAGCCCGATGATGACCACTTC
 - b. FLAG-Lin28a*:
CTGCCACCCCAGCCCAAAAAATGICACTTCTGCCAGAGC

PCR

- 1) Reaction:
 - a. 10ng DNA per reaction
 - b. 0.2 μ M primer mix per reaction
 - c. 1mM dNTPs per reaction
 - d. 0.5 μ l Phusion polymerase per reaction

Note: Add Magnesium/DMSO if required
- 2) Program:
 - a. 95°C 5 min
 - b. 95°C 1 min

- c. 69°C 1 min
- d. 72°C 10 min
- e. Repeat b-d X 15
- f. 4°C forever

Dpn1 Digest

- 1) Reaction:
 - a. 40µl PCR product per digest
 - b. 40 units Dpn1 per digest
 - c. Total volume: 50µl per digest
- 2) Incubate 2-3hrs at 37°C
- 3) Heat inactivate 20 min at 80°C
- 4) Transform 3µl DNA digest
- 5) Plate 5µl digested construct in 75µl LB+

Processing and Imaging for Scholl Analysis

1) Transfection

Neurons were transfected 48 hours prior to imaging with 10ng FL-Lin28a coding region or PCDNA3.1 (empty vector control) and 5ng soluble mCherry fluorophore per 35mm MatTek dish using Lipofectamine 2000 reagent, according to the manufacturer's instructions. Dishes were randomly assigned to conditions, and the experimenter was blinded to condition assignment throughout the imaging/analysis process.

2) Stimulation

- a. Incubate cultures in serum starvation media (0.5% B27) for 2 hours
- b. Suction media down to 90 μ l per MatTek and add 10 μ l 1 μ g/ml BDNF to a final concentration of 100ng/ml.
- c. Incubate with BDNF for 1 hour at 37°C

3) IHC

- a. Rinse briefly in warm PBS (200 μ L/dish; warm at 37°C)
- b. Suction off PBS and fix in 4% PFA/4% sucrose/PBS for 30-40 min at room temp

**Thaw PFA buffer at 37°C
- c. Remove PFA with 200 μ L pipette into PFA waste
- d. Rinse 3X with PBS

- e. Suction and permeabilize for 30-40 min in 0.2% triton X-100/PBS
- f. Rinse 3x with PBS
- g. Block in 10% BSA/PBS for at least 1 hr at room temp
- h. Primary antibody (mouse anti-mCherry) overnight in 10% BSA/PBS at 4°C
- i. Wash 3x PBS, let sit 10 min room temp
- j. Secondary antibody (Alexa 568 mouse)
- k. Wash 3X PBS, let sit 10 min room temp during each wash
- l. Add 150µL mounting media and coverslips
- m. Seal with agar

4) Imaging

Confocal images of hippocampal pyramidal neurons (determined by morphology) were acquired using a 40x objective on a Yokogawa spinning disk system (Cell Observer, Carl Zeiss). All experimental conditions were from a minimum of 3 independent cultures, no more than 4 neurons per dish.

5) Scholl analysis

Scholl analysis was performed using the Scholl plugin in ImageJ (A. Ghosh lab). Z-compressed neuronal projections were semi-automatically traced. Dendritic arborization was quantified using a circle of 15µm diameter centered on the cell soma, with subsequent circles of increasing

5 μ m increments. The number of intersections between dendritic projections and circles at differing distances from the soma were counted and analyzed.

References

- Aakalu, G., Smith, W.B., Nguyen, N., Jiang, C., and Schuman, E.M. (2001). Dynamic visualization of local protein synthesis in hippocampal neurons. *Neuron* 30, 489-502.
- Agnihotri, S., Gugel, I., Remke, M., Bornemann, A., Pantazis, G., Mack, S.C., Shih, D., Singh, S.K., Sabha, N., Taylor, M.D., *et al.* (2014). Gene-expression profiling elucidates molecular signaling networks that can be therapeutically targeted in vestibular schwannoma. *J Neurosurg* 121, 1434-1445.
- Alonso, M., Medina, J.H., and Pozzo-Miller, L. (2004). ERK1/2 activation is necessary for BDNF to increase dendritic spine density in hippocampal CA1 pyramidal neurons. *Learn Mem* 11, 172-178.
- Andero, R., and Ressler, K.J. (2012). Fear extinction and BDNF: translating animal models of PTSD to the clinic. *Genes Brain Behav* 11, 503-512.
- Andreska, T., Aufmkolk, S., Sauer, M., and Blum, R. (2014). High abundance of BDNF within glutamatergic presynapses of cultured hippocampal neurons. *Front Cell Neurosci* 8, 107.
- Arakawa, H., Hayashi, N., Nagase, H., Ogawa, M., and Nakamura, Y. (1994). Alternative splicing of the NF2 gene and its mutation analysis of breast and colorectal cancers. *Hum Mol Genet* 3, 565-568.
- Ashraf, S.I., McLoon, A.L., Sclarsic, S.M., and Kunes, S. (2006). Synaptic protein synthesis associated with memory is regulated by the RISC pathway in *Drosophila*. *Cell* 124, 191-205.
- Balzer, E., Heine, C., Jiang, Q., Lee, V.M., and Moss, E.G. (2010). LIN28 alters cell fate succession and acts independently of the let-7 microRNA during neurogenesis in vitro. *Development* 137, 891-900.
- Bassell, G.J., and Warren, S.T. (2008). Fragile X syndrome: loss of local mRNA regulation alters synaptic development and function. *Neuron* 60, 201-214.
- Bekinschtein, P., Cammarota, M., Igaz, L.M., Bevilacqua, L.R., Izquierdo, I., and Medina, J.H. (2007). Persistence of long-term memory storage requires a late protein synthesis- and BDNF- dependent phase in the hippocampus. *Neuron* 53, 261-277.
- Bhakar, A.L., Dolen, G., and Bear, M.F. (2012). The pathophysiology of fragile X (and what it teaches us about synapses). *Annu Rev Neurosci* 35, 417-443.

- Bingol, B., and Schuman, E.M. (2006). Activity-dependent dynamics and sequestration of proteasomes in dendritic spines. *Nature* 441, 1144-1148.
- Blakeley, J.O., Evans, D.G., Adler, J., Brackmann, D., Chen, R., Ferner, R.E., Hanemann, C.O., Harris, G., Huson, S.M., Jacob, A., *et al.* (2012). Consensus recommendations for current treatments and accelerating clinical trials for patients with neurofibromatosis type 2. *Am J Med Genet A* 158A, 24-41.
- Bolton, P.F., Roobol, M., Allsopp, L., and Pickles, A. (2001). Association between idiopathic infantile macrocephaly and autism spectrum disorders. *Lancet* 358, 726-727.
- Buganim, Y., Faddah, D.A., Cheng, A.W., Itskovich, E., Markoulaki, S., Ganz, K., Klemm, S.L., van Oudenaarden, A., and Jaenisch, R. (2012). Single-cell expression analyses during cellular reprogramming reveal an early stochastic and a late hierarchic phase. *Cell* 150, 1209-1222.
- Calin, G.A., Sevignani, C., Dumitru, C.D., Hyslop, T., Noch, E., Yendamuri, S., Shimizu, M., Rattan, S., Bullrich, F., Negrini, M., *et al.* (2004). Human microRNA genes are frequently located at fragile sites and genomic regions involved in cancers. *Proc Natl Acad Sci U S A* 101, 2999-3004.
- Castren, M.L., and Castren, E. (2014). BDNF in fragile X syndrome. *Neuropharmacology* 76 Pt C, 729-736.
- Chang, H.M., Triboulet, R., Thornton, J.E., and Gregory, R.I. (2013). A role for the Perlman syndrome exonuclease Dis3l2 in the Lin28-let-7 pathway. *Nature* 497, 244-248.
- Chang, T.C., Zeitels, L.R., Hwang, H.W., Chivukula, R.R., Wentzel, E.A., Dews, M., Jung, J., Gao, P., Dang, C.V., Beer, M.A., *et al.* (2009). Lin-28B transactivation is necessary for Myc-mediated let-7 repression and proliferation. *Proc. Natl. Acad. Sci. USA* 106, 3384-3389.
- Chawla, G., and Sokol, N.S. (2012). Hormonal activation of let-7-C microRNAs via EcR is required for adult *Drosophila melanogaster* morphology and function. *Development* 139, 1788-1797.
- Chendrimada, T.P., Gregory, R.I., Kumaraswamy, E., Norman, J., Cooch, N., Nishikura, K., and Shiekhattar, R. (2005). TRBP recruits the Dicer complex to Ago2 for microRNA processing and gene silencing. *Nature* 436, 740-744.
- Cheng, J.Q., Lee, W.C., Klein, M.A., Cheng, G.Z., Jhanwar, S.C., and Testa, J.R. (1999). Frequent mutations of NF2 and allelic loss from chromosome band 22q12 in malignant mesothelioma: evidence for a two-hit mechanism of NF2 inactivation. *Genes Chromosomes Cancer* 24, 238-242.

- Cheung, Z.H., Chin, W.H., Chen, Y., Ng, Y.P., and Ip, N.Y. (2007). Cdk5 is involved in BDNF-stimulated dendritic growth in hippocampal neurons. *PLoS Biol* 5, e63.
- Cho, J., Chang, H., Kwon, S.C., Kim, B., Kim, Y., Choe, J., Ha, M., Kim, Y.K., and Kim, V.N. (2012). LIN28A is a suppressor of ER-associated translation in embryonic stem cells. *Cell* 151, 765-777.
- Conner, J.M., Lauterborn, J.C., Yan, Q., Gall, C.M., and Varon, S. (1997). Distribution of brain-derived neurotrophic factor (BDNF) protein and mRNA in the normal adult rat CNS: evidence for anterograde axonal transport. *J Neurosci* 17, 2295-2313.
- Correia, C.T., Coutinho, A.M., Sequeira, A.F., Sousa, I.G., Lourenco Venda, L., Almeida, J.P., Abreu, R.L., Lobo, C., Miguel, T.S., Conroy, J., *et al.* (2010). Increased BDNF levels and NTRK2 gene association suggest a disruption of BDNF/TrkB signaling in autism. *Genes Brain Behav* 9, 841-848.
- Courchesne, E., Mouton, P.R., Calhoun, M.E., Semendeferi, K., Ahrens-Barbeau, C., Hallet, M.J., Barnes, C.C., and Pierce, K. (2011). Neuron number and size in prefrontal cortex of children with autism. *JAMA* 306, 2001-2010.
- Dai, X., Fan, W., Wang, Y., Huang, L., Jiang, Y., Shi, L., McKinley, D., Tan, W., and Tan, C. (2015). Combined Delivery of Let-7b MicroRNA and Paclitaxel via Biodegradable Nanoassemblies for the Treatment of KRAS Mutant Cancer. *Mol Pharm.*
- Dajas-Bailador, F., Bonev, B., Garcez, P., Stanley, P., Guillemot, F., and Papalopulu, N. (2012). microRNA-9 regulates axon extension and branching by targeting Map1b in mouse cortical neurons. *Nat Neurosci*.
- Daniels, S.M., Melendez-Pena, C.E., Scarborough, R.J., Daher, A., Christensen, H.S., El Far, M., Purcell, D.F., Laine, S., and Gatignol, A. (2009). Characterization of the TRBP domain required for dicer interaction and function in RNA interference. *BMC Mol Biol* 10, 38.
- Darnell, J.C., Van Driesche, S.J., Zhang, C., Hung, K.Y., Mele, A., Fraser, C.E., Stone, E.F., Chen, C., Fak, J.J., Chi, S.W., *et al.* (2011). FMRP stalls ribosomal translocation on mRNAs linked to synaptic function and autism. *Cell* 146, 247-261.
- De Palma, M., and Naldini, L. (2010). Antagonizing metastasis. *Nat Biotechnol* 28, 331-332.
- Ehlers, M.D. (2003). Activity level controls postsynaptic composition and signaling via the ubiquitin-proteasome system. *Nat Neurosci* 6, 231-242.

Ernfors, P., Kucera, J., Lee, K.F., Loring, J., and Jaenisch, R. (1995). Studies on the physiological role of brain-derived neurotrophic factor and neurotrophin-3 in knockout mice. *Int J Dev Biol* 39, 799-807.

Evans, D.G., Huson, S.M., Donnai, D., Neary, W., Blair, V., Newton, V., and Harris, R. (1992). A clinical study of type 2 neurofibromatosis. *Q J Med* 84, 603-618.

Evans, D.G., Trueman, L., Wallace, A., Collins, S., and Strachan, T. (1998). Genotype/phenotype correlations in type 2 neurofibromatosis (NF2): evidence for more severe disease associated with truncating mutations. *J Med Genet* 35, 450-455.

Fifkova, E., Anderson, C.L., Young, S.J., and Van Harrevel, A. (1982). Effect of anisomycin on stimulation-induced changes in dendritic spines of the dentate granule cells. *J Neurocytol* 11, 183-210.

Finkbeiner, S., Tavazoie, S.F., Maloratsky, A., Jacobs, K.M., Harris, K.M., and Greenberg, M.E. (1997). CREB: a major mediator of neuronal neurotrophin responses. *Neuron* 19, 1031-1047.

Fiore, R., Khudayberdiev, S., Christensen, M., Siegel, G., Flavell, S.W., Kim, T.K., Greenberg, M.E., and Schratt, G. (2009). Mef2-mediated transcription of the miR379-410 cluster regulates activity-dependent dendritogenesis by fine-tuning Pumilio2 protein levels. *EMBO J* 28, 697-710.

Foss, E.J., Radulovic, D., Shaffer, S.A., Goodlett, D.R., Kruglyak, L., and Bedalov, A. (2011). Genetic variation shapes protein networks mainly through non-transcriptional mechanisms. *PLoS Biol* 9, e1001144.

Frost, R.J., and Olson, E.N. (2011). Control of glucose homeostasis and insulin sensitivity by the Let-7 family of microRNAs. *Proc Natl Acad Sci U S A* 108, 21075-21080.

Fukunaga, R., Han, B.W., Hung, J.H., Xu, J., Weng, Z., and Zamore, P.D. (2012). Dicer partner proteins tune the length of mature miRNAs in flies and mammals. *Cell* 151, 533-546.

Gal-Ben-Ari, S., Kenney, J.W., Ounalla-Saad, H., Taha, E., David, O., Levitan, D., Gildish, I., Panja, D., Pai, B., Wibrand, K., *et al.* (2012). Consolidation and translation regulation. *Learn Mem* 19, 410-422.

Gehrke, S., Imai, Y., Sokol, N., and Lu, B. (2010). Pathogenic LRRK2 negatively regulates microRNA-mediated translational repression. *Nature* 466, 637-641.

Gingras, A.C., Raught, B., and Sonenberg, N. (1999). eIF4 initiation factors: effectors of mRNA recruitment to ribosomes and regulators of translation. *Annu Rev Biochem* 68, 913-963.

- Gingras, A.C., Raught, B., and Sonenberg, N. (2004). mTOR signaling to translation. *Curr Top Microbiol Immunol* 279, 169-197.
- Giraldez, A.J., Cinalli, R.M., Glasner, M.E., Enright, A.J., Thomson, J.M., Baskerville, S., Hammond, S.M., Bartel, D.P., and Schier, A.F. (2005). MicroRNAs regulate brain morphogenesis in zebrafish. *Science* 308, 833-838.
- Guerrero, P.A., Yin, W., Camacho, L., and Marchetti, D. (2015). Oncogenic role of Merlin/NF2 in glioblastoma. *Oncogene* 34, 2621-2630.
- Haase, A.D., Jaskiewicz, L., Zhang, H., Laine, S., Sack, R., Gatignol, A., and Filipowicz, W. (2005). TRBP, a regulator of cellular PKR and HIV-1 virus expression, interacts with Dicer and functions in RNA silencing. *EMBO Rep* 6, 961-967.
- Hammell, C.M., Karp, X., and Ambros, V. (2009). A feedback circuit involving let-7-family miRNAs and DAF-12 integrates environmental signals and developmental timing in *Caenorhabditis elegans*. *Proc Natl Acad Sci U S A* 106, 18668-18673.
- Hartmann, M., Heumann, R., and Lessmann, V. (2001). Synaptic secretion of BDNF after high-frequency stimulation of glutamatergic synapses. *EMBO J* 20, 5887-5897.
- He, X.Y., Chen, J.X., Zhang, Z., Li, C.L., Peng, Q.L., and Peng, H.M. (2010). The let-7a microRNA protects from growth of lung carcinoma by suppression of k-Ras and c-Myc in nude mice. *J Cancer Res Clin Oncol* 136, 1023-1028.
- Heldt, S.A., Stanek, L., Chhatwal, J.P., and Ressler, K.J. (2007). Hippocampus-specific deletion of BDNF in adult mice impairs spatial memory and extinction of aversive memories. *Mol Psychiatry* 12, 656-670.
- Heo, I., Ha, M., Lim, J., Yoon, M.J., Park, J.E., Kwon, S.C., Chang, H., and Kim, V.N. (2012). Mono-uridylation of pre-microRNA as a key step in the biogenesis of group II let-7 microRNAs. *Cell* 151, 521-532.
- Heo, I., Joo, C., Cho, J., Ha, M., Han, J., and Kim, V.N. (2008). Lin28 mediates the terminal uridylation of let-7 precursor MicroRNA. *Mol Cell* 32, 276-284.
- Heo, I., Joo, C., Kim, Y.K., Ha, M., Yoon, M.J., Cho, J., Yeom, K.H., Han, J., and Kim, V.N. (2009). TUT4 in concert with Lin28 suppresses microRNA biogenesis through pre-microRNA uridylation. *Cell* 138, 696-708.
- Hikasa, H., Sekido, Y., and Suzuki, A. (2016). Merlin/NF2-Lin28B-let-7 Is a Tumor-Suppressive Pathway that Is Cell-Density Dependent and Hippo Independent. *Cell Rep* 14, 2950-2961.

- Holt, C.E., and Schuman, E.M. (2013). The central dogma decentralized: new perspectives on RNA function and local translation in neurons. *Neuron* 80, 648-657.
- Horch, H.W., and Katz, L.C. (2002). BDNF release from single cells elicits local dendritic growth in nearby neurons. *Nat Neurosci* 5, 1177-1184.
- Huang, Y.S., Jung, M.Y., Sarkissian, M., and Richter, J.D. (2002). N-methyl-D-aspartate receptor signaling results in Aurora kinase-catalyzed CPEB phosphorylation and alpha CaMKII mRNA polyadenylation at synapses. *EMBO J* 21, 2139-2148.
- Huang, Y.W., Ruiz, C.R., Eyler, E.C., Lin, K., and Meffert, M.K. (2012). Dual regulation of miRNA biogenesis generates target specificity in neurotrophin-induced protein synthesis. *Cell* 148, 933-946.
- Hung, G., Li, X., Faudoa, R., Xeu, Z., Kluwe, L., Rhim, J.S., Slattery, W., and Lim, D. (2002). Establishment and characterization of a schwannoma cell line from a patient with neurofibromatosis 2. *Int J Oncol* 20, 475-482.
- Ideker, T., Thorsson, V., Ranish, J.A., Christmas, R., Buhler, J., Eng, J.K., Bumgarner, R., Goodlett, D.R., Aebersold, R., and Hood, L. (2001). Integrated genomic and proteomic analyses of a systematically perturbed metabolic network. *Science* 292, 929-934.
- Iliopoulos, D., Hirsch, H.A., and Struhl, K. (2009). An epigenetic switch involving NF-kappaB, Lin28, Let-7 MicroRNA, and IL6 links inflammation to cell transformation. *Cell* 139, 693-706.
- Inamura, N., Nawa, H., and Takei, N. (2005). Enhancement of translation elongation in neurons by brain-derived neurotrophic factor: implications for mammalian target of rapamycin signaling. *J Neurochem* 95, 1438-1445.
- Jaworski, J., Spangler, S., Seeburg, D.P., Hoogenraad, C.C., and Sheng, M. (2005). Control of dendritic arborization by the phosphoinositide-3'-kinase-Akt-mammalian target of rapamycin pathway. *J Neurosci* 25, 11300-11312.
- Je, H.S., Lu, Y., Yang, F., Nagappan, G., Zhou, J., Jiang, Z., Nakazawa, K., and Lu, B. (2009a). Chemically inducible inactivation of protein synthesis in genetically targeted neurons. *J Neurosci* 29, 6761-6766.
- Je, H.S., Lu, Y., Yang, F., Nagappan, G., Zhou, J., Jiang, Z., Nakazawa, K., and Lu, B. (2009b). Chemically inducible inactivation of protein synthesis in genetically targeted neurons. *J. Neurosci.* 29, 6761-6766.
- Jenuwein, T., and Allis, C.D. (2001). Translating the histone code. *Science* 293, 1074-1080.

- Jia, J.M., Chen, Q., Zhou, Y., Miao, S., Zheng, J., Zhang, C., and Xiong, Z.Q. (2008). Brain-derived neurotrophic factor-tropomyosin-related kinase B signaling contributes to activity-dependent changes in synaptic proteins. *J Biol Chem* 283, 21242-21250.
- Jones, K.R., Farinas, I., Backus, C., and Reichardt, L.F. (1994). Targeted disruption of the BDNF gene perturbs brain and sensory neuron development but not motor neuron development. *Cell* 76, 989-999.
- Jourdi, H., Hsu, Y.T., Zhou, M., Qin, Q., Bi, X., and Baudry, M. (2009). Positive AMPA receptor modulation rapidly stimulates BDNF release and increases dendritic mRNA translation. *J Neurosci* 29, 8688-8697.
- Juhila, J., Sipila, T., Icaý, K., Nicorici, D., Ellonen, P., Kallio, A., Korpelainen, E., Greco, D., and Hovatta, I. (2011). MicroRNA expression profiling reveals miRNA families regulating specific biological pathways in mouse frontal cortex and hippocampus. *PLoS One* 6, e21495.
- Jung, J.R., Kim, H., Jeun, S.S., Lee, J.Y., Koh, E.J., and Ji, C. (2005). The Phosphorylation status of merlin is important for regulating the Ras-ERK pathway. *Mol Cells* 20, 196-200.
- Kajiya, M., Shiba, H., Fujita, T., Takeda, K., Uchida, Y., Kawaguchi, H., Kitagawa, M., Takata, T., and Kurihara, H. (2009). Brain-derived neurotrophic factor protects cementoblasts from serum starvation-induced cell death. *J Cell Physiol* 221, 696-706.
- Kalita, K., Kharebava, G., Zheng, J.J., and Hetman, M. (2006). Role of megakaryoblastic acute leukemia-1 in ERK1/2-dependent stimulation of serum response factor-driven transcription by BDNF or increased synaptic activity. *J Neurosci* 26, 10020-10032.
- Kanhema, T., Dagestad, G., Panja, D., Tiron, A., Messaoudi, E., Havik, B., Ying, S.W., Nairn, A.C., Sonenberg, N., and Bramham, C.R. (2006). Dual regulation of translation initiation and peptide chain elongation during BDNF-induced LTP in vivo: evidence for compartment-specific translation control. *J Neurochem* 99, 1328-1337.
- Kasinski, A.L., Kelnar, K., Stahlhut, C., Orellana, E., Zhao, J., Shimer, E., Dysart, S., Chen, X., Bader, A.G., and Slack, F.J. (2015). A combinatorial microRNA therapeutics approach to suppressing non-small cell lung cancer. *Oncogene* 34, 3547-3555.
- Kawashima, H., Numakawa, T., Kumamaru, E., Adachi, N., Mizuno, H., Ninomiya, M., Kunugi, H., and Hashido, K. (2010). Glucocorticoid attenuates brain-derived neurotrophic factor-dependent upregulation of glutamate receptors via the suppression of microRNA-132 expression. *Neuroscience* 165, 1301-1311.

- Kelleher, R.J., 3rd, and Bear, M.F. (2008). The autistic neuron: troubled translation? *Cell* 135, 401-406.
- Kelleher, R.J., 3rd, Govindarajan, A., Jung, H.Y., Kang, H., and Tonegawa, S. (2004). Translational control by MAPK signaling in long-term synaptic plasticity and memory. *Cell* 116, 467-479.
- Kim, Y., Yeo, J., Lee, J.H., Cho, J., Seo, D., Kim, J.S., and Kim, V.N. (2014). Deletion of human tarbp2 reveals cellular microRNA targets and cell-cycle function of TRBP. *Cell Rep* 9, 1061-1074.
- Kluwe, L., Mautner, V., Heinrich, B., Dezube, R., Jacoby, L.B., Friedrich, R.E., and MacCollin, M. (2003). Molecular study of frequency of mosaicism in neurofibromatosis 2 patients with bilateral vestibular schwannomas. *J Med Genet* 40, 109-114.
- Kluwe, L., and Mautner, V.F. (1998). Mosaicism in sporadic neurofibromatosis 2 patients. *Hum Mol Genet* 7, 2051-2055.
- Krauss, S., Griesche, N., Jastrzebska, E., Chen, C., Rutschow, D., Achmuller, C., Dorn, S., Boesch, S.M., Lalowski, M., Wanker, E., *et al.* (2013). Translation of HTT mRNA with expanded CAG repeats is regulated by the MID1-PP2A protein complex. *Nat Commun* 4, 1511.
- Krichevsky, A.M., King, K.S., Donahue, C.P., Khrapko, K., and Kosik, K.S. (2003). A microRNA array reveals extensive regulation of microRNAs during brain development. *RNA* 9, 1274-1281.
- Krol, J., Buskamp, V., Markiewicz, I., Stadler, M.B., Ribi, S., Richter, J., Duebel, J., Bicker, S., Fehling, H.J., Schubeler, D., *et al.* (2010). Characterizing light-regulated retinal microRNAs reveals rapid turnover as a common property of neuronal microRNAs. *Cell* 141, 618-631.
- Lagos-Quintana, M., Rauhut, R., Yalcin, A., Meyer, J., Lendeckel, W., and Tuschl, T. (2002). Identification of tissue-specific microRNAs from mouse. *Curr Biol* 12, 735-739.
- Lai, K.O., Wong, A.S., Cheung, M.C., Xu, P., Liang, Z., Lok, K.C., Xie, H., Palko, M.E., Yung, W.H., Tessarollo, L., *et al.* (2012). TrkB phosphorylation by Cdk5 is required for activity-dependent structural plasticity and spatial memory. *Nat Neurosci* 15, 1506-1515.
- Lauterborn, J.C., Rex, C.S., Kramar, E., Chen, L.Y., Pandeyarajan, V., Lynch, G., and Gall, C.M. (2007). Brain-derived neurotrophic factor rescues synaptic plasticity in a mouse model of fragile X syndrome. *J. Neurosci.* 27, 10685-10694.

- Lazo, O.M., Gonzalez, A., Ascano, M., Kuruvilla, R., Couve, A., and Bronfman, F.C. (2013). BDNF regulates Rab11-mediated recycling endosome dynamics to induce dendritic branching. *J Neurosci* 33, 6112-6122.
- Lee, H.Y., Zhou, K., Smith, A.M., Noland, C.L., and Doudna, J.A. (2013). Differential roles of human Dicer-binding proteins TRBP and PACT in small RNA processing. *Nucleic Acids Res* 41, 6568-6576.
- Lee, J.Y., Kim, H., Ryu, C.H., Kim, J.Y., Choi, B.H., Lim, Y., Huh, P.W., Kim, Y.H., Lee, K.H., Jun, T.Y., *et al.* (2004). Merlin, a tumor suppressor, interacts with transactivation-responsive RNA-binding protein and inhibits its oncogenic activity. *J Biol Chem* 279, 30265-30273.
- Lee, J.Y., Moon, H.J., Lee, W.K., Chun, H.J., Han, C.W., Jeon, Y.W., Lim, Y., Kim, Y.H., Yao, T.P., Lee, K.H., *et al.* (2006). Merlin facilitates ubiquitination and degradation of transactivation-responsive RNA-binding protein. *Oncogene* 25, 1143-1152.
- Lee, R.C., Feinbaum, R.L., and Ambros, V. (1993). The *C. elegans* heterochronic gene *lin-4* encodes small RNAs with antisense complementarity to *lin-14*. *Cell* 75, 843-854.
- Li, Z., He, S.Q., Xu, Q., Yang, F., Tiwari, V., Liu, Q., Tang, Z., Han, L., Chu, Y.X., Wang, Y., *et al.* (2014). Activation of MrgC receptor inhibits N-type calcium channels in small-diameter primary sensory neurons in mice. *Pain* 155, 1613-1621.
- Liao, L., Pilotte, J., Xu, T., Wong, C.C., Edelman, G.M., Vanderklish, P., and Yates, J.R., 3rd (2007). BDNF induces widespread changes in synaptic protein content and up-regulates components of the translation machinery: an analysis using high-throughput proteomics. *J Proteome Res* 6, 1059-1071.
- Lim, J.Y., Kim, H., Kim, Y.H., Kim, S.W., Huh, P.W., Lee, K.H., Jeun, S.S., Rha, H.K., and Kang, J.K. (2003a). Merlin suppresses the SRE-dependent transcription by inhibiting the activation of Ras-ERK pathway. *Biochem Biophys Res Commun* 302, 238-245.
- Lim, K.L., Chew, K.C., Tan, J.M., Wang, C., Chung, K.K., Zhang, Y., Tanaka, Y., Smith, W., Engelender, S., Ross, C.A., *et al.* (2005). Parkin mediates nonclassical, proteasomal-independent ubiquitination of synphilin-1: implications for Lewy body formation. *J. Neurosci.* 25, 2002-2009.
- Lim, L.P., Lau, N.C., Weinstein, E.G., Abdelhakim, A., Yekta, S., Rhoades, M.W., Burge, C.B., and Bartel, D.P. (2003b). The microRNAs of *Caenorhabditis elegans*. *Genes Dev* 17, 991-1008.

- Lin, M.Y., Lin, Y.M., Kao, T.C., Chuang, H.H., and Chen, R.H. (2011). PDZ-RhoGEF ubiquitination by Cullin3-KLHL20 controls neurotrophin-induced neurite outgrowth. *J Cell Biol* 193, 985-994.
- Link, T.M., Park, U., Vonakis, B.M., Raben, D.M., Soloski, M.J., and Caterina, M.J. (2010). TRPV2 has a pivotal role in macrophage particle binding and phagocytosis. *Nat Immunol* 11, 232-239.
- Liu, Y.M., Xia, Y., Dai, W., Han, H.Y., Dong, Y.X., Cai, J., Zeng, X., Luo, F.Y., Yang, T., Li, Y.Z., *et al.* (2014). Cholesterol-conjugated let-7a mimics: antitumor efficacy on hepatocellular carcinoma in vitro and in a preclinical orthotopic xenograft model of systemic therapy. *BMC Cancer* 14, 889.
- Liu-Yesucevitz, L., Bassell, G.J., Gitler, A.D., Hart, A.C., Klann, E., Richter, J.D., Warren, S.T., and Wolozin, B. (2011). Local RNA translation at the synapse and in disease. *J Neurosci* 31, 16086-16093.
- Lugli, G., Larson, J., Demars, M.P., and Smalheiser, N.R. (2012). Primary microRNA precursor transcripts are localized at post-synaptic densities in adult mouse forebrain. *J Neurochem* 123, 459-466.
- Lugli, G., Larson, J., Martone, M.E., Jones, Y., and Smalheiser, N.R. (2005). Dicer and eIF2c are enriched at postsynaptic densities in adult mouse brain and are modified by neuronal activity in a calpain-dependent manner. *J Neurochem* 94, 896-905.
- Lugli, G., Torvik, V.I., Larson, J., and Smalheiser, N.R. (2008). Expression of microRNAs and their precursors in synaptic fractions of adult mouse forebrain. *J Neurochem* 106, 650-661.
- Manadas, B., Santos, A.R., Szabadfi, K., Gomes, J.R., Garbis, S.D., Fountoulakis, M., and Duarte, C.B. (2009). BDNF-induced changes in the expression of the translation machinery in hippocampal neurons: protein levels and dendritic mRNA. *J Proteome Res* 8, 4536-4552.
- Mansour, S.J., Matten, W.T., Hermann, A.S., Candia, J.M., Rong, S., Fukasawa, K., Vande Woude, G.F., and Ahn, N.G. (1994). Transformation of mammalian cells by constitutively active MAP kinase kinase. *Science* 265, 966-970.
- Mao, X.G., Hutt-Cabezas, M., Orr, B.A., Weingart, M., Taylor, I., Rajan, A.K., Oda, Y., Kahlert, U., Maciaczyk, J., Nikkhah, G., *et al.* (2013). LIN28A facilitates the transformation of human neural stem cells and promotes glioblastoma tumorigenesis through a pro-invasive genetic program. *Oncotarget* 4, 1050-1064.
- Marson, A., Levine, S.S., Cole, M.F., Frampton, G.M., Brambrink, T., Johnstone, S., Guenther, M.G., Johnston, W.K., Wernig, M., Newman, J., *et al.* (2008). Connecting microRNA genes to the core transcriptional regulatory circuitry of embryonic stem cells. *Cell* 134, 521-533.

- Matsuda, N., Lu, H., Fukata, Y., Noritake, J., Gao, H., Mukherjee, S., Nemoto, T., Fukata, M., and Poo, M.M. (2009). Differential activity-dependent secretion of brain-derived neurotrophic factor from axon and dendrite. *J Neurosci* 29, 14185-14198.
- Mautner, V.F., Lindenau, M., Baser, M.E., Hazim, W., Tatagiba, M., Haase, W., Samii, M., Wais, R., and Pulst, S.M. (1996). The neuroimaging and clinical spectrum of neurofibromatosis 2. *Neurosurgery* 38, 880-885; discussion 885-886.
- Mayr, F., Schutz, A., Doge, N., and Heinemann, U. (2012). The Lin28 cold-shock domain remodels pre-let-7 microRNA. *Nucleic Acids Res* 40, 7492-7506.
- Mbarek, O., Marouillat, S., Martineau, J., Barthelemy, C., Muh, J.P., and Andres, C. (1999). Association study of the NF1 gene and autistic disorder. *Am J Med Genet* 88, 729-732.
- McAllister, A.K., Katz, L.C., and Lo, D.C. (1997). Opposing roles for endogenous BDNF and NT-3 in regulating cortical dendritic growth. *Neuron* 18, 767-778.
- McAllister, A.K., Katz, L.C., and Lo, D.C. (1999). Neurotrophins and synaptic plasticity. *Annu Rev Neurosci* 22, 295-318.
- Meffert, M.K., Chang, J.M., Wiltgen, B.J., Fanselow, M.S., and Baltimore, D. (2003). NF-kappa B functions in synaptic signaling and behavior. *Nat. Neurosci.* 6, 1072-1078.
- Melo, S.A., Roperio, S., Moutinho, C., Aaltonen, L.A., Yamamoto, H., Calin, G.A., Rossi, S., Fernandez, A.F., Carneiro, F., Oliveira, C., *et al.* (2009). A TARBP2 mutation in human cancer impairs microRNA processing and DICER1 function. *Nat Genet* 41, 365-370.
- Minichiello, L., Korte, M., Wolfer, D., Kuhn, R., Unsicker, K., Cestari, V., Rossi-Arnaud, C., Lipp, H.P., Bonhoeffer, T., and Klein, R. (1999). Essential role for TrkB receptors in hippocampus-mediated learning. *Neuron* 24, 401-414.
- Morita, K., and Han, M. (2006). Multiple mechanisms are involved in regulating the expression of the developmental timing regulator lin-28 in *Caenorhabditis elegans*. *EMBO J* 25, 5794-5804.
- Moss, E.G., Lee, R.C., and Ambros, V. (1997). The cold shock domain protein LIN-28 controls developmental timing in *C. elegans* and is regulated by the lin-4 RNA. *Cell* 88, 637-646.
- Moss, E.G., and Tang, L. (2003). Conservation of the heterochronic regulator Lin-28, its developmental expression and microRNA complementary sites. *Dev Biol* 258, 432-442.

Moyhuddin, A., Baser, M.E., Watson, C., Purcell, S., Ramsden, R.T., Heiberg, A., Wallace, A.J., and Evans, D.G. (2003). Somatic mosaicism in neurofibromatosis 2: prevalence and risk of disease transmission to offspring. *J Med Genet* 40, 459-463.

Muglia, P., Vicente, A.M., Verga, M., King, N., Macciardi, F., and Kennedy, J.L. (2003). Association between the BDNF gene and schizophrenia. *Mol Psychiatry* 8, 146-147.

Nagahara, A.H., and Tuszynski, M.H. (2011). Potential therapeutic uses of BDNF in neurological and psychiatric disorders. *Nat Rev Drug Discov* 10, 209-219.

Nam, Y., Chen, C., Gregory, R.I., Chou, J.J., and Sliz, P. (2011). Molecular basis for interaction of let-7 microRNAs with Lin28. *Cell* 147, 1080-1091.

Napoli, I., Mercaldo, V., Boyl, P.P., Eleuteri, B., Zalfa, F., De Rubeis, S., Di Marino, D., Mohr, E., Massimi, M., Falconi, M., *et al.* (2008). The fragile X syndrome protein represses activity-dependent translation through CYFIP1, a new 4E-BP. *Cell* 134, 1042-1054.

Nowak, J.S., Choudhury, N.R., de Lima Alves, F., Rappsilber, J., and Michlewski, G. (2014). Lin28a regulates neuronal differentiation and controls miR-9 production. *Nat Commun* 5, 3687.

Olde Loohuis, N.F., Kos, A., Martens, G.J., Van Bokhoven, H., Nadif Kasri, N., and Aschrafi, A. (2012). MicroRNA networks direct neuronal development and plasticity. *Cell Mol Life Sci* 69, 89-102.

Ong, K.K., Elks, C.E., Li, S., Zhao, J.H., Luan, J., Andersen, L.B., Bingham, S.A., Brage, S., Smith, G.D., Ekelund, U., *et al.* (2009). Genetic variation in LIN28B is associated with the timing of puberty. *Nat Genet* 41, 729-733.

Pardon, M.C. (2010). Role of neurotrophic factors in behavioral processes: implications for the treatment of psychiatric and neurodegenerative disorders. *Vitam Horm* 82, 185-200.

Paroo, Z., Ye, X., Chen, S., and Liu, Q. (2009). Phosphorylation of the human microRNA-generating complex mediates MAPK/Erk signaling. *Cell* 139, 112-122.

Parry, D.M., Eldridge, R., Kaiser-Kupfer, M.I., Bouzas, E.A., Pikus, A., and Patronas, N. (1994). Neurofibromatosis 2 (NF2): clinical characteristics of 63 affected individuals and clinical evidence for heterogeneity. *Am J Med Genet* 52, 450-461.

Pasquinelli, A.E., Reinhart, B.J., Slack, F., Martindale, M.Q., Kuroda, M.I., Maller, B., Hayward, D.C., Ball, E.E., Degan, B., Muller, P., *et al.* (2000). Conservation of the sequence and temporal expression of let-7 heterochronic regulatory RNA. *Nature* 408, 86-89.

- Patterson, S.L., Abel, T., Deuel, T.A., Martin, K.C., Rose, J.C., and Kandel, E.R. (1996). Recombinant BDNF rescues deficits in basal synaptic transmission and hippocampal LTP in BDNF knockout mice. *Neuron* 16, 1137-1145.
- Pedersen, S.M., Chan, W., Jattani, R.P., Mackie d, S., and Pomerantz, J.L. (2015). Negative Regulation of CARD11 Signaling and Lymphoma Cell Survival by the E3 Ubiquitin Ligase RNF181. *Mol Cell Biol* 36, 794-808.
- Pepin, G., Perron, M.P., and Provost, P. (2012). Regulation of human Dicer by the resident ER membrane protein CLIMP-63. *Nucleic Acids Res* 40, 11603-11617.
- Perez, L.M., Bernal, A., San Martin, N., Lorenzo, M., Fernandez-Veledo, S., and Galvez, B.G. (2013). Metabolic rescue of obese adipose-derived stem cells by Lin28/Let7 pathway. *Diabetes* 62, 2368-2379.
- Pfeiffer, B.E., and Huber, K.M. (2006). Current advances in local protein synthesis and synaptic plasticity. *J Neurosci* 26, 7147-7150.
- Piskounova, E., Polytarchou, C., Thornton, J.E., LaPierre, R.J., Pothoulakis, C., Hagan, J.P., Iliopoulos, D., and Gregory, R.I. (2011). Lin28A and Lin28B inhibit let-7 microRNA biogenesis by distinct mechanisms. *Cell* 147, 1066-1079.
- Power, A.E., Berlau, D.J., McGaugh, J.L., and Steward, O. (2006). Anisomycin infused into the hippocampus fails to block "reconsolidation" but impairs extinction: the role of re-exposure duration. *Learn Mem* 13, 27-34.
- Prabhakar, S., Brenner, G.J., Sung, B., Messerli, S.M., Mao, J., Sena-Esteves, M., Stemmer-Rachamimov, A., Tannous, B., and Breakefield, X.O. (2010). Imaging and therapy of experimental schwannomas using HSV amplicon vector-encoding apoptotic protein under Schwann cell promoter. *Cancer Gene Ther* 17, 266-274.
- Raab-Graham, K.F., Haddick, P.C., Jan, Y.N., and Jan, L.Y. (2006). Activity- and mTOR-dependent suppression of Kv1.1 channel mRNA translation in dendrites. *Science* 314, 144-148.
- Ramachandran, R., Fausett, B.V., and Goldman, D. (2010). Ascl1a regulates Muller glia dedifferentiation and retinal regeneration through a Lin-28-dependent, let-7 microRNA signalling pathway. *Nat. Cell Biol.* 12, 1101-1107.
- Ramaswami, M., Taylor, J.P., and Parker, R. (2013). Altered ribostasis: RNA-protein granules in degenerative disorders. *Cell* 154, 727-736.
- Rehfeld, F., Rohde, A.M., Nguyen, D.T., and Wulczyn, F.G. (2015). Lin28 and let-7: ancient milestones on the road from pluripotency to neurogenesis. *Cell Tissue Res* 359, 145-160.

- Reinhart, B.J., Slack, F.J., Basson, M., Pasquinelli, A.E., Bettinger, J.C., Rougvie, A.E., Horvitz, H.R., and Ruvkun, G. (2000). The 21-nucleotide let-7 RNA regulates developmental timing in *Caenorhabditis elegans*. *Nature* *403*, 901-906.
- Riccio, A., Alvania, R.S., Lonze, B.E., Ramanan, N., Kim, T., Huang, Y., Dawson, T.M., Snyder, S.H., and Ginty, D.D. (2006). A nitric oxide signaling pathway controls CREB-mediated gene expression in neurons. *Mol Cell* *21*, 283-294.
- Rivera, C., Li, H., Thomas-Crusells, J., Lahtinen, H., Viitanen, T., Nanobashvili, A., Kokaia, Z., Airaksinen, M.S., Voipio, J., Kaila, K., *et al.* (2002). BDNF-induced TrkB activation down-regulates the K⁺-Cl⁻ cotransporter KCC2 and impairs neuronal Cl⁻ extrusion. *J Cell Biol* *159*, 747-752.
- Ruiz, C.R., Shi, J., and Meffert, M.K. (2014). Transcript specificity in BDNF-regulated protein synthesis. *Neuropharmacology* *76 Pt C*, 657-663.
- Ruttledge, M.H., Andermann, A.A., Phelan, C.M., Claudio, J.O., Han, F.Y., Chretien, N., Rangaratnam, S., MacCollin, M., Short, P., Parry, D., *et al.* (1996). Type of mutation in the neurofibromatosis type 2 gene (NF2) frequently determines severity of disease. *Am J Hum Genet* *59*, 331-342.
- Rybak, A., Fuchs, H., Smirnova, L., Brandt, C., Pohl, E.E., Nitsch, R., and Wulczyn, F.G. (2008). A feedback loop comprising lin-28 and let-7 controls pre-let-7 maturation during neural stem-cell commitment. *Nat Cell Biol* *10*, 987-993.
- Rybak-Wolf, A., Jens, M., Murakawa, Y., Herzog, M., Landthaler, M., and Rajewsky, N. (2014). A variety of dicer substrates in human and *C. elegans*. *Cell* *159*, 1153-1167.
- Santos, A.R., Comprido, D., and Duarte, C.B. (2010). Regulation of local translation at the synapse by BDNF. *Prog Neurobiol* *92*, 505-516.
- Santos, A.R., Mele, M., Vaz, S.H., Kellermayer, B., Grimaldi, M., Colino-Oliveira, M., Rombo, D.M., Comprido, D., Sebastiao, A.M., and Duarte, C.B. (2015). Differential role of the proteasome in the early and late phases of BDNF-induced facilitation of LTP. *J Neurosci* *35*, 3319-3329.
- Schratt, G.M., Nigh, E.A., Chen, W.G., Hu, L., and Greenberg, M.E. (2004). BDNF regulates the translation of a select group of mRNAs by a mammalian target of rapamycin-phosphatidylinositol 3-kinase-dependent pathway during neuronal development. *J Neurosci* *24*, 7366-7377.
- Schratt, G.M., Tuebing, F., Nigh, E.A., Kane, C.G., Sabatini, M.E., Kiebler, M., and Greenberg, M.E. (2006). A brain-specific microRNA regulates dendritic spine development. *Nature* *439*, 283-289.

Schwanhauser, B., Busse, D., Li, N., Dittmar, G., Schuchhardt, J., Wolf, J., Chen, W., and Selbach, M. (2011). Global quantification of mammalian gene expression control. *Nature* 473, 337-342.

Seggerson, K., Tang, L., and Moss, E.G. (2002). Two genetic circuits repress the *Caenorhabditis elegans* heterochronic gene *lin-28* after translation initiation. *Dev Biol* 243, 215-225.

Seizinger, B.R., Martuza, R.L., and Gusella, J.F. (1986). Loss of genes on chromosome 22 in tumorigenesis of human acoustic neuroma. *Nature* 322, 644-647.

Sempere, L.F., Freemantle, S., Pitha-Rowe, I., Moss, E., Dmitrovsky, E., and Ambros, V. (2004). Expression profiling of mammalian microRNAs uncovers a subset of brain-expressed microRNAs with possible roles in murine and human neuronal differentiation. *Genome Biol* 5, R13.

Sher, I., Hanemann, C.O., Karplus, P.A., and Bretscher, A. (2012). The tumor suppressor merlin controls growth in its open state, and phosphorylation converts it to a less-active more-closed state. *Dev Cell* 22, 703-705.

Shinohara, Y., Yahagi, K., Kawano, M., Nishiyori, H., Kawazu, C., Suzuki, N., Manabe, R., and Hirase, H. (2011). miRNA profiling of bilateral rat hippocampal CA3 by deep sequencing. *Biochem Biophys Res Commun* 409, 293-298.

Shyh-Chang, N., and Daley, G.Q. (2013). Lin28: primal regulator of growth and metabolism in stem cells. *Cell Stem Cell* 12, 395-406.

Shyh-Chang, N., Zhu, H., Yvanka de Soysa, T., Shinoda, G., Seligson, M.T., Tsanov, K.M., Nguyen, L., Asara, J.M., Cantley, L.C., and Daley, G.Q. (2013). Lin28 enhances tissue repair by reprogramming cellular metabolism. *Cell* 155, 778-792.

Smalheiser, N.R., and Lugli, G. (2009). microRNA regulation of synaptic plasticity. *Neuromolecular Med* 11, 133-140.

Smith, N.C., and Matthews, J.M. (2016). Mechanisms of DNA-binding specificity and functional gene regulation by transcription factors. *Curr Opin Struct Biol* 38, 68-74.

Spyra, M., Otto, B., Schon, G., Kehrer-Sawatzki, H., and Mautner, V.F. (2015). Determination of the mutant allele frequency in patients with neurofibromatosis type 2 and somatic mosaicism by means of deep sequencing. *Genes Chromosomes Cancer*.

Srivastava, T., Fortin, D.A., Nygaard, S., Kaech, S., Sonenberg, N., Edelman, A.M., and Soderling, T.R. (2012). Regulation of neuronal mRNA translation by CaM-kinase I phosphorylation of eIF4GII. *J Neurosci* 32, 5620-5630.

Stenvang, J., Petri, A., Lindow, M., Obad, S., and Kauppinen, S. (2012). Inhibition of microRNA function by antimiR oligonucleotides. *Silence* 3, 1.

Takamizawa, J., Konishi, H., Yanagisawa, K., Tomida, S., Osada, H., Endoh, H., Harano, T., Yatabe, Y., Nagino, M., Nimura, Y., *et al.* (2004). Reduced expression of the let-7 microRNAs in human lung cancers in association with shortened postoperative survival. *Cancer Res* 64, 3753-3756.

Takei, N., Inamura, N., Kawamura, M., Namba, H., Hara, K., Yonezawa, K., and Nawa, H. (2004). Brain-derived neurotrophic factor induces mammalian target of rapamycin-dependent local activation of translation machinery and protein synthesis in neuronal dendrites. *J Neurosci* 24, 9760-9769.

Takei, N., Kawamura, M., Hara, K., Yonezawa, K., and Nawa, H. (2001). Brain-derived neurotrophic factor enhances neuronal translation by activating multiple initiation processes: comparison with the effects of insulin. *J Biol Chem* 276, 42818-42825.

Takei, N., Kawamura, M., Ishizuka, Y., Kakiya, N., Inamura, N., Namba, H., and Nawa, H. (2009). Brain-derived neurotrophic factor enhances the basal rate of protein synthesis by increasing active eukaryotic elongation factor 2 levels and promoting translation elongation in cortical neurons. *J Biol Chem* 284, 26340-26348.

Takemoto-Kimura, S., Ageta-Ishihara, N., Nonaka, M., Adachi-Morishima, A., Mano, T., Okamura, M., Fujii, H., Fuse, T., Hoshino, M., Suzuki, S., *et al.* (2007). Regulation of dendritogenesis via a lipid-raft-associated Ca²⁺/calmodulin-dependent protein kinase CLICK-III/CaMKIgamma. *Neuron* 54, 755-770.

Tanaka, J., Horiike, Y., Matsuzaki, M., Miyazaki, T., Ellis-Davies, G.C., and Kasai, H. (2008). Protein synthesis and neurotrophin-dependent structural plasticity of single dendritic spines. *Science* 319, 1683-1687.

Tang, G., Gudsnek, K., Kuo, S.H., Cotrina, M.L., Rosoklija, G., Sosunov, A., Sonders, M.S., Kanter, E., Castagna, C., Yamamoto, A., *et al.* (2014). Loss of mTOR-dependent macroautophagy causes autistic-like synaptic pruning deficits. *Neuron* 83, 1131-1143.

Thornton, J.E., Chang, H.M., Piskounova, E., and Gregory, R.I. (2012). Lin28-mediated control of let-7 microRNA expression by alternative TUTases Zcchc11 (TUT4) and Zcchc6 (TUT7). *RNA* 18, 1875-1885.

Thornton, J.E., and Gregory, R.I. (2012). How does Lin28 let-7 control development and disease? *Trends Cell Biol.* 22, 474-482.

Tian, Q., Stepaniants, S.B., Mao, M., Weng, L., Feetham, M.C., Doyle, M.J., Yi, E.C., Dai, H., Thorsson, V., Eng, J., *et al.* (2004). Integrated genomic and

proteomic analyses of gene expression in Mammalian cells. *Mol Cell Proteomics* 3, 960-969.

Tommiska, J., Sorensen, K., Aksglaede, L., Koivu, R., Puhakka, L., Juul, A., and Raivio, T. (2011). LIN28B, LIN28A, KISS1, and KISS1R in idiopathic central precocious puberty. *BMC Res Notes* 4, 363.

Tronel, S., Milekic, M.H., and Alberini, C.M. (2005). Linking new information to a reactivated memory requires consolidation and not reconsolidation mechanisms. *PLoS Biol* 3, e293.

Tyler, W.J., Alonso, M., Bramham, C.R., and Pozzo-Miller, L.D. (2002). From acquisition to consolidation: on the role of brain-derived neurotrophic factor signaling in hippocampal-dependent learning. *Learn Mem* 9, 224-237.

Tyler, W.J., and Pozzo-Miller, L. (2003). Miniature synaptic transmission and BDNF modulate dendritic spine growth and form in rat CA1 neurones. *J Physiol* 553, 497-509.

Tyler, W.J., and Pozzo-Miller, L.D. (2001). BDNF enhances quantal neurotransmitter release and increases the number of docked vesicles at the active zones of hippocampal excitatory synapses. *J Neurosci* 21, 4249-4258.

Urbach, A., Yermalovich, A., Zhang, J., Spina, C.S., Zhu, H., Perez-Atayde, A.R., Shukrun, R., Charlton, J., Sebire, N., Mifsud, W., *et al.* (2014). Lin28 sustains early renal progenitors and induces Wilms tumor. *Genes Dev.* 28, 971-982.

Vakharia, K.T., Henstrom, D., Plotkin, S.R., Cheney, M., and Hadlock, T.A. (2012). Facial reanimation of patients with neurofibromatosis type 2. *Neurosurgery* 70, 237-243.

Vessey, J.P., Schoderboeck, L., Gingl, E., Luzi, E., Riefler, J., Di Leva, F., Karra, D., Thomas, S., Kiebler, M.A., and Macchi, P. (2010). Mammalian Pumilio 2 regulates dendrite morphogenesis and synaptic function. *Proc Natl Acad Sci U S A* 107, 3222-3227.

Viswanathan, S.R., Daley, G.Q., and Gregory, R.I. (2008). Selective blockade of microRNA processing by Lin28. *Science* 320, 97-100.

Viswanathan, S.R., Powers, J.T., Einhorn, W., Hoshida, Y., Ng, T.L., Toffanin, S., O'Sullivan, M., Lu, J., Phillips, L.A., Lockhart, V.L., *et al.* (2009). Lin28 promotes transformation and is associated with advanced human malignancies. *Nat. Genet.* 41, 843-848.

Vo, N., Klein, M.E., Varlamova, O., Keller, D.M., Yamamoto, T., Goodman, R.H., and Impey, S. (2005). A cAMP-response element binding protein-induced microRNA regulates neuronal morphogenesis. *Proc Natl Acad Sci U S A* 102, 16426-16431.

- Wang, Q.Z., Lv, Y.H., Gong, Y.H., Li, Z.F., Xu, W., Diao, Y., and Xu, R. (2012). Double-stranded Let-7 mimics, potential candidates for cancer gene therapy. *J Physiol Biochem* 68, 107-119.
- Wang, W., van Niekerk, E., Willis, D.E., and Twiss, J.L. (2007). RNA transport and localized protein synthesis in neurological disorders and neural repair. *Dev Neurobiol* 67, 1166-1182.
- Wayman, G.A., Davare, M., Ando, H., Fortin, D., Varlamova, O., Cheng, H.Y., Marks, D., Obrietan, K., Soderling, T.R., Goodman, R.H., *et al.* (2008). An activity-regulated microRNA controls dendritic plasticity by down-regulating p250GAP. *Proc Natl Acad Sci U S A* 105, 9093-9098.
- Wetmore, C., Ernfors, P., Persson, H., and Olson, L. (1990). Localization of brain-derived neurotrophic factor mRNA to neurons in the brain by in situ hybridization. *Exp Neurol* 109, 141-152.
- Wienholds, E., Kloosterman, W.P., Miska, E., Alvarez-Saavedra, E., Berezikov, E., de Bruijn, E., Horvitz, H.R., Kauppinen, S., and Plasterk, R.H. (2005). MicroRNA expression in zebrafish embryonic development. *Science* 309, 310-311.
- Wilbert, M.L., Huelga, S.C., Kapeli, K., Stark, T.J., Liang, T.Y., Chen, S.X., Yan, B.Y., Nathanson, J.L., Hutt, K.R., Lovci, M.T., *et al.* (2012). LIN28 binds messenger RNAs at GGAGA motifs and regulates splicing factor abundance. *Mol Cell* 48, 195-206.
- Wilson, R.C., Tambe, A., Kidwell, M.A., Noland, C.L., Schneider, C.P., and Doudna, J.A. (2015). Dicer-TRBP complex formation ensures accurate mammalian microRNA biogenesis. *Mol Cell* 57, 397-407.
- Wu, L., Wells, D., Tay, J., Mendis, D., Abbott, M.A., Barnitt, A., Quinlan, E., Heynen, A., Fallon, J.R., and Richter, J.D. (1998). CPEB-mediated cytoplasmic polyadenylation and the regulation of experience-dependent translation of alpha-CaMKII mRNA at synapses. *Neuron* 21, 1129-1139.
- Wulczyn, F.G., Smirnova, L., Rybak, A., Brandt, C., Kwidzinski, E., Ninnemann, O., Strehle, M., Seiler, A., Schumacher, S., and Nitsch, R. (2007). Post-transcriptional regulation of the let-7 microRNA during neural cell specification. *FASEB J* 21, 415-426.
- Xu, B., Zang, K., Ruff, N.L., Zhang, Y.A., McConnell, S.K., Stryker, M.P., and Reichardt, L.F. (2000). Cortical degeneration in the absence of neurotrophin signaling: dendritic retraction and neuronal loss after removal of the receptor TrkB. *Neuron* 26, 233-245.
- Yanaihara, N., Caplen, N., Bowman, E., Seike, M., Kumamoto, K., Yi, M., Stephens, R.M., Okamoto, A., Yokota, J., Tanaka, T., *et al.* (2006). Unique

microRNA molecular profiles in lung cancer diagnosis and prognosis. *Cancer Cell* 9, 189-198.

Yin, Y., Edelman, G.M., and Vanderklish, P.W. (2002). The brain-derived neurotrophic factor enhances synthesis of Arc in synaptoneurosomes. *Proc Natl Acad Sci U S A* 99, 2368-2373.

Yu, J., Vodyanik, M.A., Smuga-Otto, K., Antosiewicz-Bourget, J., Frane, J.L., Tian, S., Nie, J., Jonsdottir, G.A., Ruotti, V., Stewart, R., *et al.* (2007). Induced pluripotent stem cell lines derived from human somatic cells. *Science* 318, 1917-1920.

Yu, S.L., Chen, H.Y., Chang, G.C., Chen, C.Y., Chen, H.W., Singh, S., Cheng, C.L., Yu, C.J., Lee, Y.C., Chen, H.S., *et al.* (2008). MicroRNA signature predicts survival and relapse in lung cancer. *Cancer Cell* 13, 48-57.

Zeng, Y., Yao, B., Shin, J., Lin, L., Kim, N., Song, Q., Liu, S., Su, Y., Guo, J.U., Huang, L., *et al.* (2016). Lin28A Binds Active Promoters and Recruits Tet1 to Regulate Gene Expression. *Mol Cell* 61, 153-160.

Zhao, B., Wei, X., Li, W., Udan, R.S., Yang, Q., Kim, J., Xie, J., Ikenoue, T., Yu, J., Li, L., *et al.* (2007). Inactivation of YAP oncoprotein by the Hippo pathway is involved in cell contact inhibition and tissue growth control. *Genes Dev* 21, 2747-2761.

Zhu, H., Shah, S., Shyh-Chang, N., Shinoda, G., Einhorn, W.S., Viswanathan, S.R., Takeuchi, A., Grasmann, C., Rinn, J.L., Lopez, M.F., *et al.* (2010). Lin28a transgenic mice manifest size and puberty phenotypes identified in human genetic association studies. *Nat. Genet.* 42, 626-630.

Zhu, H., Shyh-Chang, N., Segre, A.V., Shinoda, G., Shah, S.P., Einhorn, W.S., Takeuchi, A., Engreitz, J.M., Hagan, J.P., Kharas, M.G., *et al.* (2011). The Lin28/let-7 axis regulates glucose metabolism. *Cell* 147, 81-94.

Zuccato, C., and Cattaneo, E. (2009). Brain-derived neurotrophic factor in neurodegenerative diseases. *Nat Rev Neurol* 5, 311-322.

Curriculum Vitae

The Johns Hopkins University School of Medicine

Alexandra M. Amen

07/2016

EDUCATION

Ph.D., expected 2016
The Johns Hopkins University School of Medicine
Advisor: Mollie K. Meffert, M.D./Ph.D.

Program in Neuroscience

Baltimore, MD

B.A., 2008
Haverford College
Advisor: Rebecca Compton, Ph.D.

Psychology/Neural and Behavioral Sciences

Haverford College

Haverford, PA

International Baccalaureate Diploma, 2004

Lincoln High School

Portland, OR

RESEARCH EXPERIENCE

Predoctoral Student, Department of Neuroscience (2010-present)

Lab of Mollie K. Meffert, M.D., Ph.D.

The Johns Hopkins University School of Medicine

Research Assistant in Cognitive Neuroscience (2008-2010)

Lab of Barry Oken, M.D.

Oregon Health and Science University

Undergraduate Research Project in Cognitive Neuroscience (2007-2008)

Lab of Rebecca Compton, Ph.D.

Haverford College

Summer Research Intern in Cellular Neuroscience (2007)

Lab of Gary Banker, Ph.D.

Oregon Health and Science University

Summer Research Student in Cellular and Molecular Biology (2006)

Lab of David Dalton, Ph.D.

Reed College

FELLOWSHIPS

2014-present NIMH Ruth L. Kirschstein National Research Service Grant
Award (F31MH098634)

TALKS AND SEMINARS

2015 Johns Hopkins Biochemistry Department Evening Research
Discussion

2015 Johns Hopkins Biochemistry Department Retreat

2015 Johns Hopkins Neuroscience Department Lunch Research Discussion

2014 Society for Neuroscience nanosymposium (invited talk) in “Synaptic
Plasticity: Molecular and Circuit Mechanisms”

2014 Johns Hopkins Biochemistry Department Evening Research
Discussion

AWARDS AND HONORS

- 2008 Society for Psychophysiological Research (SPR) student travel award
- 2008 B.A. awarded with honors, Haverford College
- 2008 Senior thesis high honors, Department of Psychology, Haverford College
- 2007 Oregon Health & Science University CROET outstanding summer research award
- 2007 Oregon Health & Science University CROET undergraduate summer fellowship

PUBLICATIONS

Manuscripts in preparation:

Amen AM, Belzberg A, Ostrow K, & Meffert MK (*in preparation*). Loss of Merlin/NF2 leads to Lin28a dysregulation and tumorigenesis in Neurofibromatosis Type 2.

Amen AM, Ruiz-Garzon CR, Shi J, Subramanian M, Pham D, & Meffert MK (*Mol Cell, under review*). A rapid induction mechanism for Lin28a in trophic responses.

Peer reviewed publications:

Amen AM, Pham D, & Meffert MK (2016). Post-transcriptional regulation by Brain-Derived Neurotrophic Factor in the nervous system. In: Menon KMJ,

Goldstrohm AC, editors. *Post-transcriptional mechanisms in endocrine regulation*. Springer International Publishing Switzerland. p. 315-338.

Fonareva I, **Amen AM**, Ellingson RM, Oken BS (2012). Differences in stress-related ratings between research center and home environments in dementia caregivers using ecological momentary assessment. *Int Psychogeriatrics* 24, 90-98.

Fonareva I, **Amen AM**, Zajdel DP, Ellingson RM, Oken BS (2011). Assessing sleep architecture in dementia caregivers at home using an ambulatory polysomnographic system. *J Geriatr Psychiatry Neurol* 24, 50-59.

Oken BS, Fonareva I, Haas M, Wahbeh H, Lane JB, Zajdel D, **Amen A** (2010). Pilot controlled trial of mindfulness meditation and education for dementia caregivers. *J Altern Complement Med* 16, 1031-1038.

Abstracts:

Amen AM, Ruiz C, Shi J, & Meffert MK (2014). Role of the Lin28/let-7 axis in gene expression regulation by BDNF. Program No. 767.03. 2014 Neuroscience Meeting Planner. Washington, DC: Society for Neuroscience, 2014. Online.

Fonareva IG, Ellingson RM, Zajdel DP, **Amen AM**, & Oken BS. Measuring evoked potentials during a GO-NOGO reaction time task in subjects' natural

environment using an ambulatory recording system. Program No. 697.15/III42. 2010 Neuroscience Meeting Planner. San Diego, CA: Society for Neuroscience, 2010. Online.

Amen A, Dodd J, Fineman SL, & Compton RJ. Individual differences in cognitive control are associated with cortisol reactivity. Program Number 123. Austin, TX: Society for Psychophysiology Research, 2008.

Chapters:

Oken BS & **Amen AM** (2010). Electroencephalography and evoked potentials in geriatrics (Martin Albert & Janice Knoefel, Eds). In *Neurological Assessment in Aging* (3rd Ed, 277-292). Oxford University Press.

Undergraduate Senior Thesis:

Amen A (2008). Monitoring the Mind: The relationship between individual differences in cognitive control and emotion regulation. Senior thesis under Rebecca Compton, Haverford College. <http://hdl.handle.net/10066/1428>

MENTORING AND TEACHING

2015	Guided the rotation project of a Biochemistry graduate student
2014	Designed and co-taught with one other graduate student a two month long undergraduate course covering modern methods in neuroscience

- 2014 Mentored a Johns Hopkins undergraduate student
- 2013-2016 Mentored a Johns Hopkins undergraduate student
- 2011-2014 Guided the projects of a Johns Hopkins Neuroscience Master's student
- 2013 Guided the rotation project of a Johns Hopkins Biochemistry and Molecular Biology graduate student
- 2012 Guided the rotation project of a Johns Hopkins Biochemistry and Molecular Biology graduate student
- 2012 Guided the rotation project of a Johns Hopkins Neuroscience graduate student
- 2012 Teaching assistant, Neuroscience and Cognition (Merit-based)
- 2010-2013 Tutored high school students through the Johns Hopkins mentorship program "Thread"